5-2018

IDENTIFYING MOLECULAR TARGETS AND VALIDATING NOVEL THERAPIES FOR OVARIAN CANCER

Alejandro Villar-Prados

IDENTIFYING MOLECULAR TARGETS AND VALIDATING NOVEL THERAPIES FOR

OVARIAN CANCER

By

Alejandro Villar-Prados, B.S.

APPROVED:

Anil K. Sood, M.D.
Advisory Professor

Swathi Arur, Ph.D.

Russell R. Broaddus, M.D., Ph.D.

Jeffrey N. Myers, M.D., Ph.D.

Jason Roszik, Ph.D., MBA

APPROVED:

Dean, The University of Texas
MD Anderson Cancer Center UTHealth Graduate School of Biomedical Science

IDENTIFYING MOLECULAR TARGETS AND VALIDATING NOVEL THERAPIES FOR

OVARIAN CANCER

A

DISSERTATION

Presented to the Faculty of

The University of Texas

MD Anderson Cancer Center UTHealth

Graduate School of Biomedical Sciences

In Partial Fulfillment

of the Requirements

for the Degree of

DOCTOR OF PHILOSOPHY

By

Alejandro Villar-Prados, B.S.

Houston, Texas

May, 2018

DEDICATION

I would like to dedicate this work to all of my immediate family in Puerto Rico and my wonderful wife, Amanda. R. Haltom, Ph.D. The completion of this dissertation would have not been possible without your constant support and unconditional love. All of you have provided the foundation and stepping stones that have made me the person who I am today, which allowed me to keep moving forward and achieve my goals and dreams.

ACKNOWLEDGMENTS

First and foremost, I want to express my greatest gratitude to my Ph.D. mentor, Dr. Anil K. Sood, for extending your hand to me and taking the role of becoming my scientific mentor. During these past two and a half years, the training environment you have provided for me has nourished my scientific growth, sparked my curiosity and motivated me to become an exceptional physician scientist. The experience in your laboratory has shown me how the discoveries we make as a team can have a direct impact on cancer patient care. Your work ethic and constant support that you have shown to your trainees are qualities that I wish to incorporate and pass on to my future trainees. I would also like to thank all current and some past Sood laboratory members, for your guidance and allowing me to partake in various collaborative efforts.

Next, I want to thank and acknowledge my advisory committee members: Drs. Swathi Arur, Russell Broaddus, Jason Roszik and Jeffrey Myers. Your continuous input and support has been a pivotal factor for my progress and to proudly present my findings in this dissertation. I would specially want to thank Dr. Arur and Dr. Broaddus for your guidance during the completion of my entire Ph.D. studies. Your scientific rigor and your passion for aiding students in and outside the laboratory environment has been integral for my formative training and development as a scientist.

Next, I would like to acknowledge the leadership of the combined M.D./Ph.D. program between The University of Puerto Rico and The University of Texas MD Anderson Cancer for giving me the opportunity of being part of this wonderful program. In particular, I want thank Dr. Michelle Barton for her academic advice, tough love approach and bestowing confidence within myself. I want to also extend my appreciation to Dr. Elizabeth Travis as well as the leadership at the University of Puerto

iv

Rico Medical School for giving me the opportunity to complete the combined M.D./Ph.D. track. I would also like to thank the students and leadership at the UT Houston M.D./Ph.D. program for making me feel, since the very beginning of my Ph.D. training, as an integral part of the program despite coming from a different institution. I also would like to thank all of the wonderful people that work at the MD Anderson Cancer Center-UTHealth Graduate School of Biomedical Sciences for your support and guidance.

Last but not least, I would like to thank all of the wonderful people I have met at the Genetics and Epigenetics Graduate Program. Being part of this program has taught me the true meaning of collaborative science. I want to acknowledge the amazing faculty of this program for their passion of training students. I particularly want to thank Elisabeth Lindheim for your friendship, kind advice and for being the heart and soul of the Genetics and Epigenetics Graduate Program. In this program, I have made many invaluable colleagues, but more importantly, lifelong friends. It is also thanks to this program that I was able to meet my wife, Dr. Amanda R. Haltom. The impact this program has changed not only my perspective on science but also my personal life, which is something I will cherish for the rest of my days.

IDENTIFYING MOLECULAR TARGETS AND VALIDATING NOVEL THERAPIES FOR OVARIAN CANCER

Alejandro Villar-Prados, B.S.

Advisory Professor: Anil K. Sood, M.D.

Re-purposing of targeted therapies for additional tumor types is a promising avenue for expanding treatment options for cancer patients, however accurately predicting what re-purposed targeted therapy will be effective remains challenging. To address this need, we developed a Therapy Predicting Tool (TPT) that accurately predicts the beneficial therapeutic effect of clinically relevant targeted therapies and the downstream pathways they may impact in the cancer of interest. Using ovarian cancer as a model to biologically validate our tool, we determined that Bromodomain and Extra-Terminal motif inhibitors (BETis), which target proteins such as BRD4, held the greatest promise to produce therapeutic effects and impact relevant oncogenic gene targets, such as Notch3, in this disease. In our pre-clinical models, we demonstrated that BETis produce therapeutic effects and prolong survival. Furthermore, we discovered that BRD4 directly regulates Notch3 transcription and its downstream targets in ovarian cancer. Our findings provide a basis for further exploration and application of our tool to identify and re-purpose targeted therapies for specific tumor types.

TABLE OF CONTENTS

LIST OF ILUSTRATIONS

LIST OF TABLES

ABBREVIATIONS

FDA: Food and Drug Administration

PARP: poly (ADP-ribose) polymerase

PARPi: poly (ADP-ribose) polymerase inhibitors

BER: base excision repair

SSDB: single strand DNA breaks

XRCC1: X-ray cross-complementing gene 1

VEGF: vascular endothelial growth factor

TCGA: The Cancer Genome Atlas

GTEx: Genotype-Tissue Expression Project

GEO: Gene Expression Omnibus

CCLE: Cancer Cell Line Encyclopedia

CMAP: Connectivity Map

CTRP: Cancer Therapeutics Response Portal

TPT: Therapy Predicting Tool (TPT)

HGSOC: high grade serous ovarian cancer

STIC: serous tubal intraepithelial carcinoma

BETis: bromodomain and extra terminal domain inhibitors

BET: bromodomain and extra terminal domain

PTEF-b: positive transcription elongation factor b

BRD4: bromodomain containing protein 4

RPPA: reverse phase protein array

GS: γ-secretase proteolytic complex

NICD: Notch intracellular domain

GSi: γ-secretase inhibitors

EdU: 5-ethynyl-2′-deoxyuridine

IP: intra-peritoneal

IHC: immunohistochemistry

PCR: polymerase chain reaction

qRT-PCR: quantitative real time polymerase chain reaction

ChIP: chromatin immunoprecipitation

ChiP-PCR: chromatin immunoprecipitation polymerase chain reaction

CADASIL: autosomal dominant arteriopathy with subcortical infarcts and

leukoenchephalopathy

NICD3: Notch3 intracellular domain

miR: micro RNA

PDX: patient derived xenograph

CHAPTER I

INTRODUCTION:

RATIONAL RE-PURPOSING OF TARGETED CANCER THERAPIES

Targeted Therapies in Cancer

The innumerable advancements in understanding the complex molecular mechanisms that drive cancer initiation and progression in recent decades have paved the way for the development of targeted molecular therapies (1, 2). The success of targeted therapies rests on the principle of designing either small molecules or antibodies that inhibit a biological process preferentially altered in a specific cancer type (1, 2). By taking this approach, researchers and clinicians alike strive for precise treatment of specific cancers that improve patient outcomes while minimizing the cytotoxic effects that are inherent to standard chemotherapy treatments (1, 2). The potential of targeted therapies has gathered the attention of a multitude of pharmaceutical companies invest billions of dollars to further develop and test promising targeted therapies and make them accessible to cancer patients (3, 4).

The design of targeted cancer therapies is aimed at inhibiting key molecules involved in tumor intrinsic and/or extrinsic biologic processes that promote tumor growth and progression. An example of a targeted therapy that attacks tumor intrinsic cellular processes comes in the form of the recently U.S. Food and Drug Administration (FDA) approved poly ADP-ribose polymerase (PARP) inhibitor (PARPi), olaparib (5). PARP enzymes are involved in the repair of single strand DNA breaks (SSDB) and are part of the base excision repair (BER) machinery (6). When PARP enzymes detect a SSDB, they can bind directly to that region of DNA, begin adding ADP-ribose sugar chains onto itself, which serves to signal for the recruitment of DNA ligase III, DNA polymerase β and X-ray cross-complementing gene 1 (XRCC1) protein to fully repair the segment of DNA (6). Excitement over the use of PARPi came after the observation

that when PARPis are used in cells deficient in BRCA1 and 2 proteins, which are needed for homologous recombination (HR) to repair double strand DNA breaks, it produces synthetic lethality (7). In the context of cancer, loss of function of BRCA1 or 2 results in increased genomic instability, which is a hallmark of the disease (5, 6, 8). Indeed, patients who have germline mutations in either BRCA1 or 2 have a significantly higher risk of developing breast and ovarian cancers (9). However, treating BRCA1/2 deficient cells with PARPis, deprives them of alternative pathways for DNA repair, resulting in accumulating genotoxic stress and lead to cell death (5, 6). This understanding of the basic biology of DNA repair mechanisms prompted further investigation of PARPi in patients with germline BRCA1/2 mutations (10). In 2014, olaparib was FDA approved for the treatment of patients with ovarian cancer with germline mutations in BRCA1/2 (5, 9, 10).

As mentioned above, targeted therapies have also been developed to target the tumor micro-environment, the non-cancer cells and proteins that nourish the growth of cancer cells (8). The microenvironment of the tumor is comprised of fibroblasts, infiltrating immune cells, extracellular matrix, and new blood vessels (11). As with any other tissue in our body, solid tumors need a supply of oxygenated blood in order to grow and thrive (11). To achieve this, tumors promote the generation of new blood vessels, or angiogenesis, by secreting vascular endothelial growth factor (VEGF) (11). VEGF is a potent inducer of endothelial cell proliferation and migration, which is necessary for the formation of new blood vessels (12). By secreting VEGF, cancer cells recruit endothelial cells to the micro-environment, inducing the formation of new blood vessels (11). Researchers recognized this opportunity for targeted therapy and developed bevacizumab, an IgG antibody that directly binds and sequesters secreted VEGF. Bevacizumab quenches this effect by binding directly to VEGF, preventing it

from interacting with the vascular endothelial growth factor receptors 1 and 2 (VEGFR1/2) present in the surface of endothelial cells (11, 12). Preclinical studies demonstrated promising anti-tumor effects in various solid tumors, which has led to the use of bevacizumab in cancer patients, such as those with metastatic colorectal or ovarian cancer (9, 12).

Despite the promise of the targeted therapies described above, due to the natural genomic heterogeneity of cancer, most tumors evolve ways to acquire resistance to these therapies, resulting in only modest improvements in patient outcomes (2). Multiple reports have been published related to potential mechanisms by which ovarian cancer cells can acquire resistance to PARPi, including developing secondary mutations in *BRCA1* and *BRCA2* genes which can restore their function (5, 13, 14). In the case of bevacizumab, reports by our group have shown that resistance to bevacizumab in ovarian cancer can be achieved by both tumor intrinsic and extrinsic mechanisms (15, 16). In the wake of this challenge, various active areas of research have risen to mitigate this problem, such as understanding the molecular mechanisms of resistance to targeted therapies in order to overcome them and identifying novel biomarkers in order to develop new targeted therapies. Unfortunately, these approaches can be both time consuming and resource intensive (1, 2). Thus, a third area of research has emerged to maximize the use of already developed and clinically tested targeted therapies, or re-purposing targeted cancer therapies (17).

The re-purposing of targeted therapies has gain momentum in the past years because it is cost effective and allows for quick expansion of therapeutic options clinicians can have at their disposal to treat a cancer patients by diminishing the time needed for pre-clinical testing (1). A limitation of this approach resides in the ability to accurately predict which re-purposed targeted therapy will yield the best result in the

4

cancer of interest. Thus, researchers have turned to bioinformatics in order to systematically and accurately predict what re-purposed therapies will produce the best patient outcomes.

Role of Bioinformatics in Re-purposing Targeted Therapies and the Therapy Predicting Tool

Accurately determining which re-purposed therapy will have the greatest impact in the cancer of interest remains challenging, which researchers are trying to address using bioinformatics. The unprecedented advancements in next generation sequencing and array technologies have propelled a new era of bioinformatics. Thanks to this, researchers have been able to generate and centralize massive amounts of expression and gene mutation data on publicly available databases. Some of these databases include The Cancer Genome Atlas (TCGA), the Genotype-Tissue Expression project (GTEx) for assessing normal tissue gene expression, cBioPortal for cancer genomics, the Gene Expression Omnibus (GEO) as well as the Broad Institute's Cancer Cell Line Encyclopedia (CCLE), Connectivity Map (CMAP) and Cancer Therapeutics Response Portal (18-23). Researchers and bioinformaticians alike are working side by side to develop computational algorithms for mining these databases. The intent is to rationally identify, based on the mutational status of a tumor, the best therapeutic strategy to treat cancers and produce better outcomes (24). The aim of generating such methods is to quickly stratify patients according to their tumor genomic landscape, personalize their treatment regimen, reduce the amount of side effects by smarter treatment options and ultimately extend survival (17, 24). Furthermore, by employing strategies for the re-purposing of targeted therapies, clinicians can rapidly increase treatment options to

cancer patients and reducing the extended time and cost required for new drug development.

There are still a set of challenges related to the effective use of computational databases listed above. Each of these databases has an enormous breadth of information, but discriminating between biological relevance and artifacts can be difficult. This difficulty is enhanced when trying to create computational models that incorporate information from several databases. Another challenge is biological validation for these computational models (17). By nature, cancer is an extremely heterogeneous and complex disease; thus, even if a promising gene signature is identified that can lead to the use of a specific therapy, this does not mean that targeting the genes or pathways in the gene signature will produce a positive biological effect (17).

The limitations described above, of course, has not deterred researchers from developing computational algorithms that can accurately identify potential targeted therapies that can benefit patients with specific tumor types (24-27). In a recent study by San Lucas *et al.,* the group developed an *in silico* tool that uses TCGA, CMAP and CCLE data sets to identify and match cancer gene signatures with cell lines harboring similar alterations and test whether specific drug candidates are effective (25). The authors were able to provide some biological validation by using cancer cell lines, but did not perform any *in vivo* validation, nor did the group incorporate databases such as GTEx to compare expression differences between cancer and normal tissues. Incorporation of GTEx would allow for better accuracy for relevant gene targets because it provides baseline expression levels of that gene. In another recent publication by Jianting Sheng *et al.,* the author created a similar tool but it can also predict drug sensitivity signatures based on the genomic landscape of the cancer cells

6

of interest and identify candidate compounds (26). This approach, although promising, also lacked extensive biological validation to confirm the accuracy of the computational algorithm.

To build upon the concept of accurately and systematically identifying and re-purposing targeted cancer therapies that will have positive patient outcomes, we developed a novel Therapy Predicting Tool (TPT). The principal purpose of the TPT is to determine which currently available targeted therapies that are in phase I clinical trials can be re-purposed for other tumor types to improve patient outcomes (**Figure 1-1**). Our algorithm incorporates gene and protein expression data from various databases, such as TCGA and GTEx, to simultaneously detect genes that have high expression in various cancer types in comparison to their normal organ counterparts, the impact of this high expression on patient survival, and specific drugs in phase I development that are available to target those genes (**Figure 1-1**). Furthermore, the TPT identifies potential functional relationships using tumor mRNA sequencing and reverse phase protein array (RPPA) data by comparing expression of the target gene queried with that of other upregulated genes in the cancer types of interest. This expression data is further complemented by associating gene alterations of a specific cancer with those of normal tissues by using both copy number and protein expression data. The TPT thus allows easy and rational search for potential drug candidates for specific tumor types. Based on our tool's premise, we sought to validate the accuracy of our tool using ovarian cancer as tumor model and carry out extensive biological validation in both *in vitro* and *in vivo* pre-clinical models.
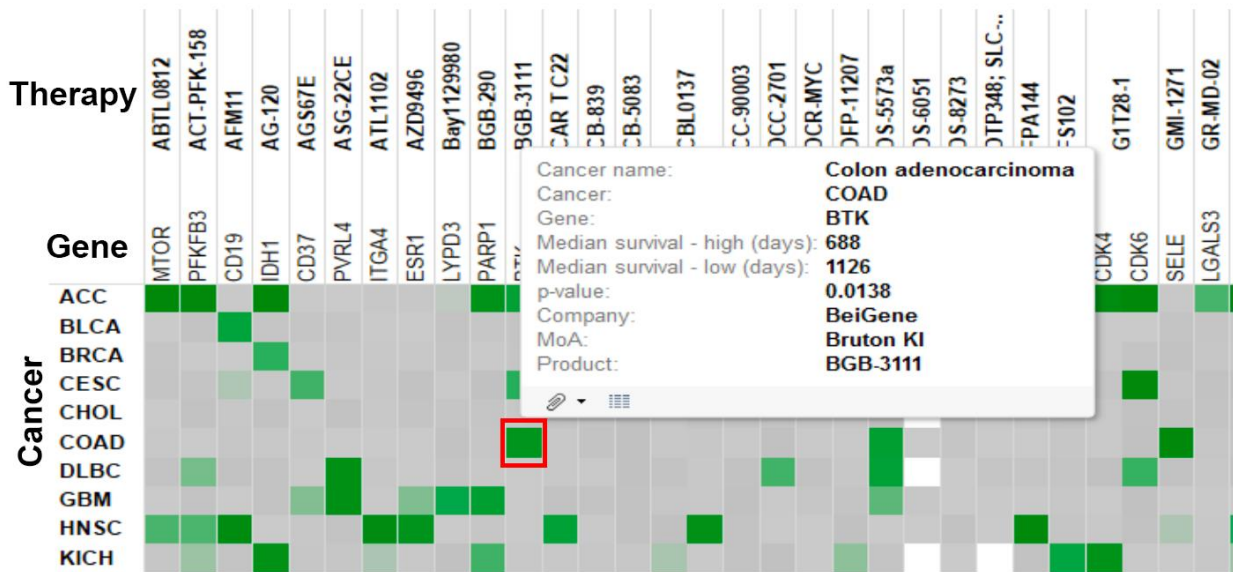
Figure -1-1. Therapy Predicting Tool correlation of targeted therapy pairing with altered gene expression in specific tumor types.

A screenshot example of one of the data outputs provided by the TPT. On the y-axis are a few cancer types matched to a variety of gene targets which have high expression in tumors, matched with currently available phase I clinical trial targeted therapy. Green squares represent a significant association between the expression of genes and its impact on patient survival and. The red square is a pop up window which provides specific information about the cancer chosen, the gene of interest, targeted therapy with mechanism of action and effect on overall survival by targeting that gene.

CHAPTER II

INTRODUCTION:

The Potential Role of Bromodomain and Extra-Terminal motif inhibitors and Notch3 Signaling in Ovarian Cancer

Ovarian Cancer

To proceed and begin validation of our TPT, we focused on ovarian cancer as a disease model. Ovarian cancer is the deadliest gynecologic disease in women today (9, 28). In the United States alone, there is an incidence of roughly 22,280 cases and 14,240 women are expected to die every year of the disease (28). Ovarian cancer serves as an umbrella term since there exists a plethora of subtypes within the disease due to the various cell types that make up the normal ovary (9, 29). These different cell types have different developmental origins (29). The germ cells are derived from endoderm that migrates to the gonadal ridge, giving rise to the future oocytes (29). Interstitial cells are responsible for the secretion of hormones such as estrogen and epithelial cells (29). Surface epithelial cells are derived from the Mullerian ducts and cover the surface of the ovary (29). Each of these cell types can give rise to distinct types of ovarian cancer, such as cancers of epithelial cell origin, germ cell derived tumors and stromal sex-chord tumors (29). The most prevalent of these tumors are the cancers of epithelial origin which are further divided into different subtypes, including high grade serous, low grade serous, clear cell carcinoma, endometrioid adenocarcinoma and mucinous carcinoma (9, 29). For the remainder of this work, including the analysis done by the TPT, when referring to ovarian cancer, I will be referring to epithelial subtypes. Each one of these epithelial derived cancers have distinct histopathological and molecular characteristics which dictate disease progression, treatment options and survival (9). From the epithelial subtypes, high grade serous ovarian cancer (HGSC) has the highest incidence in women (9). HGSC is characterized for displaying an elevated degree of genomic instability and is thought to

originate from the epithelial cells found in the fallopian epithelium of the uterine horn known as serous tubal intraepithelial carcinoma (STIC) (30, 31). Patients with HGSC are typically diagnosed at later stages of the disease and display dissemination of tumor nodules throughout the peritoneal cavity (29). Furthermore, despite initial positive response to chemotherapy agents in patients with HGSC, it has a high probability of recurrence (28).

For most of the ovarian cancer types described above, including HGSC, the main therapy modality is cytoreductive surgery (9). The goal of surgery is to remove as much tumor as possible, which correlates with better survival outcomes (9, 32). Following surgery, most patients receive adjuvant therapy with platinum and taxol based chemotherapy (9). As described above, despite the use of the modalities, patients with advanced HGSC have a recurrence rate (approximately 80%) (9). Faced with this reality, clinicians and basic researchers alike are exploring ways not only to maximize current treatment modalities of the disease but to also identify novel therapeutics. As described in Chapter I, one attractive avenue to expand treatment options for ovarian cancer patients is the incorporation of molecular targeted therapies such as bevacizumab and PARPi (9). The use of both of these therapies has shown to increase patient survival (9). However, much like many other tumor types and despite promising results, ovarian cancer inevitably develops resistance mechanisms to these targeted therapies (15, 16, 33). Thus, it has become imperative to investigate methodologies that can rapidly identify clinically ready therapies that can be re-purposed and quickly expand therapeutic options for ovarian cancer patients.

Identifying the Bromodomain and Extraterminal Domain protein BRD4 as a Therapeutic Avenue for Ovarian Cancer

To identify novel therapeutics for ovarian cancer patients, we turned to our TPT. Our analysis revealed that for ovarian cancer, our top candidate targeted therapies to be re-purposed were the epigenetic small molecule inhibitors known as bromodomain and extra terminal domain Inhibitors (BETis). BETis are a class of inhibitors which target the BET family of proteins, including BRDT (only expressed in testis), BRD2, BRD3 and BRD4 (34-36). BET proteins are widely regarded as epigenetic readers and act as molecular scaffolds that recruit various components of the gene transcription machinery (36). The BET proteins achieve this due to the presence of functional domains called bromodomains (36). These functional domains allow BET proteins to bind directly to acetylated histones, which are markers of transcriptionally active genes, at either gene promoters and/or enhancers regions (**Figure 2-1A**) (34, 36). BETs can recruit factors such as the mediator complex at enhancer sequences or positive transcription elongation factor b (PTEF-b) at gene promoters to facilitate the transcription of the target gene (35-39) (**Figure 2-1A**). It is also important to note that BET proteins can also be recruited to gene promoters independently of their binding to acetylated histones by directly interacting with other cell transcription factors, potentially independent of its bromodomains (38). BETis bind to the bromodomain of BET proteins and block the ability of BET proteins to interact with acetylated chromatin, resulting in a decrease in gene transcription (**Figure 2-1B**) (35).

Out of the BET proteins, one that has gathered much attention in the past 4 to 5 years is the bromodomain containing protein 4 (BRD4). BRD4 is over-expressed in a wide range of cancers and is known to be a key regulator of cell cycle progression by regulating expression of genes necessary for G_1/S phase and G_2/M phase transition (39-42). The prominent role of BRD4 in cancer growth and progression came after initial studies with the BETi JQ1 (35, 43, 44).
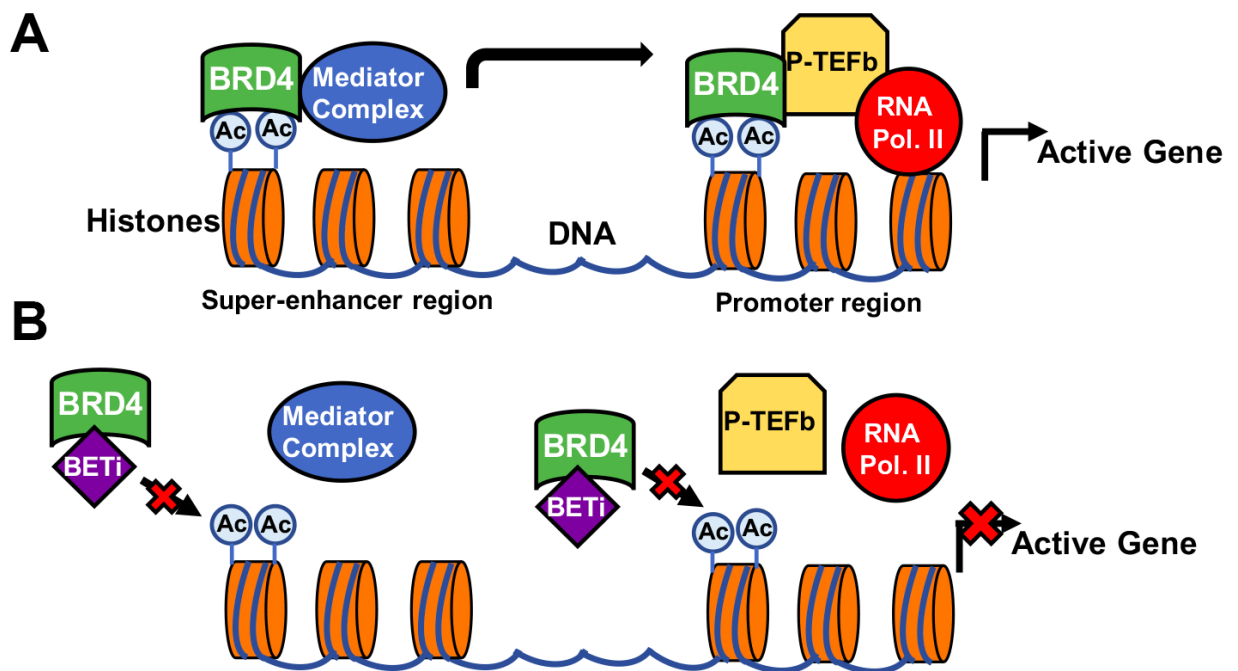
Figure 2-1. Mechanism of BRD4 (BET protein) mediated transcription and how BETis interfere with their function. (**A**) Recruitment of BRD4 to either gene super-enhancer or promoter regions by binding to acetylated chromatin. Upon binding, it can recruit protein complexes such as Mediator or P-TEGFb to promote RNA polymerase II (RNA Pol. II) activation. (**B**) Mechanism of action of BETis by which the inhibitors bind to the bromodomains of BRD4 and block its ability to interact with acetylated chromatin. Figure adapted from Panagis Filippakopoulos and Stefan Knapp, Nature Reviews: Drug Discovery, 2014 (35).

Using this drug, pioneer studies conducted by Filippakopoulos P. *et al.*, Delmore *et al.* and Mertz J.A. *et al.* observed that JQ1 was not only able to produce anti-growth effects in these models but it was also able to downregulate the oncogene *MYC* using multiple myeloma and acute myelogenous leukemia tumor models (43-45). These findings opened the avenue of using epigenetic targeted therapies to indirectly downregulate expression of key oncogenes which were proven difficult to directly target in the past (34). Following this initiative, various groups have identified additional gene targets downstream targets of BRD4 in various cancer and non-cancer models (46-53).

Another tumor model in which the inhibition of BRD4 using BETis has produced promising results is in midline NUT carcinoma (54, 55). This rare cancer is characterized by growth of malignant and undifferentiated squamous epithelial cells that invades midline structures (54). The molecular mechanism that gives rise to these tumors is due to the creation of fusion proteins that arise from chromosomal re-arrangements (54). The most commonly observed fusion is of the *NUT* gene with *BRD4* that results in constitutive expression of BRD4 in these cells (54). This overexpression of BRD4 pushes the cancer cells to persist in an undifferentiated state (54). Treatment of these tumors with BETis promotes the cancer cells to differentiate and inhibits their growing (54). Due to these observations described here and in leukemia models, the interest in further studying the roles of BRD4 and the use of BETis in cancer has grown exponentially (34). Furthermore, research is also pointing to the use BETis outside of cancer to treat diseases where acute and chronic inflammation is present (35). It is thanks to these research advancements that the multiple BETis are currently being tested in clinical trials (34).

In ovarian cancer, our TPT predicted that the use BETis would provide a beneficial survival effect in ovarian cancer patients. To further investigate the

14

oncogenic role of BRD4 in ovarian and externally validate our TPT predictions, we used the GTEx and TCGA databases (outside of the TPT) to confirm the expression of BRD4 compared to normal ovary tissue and how it correlates with patient survival (**Figure 2-2**). Our results show that BRD4 is over-expressed in ovarian cancer when compared to normal ovarian tissue using the GTEx database. Furthermore, TCGA analysis revealed that patients with higher tumor levels of BRD4 also have a worse survival rate (**Figure 2-2B,** $p < 0.02$). Taken together, these bioinformatics findings set the base for further explore the role of BRD4 and the therapeutic use of BETis in ovarian cancer patients.

Role of Notch3 Signaling in Ovarian Cancer

In our initial analysis, we observed that BRD4 overexpression strongly correlated with Notch3 upregulation in ovarian cancer (**Figure 2-3**). This observation was particularly interesting given the pro-tumorigenic effect of Notch3 over-expression in ovarian cancer (56-59). The Notch3 receptor belongs to the Notch family of transmembrane receptors and ligands (60). In mammals, there are a total of four Notch receptors and five transmembrane Notch ligands (61). Notch signaling activation follows an elegant sequence of downstream molecular events (**Figure 2-4**). Upon interaction with its ligand, the Notch receptors undergo a series of proteolytic cleavages by the γ-secretase complex (GS) located on the cell plasma membrane, resulting in the release of the Notch intracellular domain (NICD) (**Figure 2-4**) (61). The NICD is then translocated to the cell nucleus where it can form a complex with the DNA binding protein RBPJκ (61).
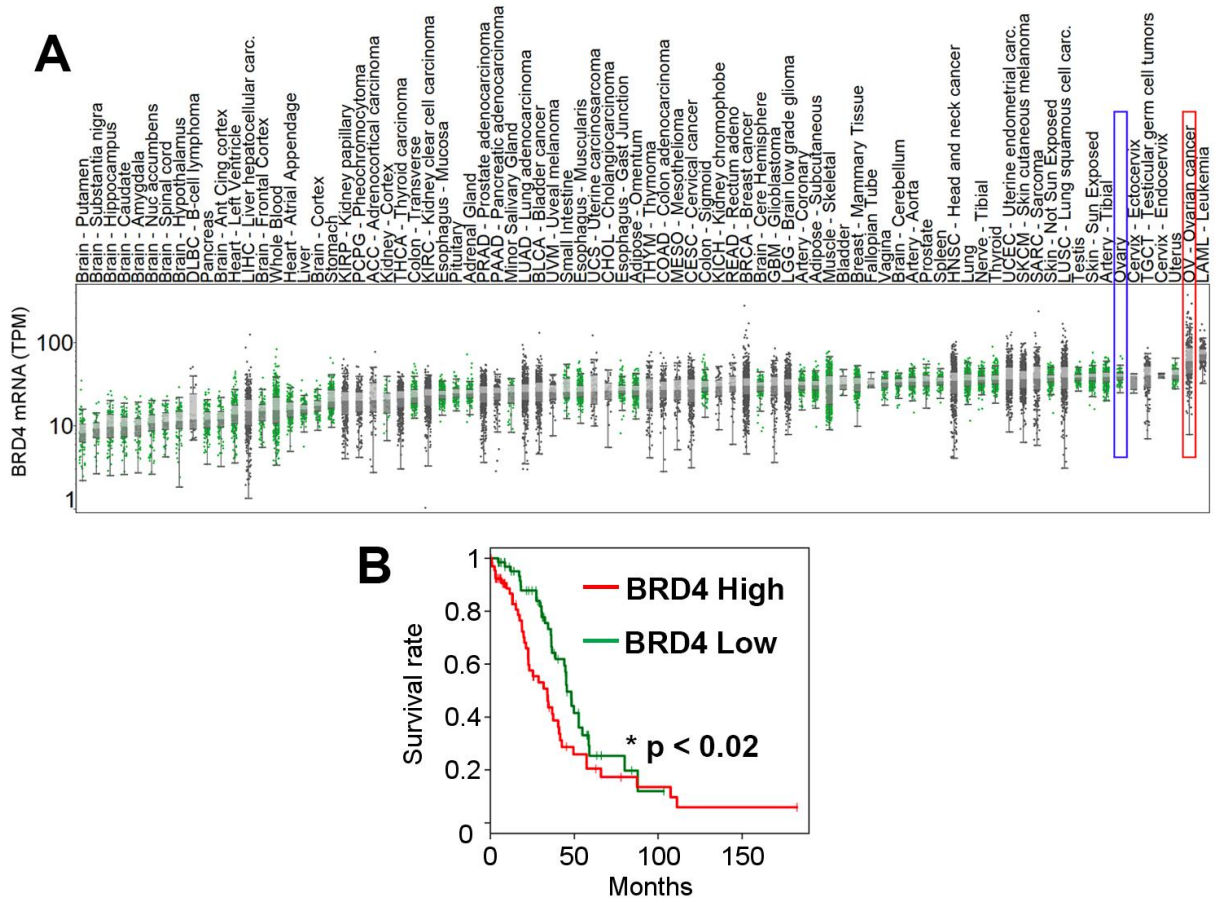
Figure 2-2. BRD4 is over-expressed in ovarian cancer and correlates with significantly worse patient survival. (A) GTEx results comparing expression of BRD4 mRNA as transcripts per million (TPM) in normal ovarian tissue (blue rectangle) compared to ovarian carcinoma (red rectangle). (B) Survival plot of ovarian cancer patients with high BRD4 mRNA expression (red line) versus low expression (blue line). Statistical analysis was done by running the log-rank test in the R "survival" package.
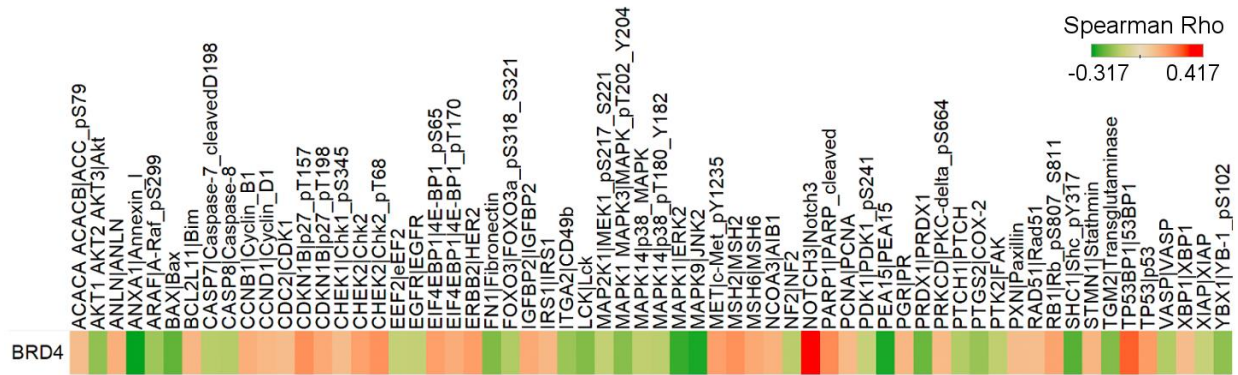
Figure 2-3. BRD4 expression highly correlates with Notch3 over-expression in ovarian cancer. Heat map comparison of BRD4 mRNA levels with the expression levels of proteins gathered from reverse phase protein array (RPPA) form molecular pathways that are frequently altered in ovarian cancer. A spearman Rho less than zero means the two genes have an inverse correlation (high BRD4 correlates with decreased expression of that gene), and a Spearman Rho of greater than zero indicates that BRD4 expression is positively correlated with the specific gene.
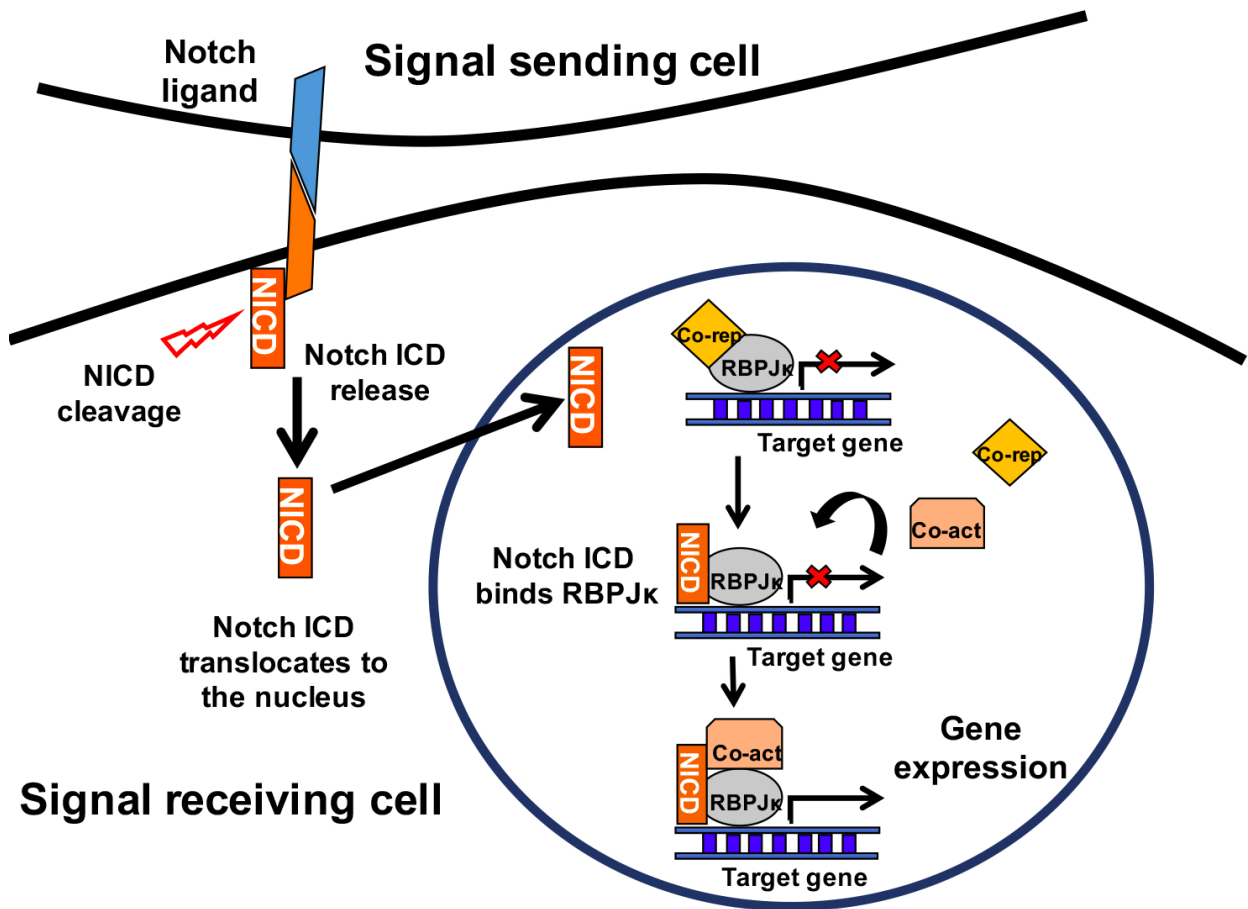
Figure 2-4. Molecular overview of Notch signaling. Interaction of the Notch ligand with the Notch receptor induces a series of proteolytic changes on the receptor that results in the release of the Notch intracellular domain (NICD). The NICD is then translocated to the cell nucleus. In the nucleus, it can directly bind to RBPJκ. RBPJκ is constitutively bound to genomic loci that correspond to Notch target genes where it is bound to transcriptional co-repressors (Co-rep). When the NICD binds to RBPJκ, the NICD displaces the Co-rep and recruits transcriptional co-activators (Co-act). This then allows for the active transcription of Notch downstream target genes. Figure adapted and modified from Kopan and Ilagan, Cell Reviews, 2009 (61)**.**

The NICD/RBPJκ complex recruits additional transcriptional co-activator proteins such as mastermind like-1 (MAM1), a histone acetyltransferase, inducing expression of target either at gene promoter or enhancer regions (60, 61). Common Notch signaling target genes include the Hes and Hey family of transcription factors, which in turn regulates the transcription of other genes (61). Interestingly, downstream targets of Notch signaling can be tissue and context dependent, which can result in the transcription of distinct downstream gene (60, 62, 63). This demonstrates how the singular activation of a Notch receptor, can have broad implications on the cells transcriptional network.

Notch3 signaling, as with all of the other Notch receptors, has been attributed to a plethora of biological processes both in normal development and in disease (60, 64, 65). In the context of development, Notch3 expression plays a significant role in the development of the mammalian arterial vascular system and in adults is mostly expression in arterial smooth muscle cells (66, 67). This is further evidenced by mouse genetic studies whereby Notch3 whole body knockout produces incomplete differentiation of arterial vessels (66). In the setting of disease, Notch3 over-expression have been implicated to play a role in the development of vascular pathologies such as pulmonary arterial hypertension, as well as cancers including ovarian cancer (57, 65, 68-73).

In ovarian cancer, Notch3 is commonly over-expressed, partly due to gene copy number amplification at its genomic locus in human chromosome 19 (57, 74). Notch3 over-expression in ovarian cancer is associated with increased chemo-resistance, recurrence in treated patients and with worse overall patient survival (57, 58, 74, 75). Strategies to directly target and downregulate Notch3 signaling in ovarian cancer

remain challenging. One avenue to inhibit Notch3 signaling is to inhibit γ-secretase, a class of inhibitors known as γ-secretase inhibitors (GSi) (76). GSis inhibit the γ-secretase protein complex, which is responsible of cleaving the Notch receptors upon activation (**Figure 2-4**) (60). This impedes the release of the NICD and its translocation to the nucleus (60, 76). In pre-clinical models, the use of GSis can sensitize Notch3-overexpressing cells to cisplatin (77). Despite these findings, the use γ-secretase inhibitors have not been effective in the clinic owing to their toxic side effects (76).

The TPT demonstrated that BRD4 over-expression highly correlates with Notch3 upregulation in ovarian cancer. Interestingly, both *BRD4* and *NOTCH3* are located on the short arm of chromosome 19, a locus that is frequently amplified in ovarian cancer (78). There is a similar genomic geographical relationship between the rest of the mammalian Notch receptors and the BET proteins: *BRD2* is adjacent to *NOTCH4* on chromosome 6, *BRDT* is adjacent to *NOTCH2* on chromosome 1 and *BRD3* is adjacent to *NOTCH1* chromosome 9 (41). This observation has led to the hypothesis of a functional relationship between these gene families (41). BRD4's ability to be a transcriptional activator and regulating the expression oncogenes such as *MYC* in other tumor models raises the possibility of utilizing BETis to inhibit Notch3 signaling in ovarian cancer (43). This is especially attractive from a clinical point of view because BETis are better tolerated by patients than GSis (34, 76). This provides further rationale to biologically validate our TPT and test the main hypothesis that the use BETis are a beneficial therapeutic avenue in ovarian cancer by targeting the Notch3 pathway.

CHAPTER III

MATERIALS AND METHODS AND RESULTS:

BIOLOGICAL VALIDATION OF THE TPT AND EXPLORING THE FUNCTIONAL RELATIONSHIP BETWEEN BRD4 AND NOTCH3 IN OVARIAN CANCER

MATERIALS AND METHODS:

Development of the Therapy Predicting Tool

To predict novel indications for targeted therapeutics, we applied an integrated visualization interface using publicly available TCGA and GTEx data. The tool contains the following main components: (i) Survival analysis from Kaplan-Meier was performed using log-rank p-values and median overall and progression-free survival times to compare sample sets with low and high protein expression in the tumor. The low and high groups are defined using the median expression level, or the lowest and highest quartiles. (ii) Tumor mRNA expression levels are analyzed using a heat map showing median-centered median expression levels. (iii) Association of targets with copy number gain or loss in the tumor is analyzed in a manner similar to that of mRNA expression. (iv) Normal-tissue expression levels, which can also help identify ideal cancer-specific targets, are examined using a heat map similar to that for tumor mRNA expression.

The TPT also includes large-scale correlation calculations (Spearman rank correlation coefficients) to provide information and insight on possible associations with protein expression and phosphorylation. Furthermore, using TCGA copy number and gene expression data, the TPT determines which copy number changes are associated with significant alterations in gene expressions.

Reagents and antibodies

For *in vitro* experiments, we used the BETi CPI203, purchased from Sigma-Aldrich (#SML1212), and the BETi CN210, kindly provided by ConverGene. The inhibitors were re-suspended in dimethyl sulfoxide (DMSO; #D2650; Sigma-Aldrich) to make a working stock of 10 mM. DMSO diluted at 1:1,000 was used as the vehicle

control for all *in vitro* experiments. For Western blots, we used the following antibodies: Notch3 (#D11B8; Cell Signaling Technology; 1:1,000), Hes1 (#D6P2U; Cell Signaling Technology; 1:700), BRD4 (#A700-004; Bethyl Laboratories; 1:5,000), and vinculin (#V9131; Sigma-Aldrich; 1:10,000). For IHC analysis of paraffin sections, the following antibodies were used: BRD4 (#A700-004; Bethyl Laboratories; 1:100), Notch3 (#ab23426; Abcam; 1:100), Ki67 (#RB-9043-P1; NeoMarkers, 1:200), and cleaved caspase-3 (#9661S; Cell Signaling Technology; 1:100). For doxycycline induction of shRNA *in vitro*, we treated cells with 100 ng/mL of doxycycline (#D9891; Sigma-Aldrich). For *in vivo* induction of BRD4 shRNA, mice harboring OVCAR 5 tumors were placed on a daily 200 mg/kg doxycycline-chow diet (#14727450; Fisher Scientific).

Cell lines and tissue culture

The human ovarian cell lines used in this study were obtained from the American Type Culture Collection (ATCC) and The University of Texas MD Anderson Cancer Center Characterized Cell Line Core Facility, except for OVCAR 432, which was kindly provided by Dr. Ronny Drapkin (Dana-Farber/Harvard Cancer Center). Cell lines' identities were validated via short tandem repeat DNA profiling carried out by the Characterized Cell Line Core Facility. Routine mycoplasma testing was carried out using the ATCC PCR Universal Mycoplasma Detection Kit (#30-1012K). The cell lines OVCAR 3, OVCAR 432, A2780, HeyA8, and OVCAR 8 were cultured in HyClone Roswell Park Memorial Institute 1640 medium (RPMI; #SH30027.01; GE Healthcare Life Sciences) media supplemented with 15% fetal bovine serum (FBS) (Sigma-Aldrich) and 0.2% gentamicin (#50146970, Fisher). OVCAR 4 cells were grown in RPMI supplemented with 10% FBS and 0.2% gentamicin (#50146970, Fisher). The generation and culture of OVCAR 4ip1 cells is described below. OVCAR 5 cells were

cultured in Dulbecco Modified Eagle Medium (DMEM; #10-013-CV; Corning) supplemented with 10% FBS and 0.2% gentamicin. All cells were grown in incubators kept at 37°C with 5% CO_2. For maintenance and passage of cultured cells, cells were washed twice with 1× HyClone phosphate-buffered saline (PBS; #SH30256.01; GE Healthcare Life Sciences) and trypsinized using 0.25% HyClone trypsin (#SH30042.01; GE Healthcare Life Sciences). Cells expressing doxycycline-inducible shRNA constructs were grown in complete media supplemented with Tet System Approved FBS (#631107; Takara) to avoid induction of BRD4 shRNA expression in culture.

Cell siRNA transfections

All siRNA sequences (**Table 3-1**) were purchased from Sigma-Aldrich. Cells were seeded in six-well plates at a density that yielded 50% confluency after 24 hours of plating (150,000 to 200,000 cells/well). The next day, about 2.6 μg (0.196 nmol) of siRNA sequences against BRD4 (Table S1) was mixed at a 1:3 ratio with Lipofectamine RNAiMAX (#13778500; Thermo Fisher Scientific) were prepared in serum-free media for 30 minutes. Then, the transfection complex was added to cells that had been washed twice with PBS and re-fed with serum-free media beforehand. Cells were incubated with the siRNA/RNAiMAX complex for 6 hours in a 37°C, 5% CO_2 tissue culture incubator and re-fed with complete media after the 6 hour incubation. Cells were then harvested for both qPCR and Western blot analysis to verify BRD4 knockdown.

For transfection in 96-well plates, cells were plated at a density of 7,000 to 10,000 cells per well in technical replicates of 10 wells per siRNA sequence used. The next day, cells were transfected with siRNA in serum-free media and incubated for 6

hours in the tissue culture incubator. Cells were then re-fed with complete media and subjected to MTT viability assays.

MTT viability assays

Specified cell lines were seeded in 96-well plates at an initial density of 3,000 cells per well in quadruplicate technical replicates. Once cells were attached, after 24 hours, culture media were removed and replaced with 150 μL of culture media with escalating concentrations of CPI203 or CN210 (0.01, 0.1, 0.5, 1.0, 5, and 10 μM). We used DMSO (1:1000 dilution) as a vehicle control. After 72 hours of cell growth in the tissue culture incubators, 50 μL of 1.5 mg/mL MTT (#J19265; Affymetrix) solution was added to each well of the 96-well plates and incubated for 2 hours in the tissue culture incubator. Then, media with MTT reagent were discarded, and 100 μL of DMSO was added to each well, completely re-suspending the MTT byproduct metabolized formazan. Plates were then analyzed using a plate spectrophotometer reader at an absorbance of 540 nm. To calculate cell viability percentage, the mean absorbance values for each treatment were normalized to DMSO vehicle–treated wells.

Colony formation assays

The indicated cell lines were plated in six-well plates in single-cell suspensions at a density of 1,000 cells per well and in technical triplicates. Twenty-four hours after seeding, cells were re-fed with fresh media containing either DMSO (1:1000 dilution) or the specified BETi (CPI203 or CN210) at 1 μM. Cells were left growing in a tissue culture incubator for 7 to 10 days. Afterward, the cells were washed three times with ice-cold PBS, fixed with ice-cold 100% methanol for 10 minutes. After 10 minutes, the methanol was discarded and cells were stained with crystal violet solution (Sigma-Aldrich; 0.5% crystal violet with 20% methanol in Milli-Q water [EMD Millipore]) for 30

minutes at room temperature with light agitation. Lastly, the crystal violet was discarded, and the cells were washed with de-ionized Milli-Q water three times and left to dry at room temperature overnight.

EdU incorporation assay and Annexin V staining

Cells were plated in technical duplicates per experiment in six-well plates at a density of 50,000 cells per well. The next day, cells were treated with the specified BETi or were transfected with siRNA. BETi-treated cells were harvested 72 hours after treatment. siRNA-transfected cells were harvested 96 hours after transfection. Harvested cells were then pulsed with EdU for 1.5 hours and processed using the Click-iT Plus EdU Alexa Fluor 488 Flow Cytometry Assay Kit (#C10632; Thermo Fisher) following the manufacturer's protocol. For Annexin V staining, we used the BD Biosciences FITC Annexin V Apoptosis Detection Kit I (#556547; BD Biosciences) and followed the manufacturer's protocol. For flow cytometry data collection and analysis, we used the Beckman Coulter Gallios Flow Cytometer.

RNA extraction and qPCR analysis

Cells that were either treated with a BETi or transfected with siRNA were washed with PBS and placed in TRIzol (Ambion TRIzol Reagent, #15596018; Thermo Fisher Scientific). For RNA extraction and purification, the Direct-zol column kit (#11-331; Genesee Scientific) was used following the manufacturer's protocol (including the DNase step). RNA was eluted with DNase- and RNase-free water, and the amount of RNA was quantified with the NanoDrop 2000 (Thermo Scientific). Any RNA that was not used immediately for reverse transcriptase reaction to create complementary DNA (cDNA) was stored at -80°C.

For cDNA synthesis, 1 μg of purified RNA was converted to cDNA using the Verso cDNA Synthesis Kit (#AB1453/B; Thermo Fisher Scientific) following the manufacturer's protocol. If not used immediately, newly synthesized cDNA was stored at –20°C. For qPCR analysis, we used Power SYBR Green PCR Master Mix (#4367659; Applied Biosystems) using the primers listed in Table S1 loaded in 96-well plates (#AB-1100; Thermo Scientific) and ran samples using the Applied Biosystems 7500 Real-Time PCR System. Data analysis was done using Applied Biosystems 7500 software version 2.3 to determine relative $\Delta\Delta$CT quantification (fold change = $2^{-\Delta\Delta CT}$) using *RPLP0* (also known as 36B4) as a housekeeping gene. See primer sequences in **Table 3-1.**

Western blot analysis

Cells treated with the indicated BETi or transfected with siRNA were harvested and lysed with radioimmunoprecipitation assay buffer (RIPA) (25 mM Tris [pH 7.5], 150 mM NaCl, 0.1% sodium dodecyl sulfate, 0.5% sodium deoxycholate, 1% Triton X) supplemented with, for each experiment, single-use phosphatase and protease inhibitors (#78442; Thermo Scientific). Protein concentrations for lysed samples were determined using the Micro BCA Protein Assay Kit (#23235; Thermo Fisher Scientific) following the manufacturer's protocol. For all Western blots, 30 μg of total cell lysate diluted with 2× Laemmli sample buffer (#1610737; Bio-Rad) was loaded in either 6% or 10% sodium dodecyl sulfate denaturing polyacrylamide gels. Protein was then transferred to a nitrocellulose membrane, blocked with 5% non-fat dry milk (#AB10109-01000; AmericanBio) in Tris-buffered saline (TBS)-T (0.1% Tween-20) for 1 hour at room temperature, and incubated with the indicated antibodies diluted in 5% milk in TBS-T overnight at 4°C with light agitation. The next day, the membrane was washed

three times with TBS-T for 10 minutes with light agitation. After the last wash, the membrane was incubated with species-specific secondary antibodies conjugated to horseradish peroxidase (#NA931V and #NA934V; GE Healthcare), diluted 1:2,500 in 5% milk in TBS-T, for 1 hour at room temperature with light agitation. The membrane was then washed three times in TBS-T and finally developed using Western Lightning Plus ECL (#NEL105001EA; Perkin Elmer) on x-ray film (#F-BX57; Phenix). For re-probing of Western blots, we stripped membranes with Restore PLUS Western Blot Stripping Buffer (#46430 Thermo Fisher Scientific), re-blocked them with 5% milk TBS-T, and incubated them with primary antibody.

Cloning of inducible shRNA constructs and lentiviral production

To generate and clone shBRD4 sequences into doxycycline-inducible lentiviral expression vectors, we first designed the sequences on the basis of validated shRNA sequences from the Sigma-Aldrich MISSION shRNA library **(Table 3-1).** Oligonucleotides (oligos) were cloned into a Tet-pLKO-puro lentiviral vector (plasmid #21915; Addgene) in accordance with Addgene's on-line protocol (https://www.addgene.org/tools/protocols/plko/). For oligo duplex annealing, 1 μL of each oligo (100 μM) was combined with 1 μL of 10× T4 ligase buffer (#B0202S; New England Biolabs [NEB]), 1 μL of T4 polynucleotide kinase (#M0201S; NEB), and 6 μL of water, and the reaction was incubated at 37°C for 30 minutes in a Master cycler (Eppendorf). Next, the temperature was increased to 95°C and decreased by 5°C every 1 minute until reaching 25°C. The oligo duplex was then ligated to the Tet-pLKO-puro vector cut previously with BshTI (#FD1464; Thermo Fisher Scientific) using 2 μL of the newly formed oligo duplex, 3 μL of gel-purified cut Tet-pLKO-puro vector, 1 μL of T7 ligase (#M0318S; NEB), 1 μL of 2× T7 ligase buffer, and 3 μL of nuclease-free

water. The ligation was incubated at 25°C for 1 hour. The ligation product was then transformed in NEB Stable Competent *Escherichia coli* (#C3040I) following the NEB protocol, plated on ampicillin plates, and grown at 30°C for 16 hours. Colonies were picked and grown in LB media (#12795027; Thermo Fisher Scientific) supplemented with ampicillin (#BP1760-5; Fisher BioReagents). Plasmid DNA was purified using the QIAGEN Plasmid Plus Midi Kit (#12945) following the manufacturer's protocol and sequenced in the MD Anderson Cancer Center Sequencing and Microarray Facility to confirm the presence of the BRD4 shRNA sequence using the sequencing primer 5′ GGCAGGGATATTCACCATTATCGTTTCAGA.

For lentiviral production, HEK 293T cells (grown in DMEM, 10% FBS, and 0.2% gentamicin) were transfected using Lipofectamine 2000 (#11668500; Thermo Fisher Scientific) with 10 µg of Tet-pLKO-puro plasmid containing either the shBRD4 sequence or the shControl non-targeting sequence (Table S1), along with 5 µg of psPAX2 (#12260; Addgene) and 2.5 µg of pMD2.G (#12259; Addgene) lentiviral helper plasmids. Supernatant containing newly generated virus was centrifuged to clear any cell debris and syringe-filtered using a 0.45-µm filter (#190-2545; Thermo Fisher Scientific). For infection of OVCAR 5 cells, cells were plated at 50% confluency in six-well plates, were incubated with 2 mL of newly produced virus along with polybrene at a 1:1,000 dilution (#sc-134220; Santa Cruz Biotechnology) for 24 hours, and were then re-fed using complete media. Lastly, cells were positively selected using puromycin (#A11138-03; Gibco). Surviving cells were expanded and used for subsequent *in vitro* and *in vivo* experiments.

For labeling cells with luciferase for IVIS imaging, cells were infected with the lentiviral vector pGreenFire1-CMV (#TR011PA-1; System Biosciences), which co-

expresses green fluorescent protein, using the protocol described above. Cells were then sorted at the MD Anderson Flow Cytometry and Cellular Imaging Core Facility for green fluorescent protein positivity and used for subsequent *in vivo* experiments.

Immunohistochemistry analysis of tumor nodules

Harvested tumor nodules were embedded in paraffin blocks and sectioned by the MD Anderson Research Histology, Pathology, and Imaging Core. Slides were de-paraffinized as follows. First, slides were placed in 60°C for 30 minutes. Next, we did one incubation in 100% xylene (#C8H10, Fisher Chemical) for 4 minutes followed by another xylene incubation for 3 minutes. Next were two incubations with 100% ethanol for 2 minutes, two incubations with 95% ethanol for 2 minutes, one incubation in 80% ethanol for 1 minute, and two final incubations in Milli-Q water for 5 minutes each. For antigen retrieval to stain for Notch3 and cleaved caspase-3, slides were placed in a vegetable steamer (Hamilton Beach) in sodium citrate (pH 6) buffer for 25 minutes. For antigen retrieval for staining with Ki67, we used Diva Decloaker (#DV2004MX; Biocare Medical) instead of sodium citrate. Endogenous tissue peroxidase activity was quenched with 3% hydrogen peroxide in 100% methanol for 12 minutes. Slides were then washed and blocked with 5% goat serum in PBS for 1 hour at room temperature and we added primary antibody diluted in 5% goat serum in PBS overnight at 4°C in a humidified chamber. BRD4, Notch3, and cleaved caspase-3 were diluted at 1:100, while Ki67 was diluted at 1:200. For Notch3, BRD4, and cleaved caspase-3, slides were washed three times with PBS for 5-minute intervals and then incubated with biotinylated anti-rabbit antibody (#GR602H; Biocare Medical) for 20 minutes at room temperature. Then, slides were washed three times with PBS for 5 minutes at room temperature and then incubated with a streptavidin horseradish peroxidase label

(#HP604H; Biocare Medical) for 20 minutes at room temperature and washed three times with PBS for 5 minutes at room temperature. For Ki67 IHC staining, we incubated slides with secondary anti-rabbit antibody conjugated to horseradish peroxidase (#111-036-047; Jackson ImmunoResearch) diluted in 5% goat serum in PBS at a 1:500 dilution for 1 hour at room temperature. After secondary antibody incubation, slides were again washed with PBS and then briefly washed with PBS containing Brij 35 (#858366; Sigma-Aldrich) and placed in DAB (#750118; Thermo Fisher Scientific). Upon color change, slides were rinsed in de-ionized Milli-Q water, counter-stained with hematoxylin (#GHS316; Sigma-Aldrich) for 15 seconds, rinsed in water again, and left to dry. When completely dry, slides were mounted with coverslips with permount (#sp15-100; Fisher Scientific). Slides were imaged using the Leica DM4000 B LED microscope. For quantification of cleaved caspase-3, Ki67, and BRD4 staining, five random high-power field photos were taken, and stained cells were counted manually using ImageJ software.

In vivo experiments

For all *in vivo* mouse experiments, female athymic (NCr-nude) mice were used, purchased from Taconic Biosciences. Mice were taken care of in accordance with the American Association for Assessment and Accreditation of Laboratory Animal Care and the U.S. Public Health Service policy on Humane Care and Use of Laboratory Animals. All studies and experiments carried out in this work were also supervised and approved by the MD Anderson Institutional Animal Care and Use Committee. All mice used were 10 to 15 weeks old at the time of tumor intraperitoneal injection cell injections. For OVCAR 5 cells, we injected 1×10^6 cells intraperitoneally per mouse. For OVCAR 4ip1 cells, we injected 2×10^6 cells per mouse. Tumor cells to be injected were first grown in

the indicated media in tissue culture incubators until reaching 70% confluency. The cells were then trypsinized, washed twice with PBS (to remove any residual trypsin) and finally re-suspended in ice-cold Hank's Balanced Salt Solution (#21-021-CV; Cellgrow). For determining the presence of tumors, mice were injected with 200 μL of 14.7 mg/mL luciferin (#LUCK-1G; Gold Bio) and imaged using the IVIS. Any non-tumor bearing mice were removed from the experiment. After injection and confirmation of tumor presence, mice were randomly assigned to the treatment groups described in main text. During the course of all *in vivo* experiments, the primary investigator was not blinded to the allocation of each treatment group, but at the time of tumor dissections, all investigators involved were blinded to group allocations to determine the outcome of the experiment.

For CPI203 experiments, 10 mice were initially calculated for each treatment group since this sample size gave an 80% power to detect a 50% decrease in tumor weights and nodules with a 95% confidence. Tumor cell take rates were not 100%, thus the final mouse number per group are specified in the figure legends of each experiment. Mice were treated daily with either 10 mg/kg CPI203 diluted in PBS or with PBS alone, injected intraperitoneally. After 21 days of treatment, mice were euthanized, and tumor nodule numbers and weights were recorded accordingly. Harvested nodules were then placed in 10% buffered formalin phosphate (#SF100-4; Fisher Scientific) for subsequent embedding in paraffin blocks for IHC staining. For tumor weights and nodule analysis, we tested for and excluded outliers using the ROUT analysis provided by Graph Pad Prism 7 software package to identify for multiple outliers present in each treatment group (Q = 1%). One outlier was removed from CPI203 treated OVCAR 5 tumor bearing mice (Fig. 3C and Fig. S3A).

For CN210 *in vivo* experiments, we re-suspended CN210 in 30% solution of Kolliphor (#42966-1KG; Sigma-Aldrich) diluted in water and adjusted with 1.05 equivalent of 0.1 N HCl for dosing. Sonication was done to completely dissolve all CN210. CN210 was delivered orally at 50, 100 or 200 mg/kg daily for 2 days to OVCAR 5 tumor-bearing mice, with n = 3 mice per group. Twenty-four hours after the final dose, mice were euthanized and tumors were harvested for Notch3 IHC staining.

For survival experiments, luciferase-labeled OVCAR 5 cells expressing either doxycycline-inducible shBRD4 or non-targeting shControl (described in supplementary material) were grown in DMEM, 10% Tet System approved FBS, and 0.2% gentamicin to 70% confluency and injected into the peritoneal cavities of mice. The mice were then imaged 7 days later using IVIS imaging and, upon confirmation of tumor establishment, were started on a 200 mg/kg doxycycline-chow diet. Mice were monitored daily, and once they became moribund owing to disease burden, they were euthanized and tumors were harvested for IHC staining.

Generation of OVCAR 4ip1 cells

OVCAR 4 parental cells were labeled with luciferase, as described above, and injected (2×10^6) into the peritoneal cavities of nude athymic mice. Three weeks after injection, tumor nodules were harvested, placed in sterile serum-free RPMI, and processed in the laboratory under sterile conditions. Briefly, tumor cells were dissociated using the gentle MACS dissociator (Miltenyi Biotec). Recovered tumor cells were then cultured in RPMI with 10% FBS and 0.2% gentamicin. Cells were then expanded and underwent short tandem repeat DNA fingerprinting analysis to confirm the identity of OVCAR 4 cells and underwent mycoplasma testing before their injection into mice

Liposome nanoparticle preparation and delivery in vivo

In vivo delivery of siBRD4 2 was achieved by incorporating the siRNA in a previously described DOPC liposomal particle delivery system (79). Briefly, DOPC and siRNA were combined at a ratio of 1:10 (siRNA to DOPC) in the presence of excess tertiary butanol. Tween-20 was then added to the mixture at a ratio of 1:10 (Tween-20 to DOPC/siRNA mixture). This combination was mixed in a vortexer, frozen in a bath of acetone and dry ice, lyophilized, and kept at $-20°C$ until needed for *in vivo* injections. For *in vivo* administration, the DOPC/siRNA mixture was hydrated in sterile PBS without calcium or magnesium at room temperature to a concentration of 25 μg/mL and injected in doses of 200 μL, for a total of 5 μg per OVCAR 5 tumor-bearing mouse, in the peritoneal cavities of mice twice a week. After three treatments, mice were euthanized, and tumor nodules were harvested for IHC staining.

ChIP and ChIP PCR

For ChIP experiments, cells were plated in 15-cm tissue culture dishes and grown until reaching 70% to 80% confluency. Then, the cells were harvested, and chromatin was isolated and sheared according to the protocol of the Active Motif ChIP-IT Express kit (#53008). For each ChIP reaction, 25 μg of isolated chromatin was used with 5 μg of BRD4 antibody (#A700-004; Bethyl Laboratories) or normal rabbit immunoglobulin G (IgG) (#2729S; Cell Signaling Technology) and incubated with ChIP-IT Protein G Magnetic Beads (Active Motif) overnight with light agitation at 4°C. The next day, the beads were washed, and chromatin was eluted. The eluted chromatin was processed according to the manufacturer's protocol to eliminate any chromosomal protein from genomic DNA and was used for ChIP PCR reactions. See primers used in

Table 3-1. For regular PCR reactions, we used the AccuPrime GC-Rich DNA Polymerase kit (#12337016; Thermo Fisher Scientific). The following thermocycler (Eppendorf vapo.protect Mastercycler) conditions were used: 94°C for 2 minutes of initial denaturing, then 36 cycles at 94°C for 30 seconds, 60°C for 30 seconds, and 72°C for 30 seconds. PCR products were then loaded in a 2% agarose gel made with 1× TBE buffer (1.0 M Tris, 0.9 M boric acid, and 0.01 M ethylenediaminetetraacetic acid; #15581-028; Invitrogen UltraPure) and run for 120 volts alongside a 100- to 3,000-bp DNA ladder (#DNAL-100BP; Phenix). The gel was stained with ethidium bromide and imaged under ultraviolet light. For qPCR reactions, isolated DNA was further purified using the Active Motif ChIP DNA Purification Kit (#58002), and qPCRs were run using SYBR Green reagent using the Applied Biosystems 7500 Real-Time PCR System. To calculate fold enrichment, the DNA amount of normal rabbit IgG was used as a normalizing value.

RPPA and NetWalker analysis

OVCAR 4 and OVCAR 5 cells were cultured in either DMSO or 1 μM CPI203 for 48 hours. Then, cells were harvested and lysed with radioimmunoprecipitation assay buffer (RIPA) supplemented with phosphatase and protease inhibitors and diluted to a concentration of 1.5 μg/μL, which was mixed with 4× sample buffer (40% glycerol, 8% sodium dodecyl sulfate, and 0.25 M Tris, pH 6.8) with no bromophenol blue, to which β-mercaptoethanol was added in a 1:10 ratio before use. Samples were prepared in biologic duplicates, and a total of 40 μL of samples was submitted to the MD Anderson RPPA Core Facility and run using a validated set of antibodies (80). Initial protein expression analysis provided by the core was done using the R statistical software package (http://cran.r-project.org). To create a *NOTCH3* gene signature in our ovarian

cancer samples and study changes in expression of those genes after CPI203 treatment, we used NetWalker analysis software (81). Changes in expression were determined by means of normalized log2 of DMSO-treated cells compared with CPI203-treated cells. The generation of the final network is described in the Results.

Statistical analysis

Statistical analyses of *in vitro* and *in vivo* experiments were done using GraphPad Prism 7. To determine whether differences between two groups were significant, we used a two-tailed Student *t*-test (equal variance) or one-way analysis of variance (ANOVA) for multiple group comparisons. For these analyses, a p value < 0.05 was considered significant. Results are presented as the mean ± standard deviation of the mean. To test for outliers in our *in vivo* experiments, we used ROUT analysis provided by Graph Pad Prism 7 software package to identify for multiple outliers present in each treatment group (Q = 1%). For survival curve comparison analysis, we used the Log-rank (Mantel-Cox) test. For TCGA analysis, Spearman's rank correlation test was performed using 309 to evaluate the correlation between expression levels of *BRD4* and other genes of specified in Fig. S1. The same test was applied to investigate the correlation between *BRD4* gene expression and copy number within 303 ovarian cancer patients. For these analysis, we chose a p value of 3×10^{-4} as the cutoff to evaluate significant correlations.

Construct	Sequences	
siRNAs	**Forward (5′-3′)**	**Reverse (5′-3′)**
siControl	GCGACAGCUGGGCUGAAUA[dT][dT]	UAUUCAGCCCAGCUGUCGC
siBRD4 1	CUGAUUACUAUAAGAUCAU	AUGAUCUUAUAGUAAUCAG
siBRD4 2	CUGGAAUGCUCAGGAAUGU	ACAUUCCUGAGCAUUCCAG
qPCR primers	**Forward (5′-3′)**	**Reverse (5′-3′)**
BRD4	AGTCCAGCTCCTCTGACAGC	GATGGTGCTTCTTCTGCTCC
NOTCH3	GCTCTGGAGCCAATGCCAAC	CAGTCTCGCCAGTACGGTCA
HES1	TCAACACGACACCGGATAAAC	GCCGCGAGCTATCTTTCTTCA
36B4	ATCAACGGGTACAAACAGAGTCCTG	AAGGCAGATGGATCAGCCAA-GAAG
ChIP PCR primers	**Reverse (5′-3′)**	**Reverse (5′-3′)**
NOTCH3	GAAGGAGGGAGGAGGGGA	TTGGGGGTTCTTGCACTC
MYC	CTTACAACACCCGAGCAAGGAC	GCTGCTGGTTTTCCA-CTACCC
NOTCH2	TGAGCCTTTGAAGCAGGAGGAG	CATCTTCTCGGTC-GCCTCCTC
shRNAs	**Top oligo (5′-3′)**	**Bottom oligo (5′-3′)**
shControll	CCGGCCTAAGGTTAA-GTCGCCCTCGCTC-GAGCGAGGGCG-ACTTAACCTTAGGTTTTTG	AATTCAAAAACC-TAAGGTTA-AGTCGCCCTCGCTCGA-GCGAGGGCG-ACTTAACCTTAGG
shBRD4	CCGGCCTGGAGATGACAT-AGTCTTACTCGAGTAAGA-CTATGTCATCTCCAGGTTTTTG	AATTCAAAAACCTGGAGA-TGACATAGTCTTACTCGA-GTAAGACTATGTCATCTCCAG-G

Table 3-1. siRNAs, qPCR primers, ChIP primers, and shRNA sequences used in this study.

RESULTS

TPT identifies BRD4 as a therapeutic avenue to target Notch3 in ovarian cancer

We first employed the TPT to identify promising, clinically relevant targeted therapies at the phase I clinical trial stage that can be re-purposed for ovarian cancer. Our analysis revealed BETis, which inhibit the bromodomain containing the protein BRD4 and have shown promise in other tumor models, as a top candidate (43, 82, 83). On the basis of these findings, we proceeded with an *in silico* validation of the TPT in which we explored the role of BRD4 in ovarian cancer. Independently probing gene expression data of TCGA and GTEx databases revealed that mRNA expression of BRD4 is highly upregulated in ovarian cancer compared with that in normal ovarian tissues (**Figure 2-2A**). In validation of this result, using patient data sets from the TCGA independent of the TPT, we found that in ovarian cancer, an increase in *BRD4* copy number strongly correlated with increased BRD4 mRNA expression (**Figure 3-1A**). TCGA analysis also revealed that increased BRD4 expression in ovarian cancer correlated with a significant decrease in survival (**Figure 2-2B,** $p < 0.02$). Taken together, these computational analyses results provided the initial justification to investigate the biologic impact of BRD4 inhibition in pre-clinical ovarian cancer models.

A critical feature of the TPT is that it correlates expression of a target gene with the expression of oncogenic proteins associated with the cancer of interest to reveal potential novel functional relationships. The anti-tumor effect of BETis has been attributed to downregulation of the expression of oncogenes such *MYC,* which cannot be directly targeted (43, 44).
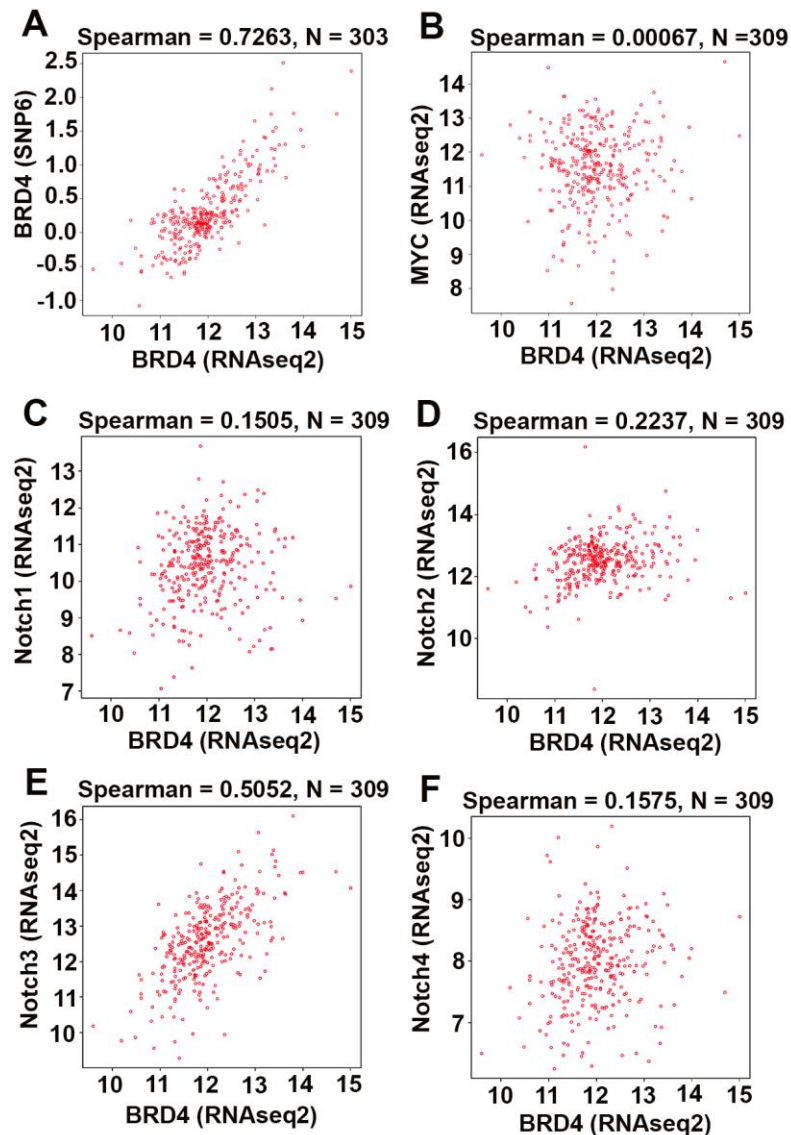
Figure 3-1. TCGA correlation analysis of BRD4 expression in ovarian cancer. (**A**) Correlation plot comparing BRD4 copy number alterations and mRNA gene expression in ovarian cancer. **** $p < 1 \times 10^{-10}$. (**B-F**) Correlation between BRD4 and MYC (**B**), NOTCH1 (**C**), NOTCH2 (**D**), NOTCH3 (**E**), and NOTCH4 (**F**) expression in ovarian cancer patient tumor samples. * $p < 0.0003$, **** $p < 1 \times 10^{-10}$. Spearman's rank correlation test was performed using 309 patient samples to evaluate the correlation between expression levels of BRD4 and other genes of specified. For these analysis, we chose a p value of 3×10^{-4} as the cutoff to evaluate significant correlations.

Thus, using our tool, we sought to identify novel downstream molecular targets that could be impacted by BRD4 inhibition in ovarian cancer. Comparing BRD4 mRNA levels with RPPA data on proteins in TPT, we determined that BRD4 levels strongly correlate with expression of Notch3 (**Figure 2-3**). Notch3 has been shown to be highly upregulated in ovarian cancer and correlates with increased proliferation, increased chemo-resistance, and decreased survival but has proven difficult to target directly (57-59, 84, 85). To investigate whether this correlation between BRD4 and Notch3 upregulation is exclusive to the Notch3 receptor, we probed the ovarian cancer TCGA data set. Our analysis revealed that there is indeed a high correlation between Notch3 and BRD4 expression in ovarian cancer (Spearman coefficient, 0.5052; $p < 2.2 \times 10^{-16}$) (**Figure 3-1E**), but increased *BRD4* expression did not significantly correlate with expression of *MYC* (Spearman coefficient, 0.00067; p = 0.906728)*, NOTCH1* (Spearman coefficient, 0.1505; p = 0.004644) and *NOTCH4* (Spearman coefficient, 0.1575; p = 0.003159) receptors (**Figure 3-1B, 1C and 1F**). We did observe a significant correlation between *BRD4* expression and the *NOTCH2* receptor (Spearman coefficient, 0.2237, $p = 7.58 \times 10^{-5}$) but the Spearman coefficient was not as high nor the p value was not as small when compared to *BRD4* and *NOTCH3* (Spearman coefficient, 0.5052; $p < 2.2 \times 10^{-16}$, **Figure 3-1E and 1D**)*.

BRD4 inhibition has a therapeutic effect in pre-clinical ovarian cancer models

Next, to biologically validate our *in silico* findings, we evaluated the therapeutic effect of BRD4 inhibition in ovarian cancer *in vitro.* BETis have proven effective in other tumor models, including multiple myeloma and NUT midline carcinoma, which propelled the use of BETis in clinical trials (34, 43, 86).
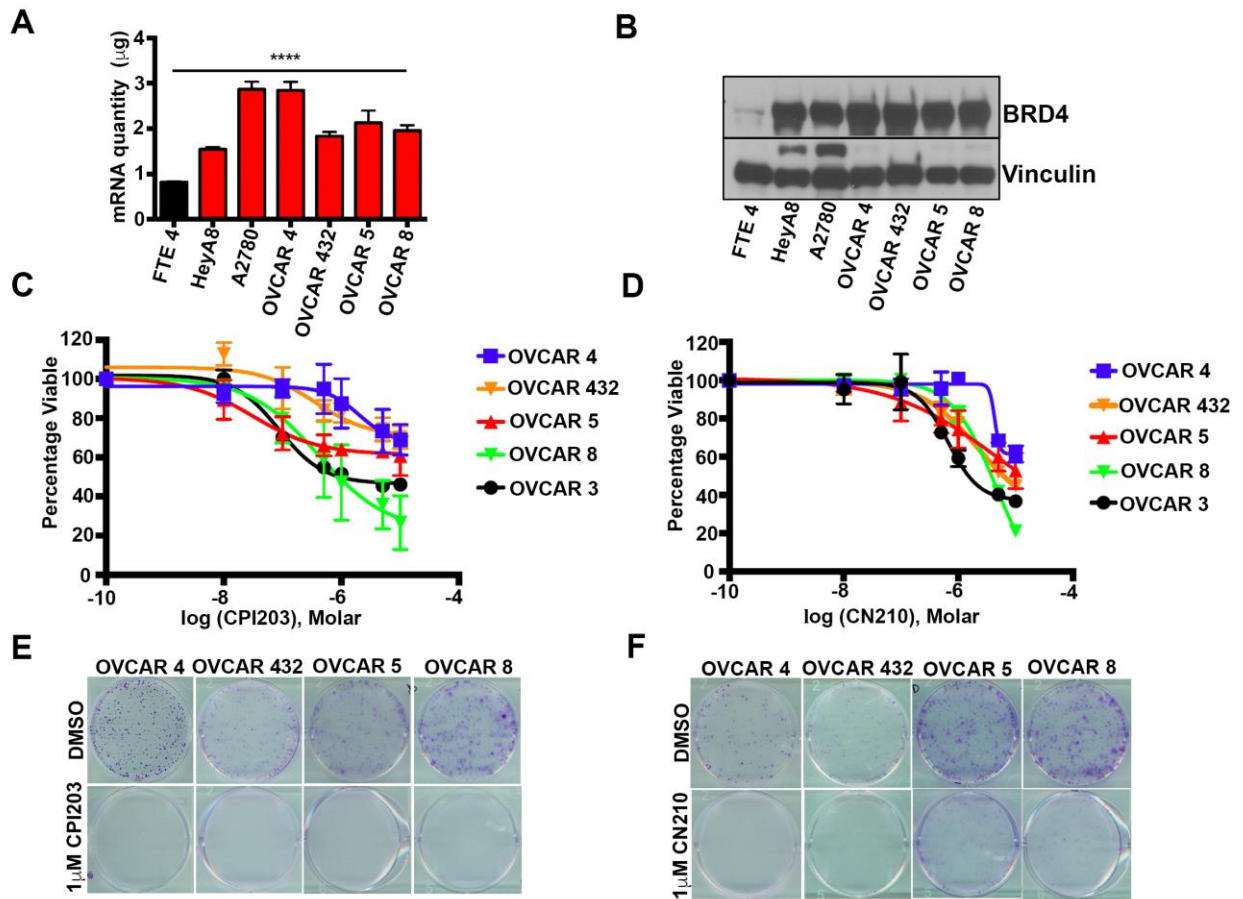
Figure 3-2. BETi treatments decreases cell viability in ovarian cancer cell lines. (**A**) Standard curve qRT-PCR analysis of relative BRD4 mRNA levels in ovarian cancer cell lines compared with human isolated primary fallopian tube epithelial cells (FTE 4). Experiment done in 2 independent biological duplicates, **** $p < 0.001$. One way ANOVA was used to test for significance. (**B**) BRD4 protein levels in ovarian cancer cells relative to those of FTE 4. Experiment done in 2 independent biological duplicates. (**C and D**) MTT viability assays of ovarian cancer cells treated for 72 hours with BETi CPI203 or CN210, respectively. Experiment done in 3 independent biological duplicates. (**E and F**) Colony formation assay of ovarian cancer cells treated for 10 days with BETi CPI203 or CN210, respectively. Experiment done in 3 independent biological duplicates.

We first tested BRD4 expression in a panel of well-established ovarian cancer cell lines. All ovarian cancer cell lines tested had substantially higher BRD4 mRNA and protein levels than did freshly isolated patient-derived primary fallopian tube epithelial (FTE4) cells (**Figure 3-2A and 2B**). FTE4 cells were used as a control given the growing evidence of fallopian tube epithelial cells being one etiological source for ovarian epithelial cancer (31, 87). The over-expression of BRD4 in ovarian cancer cells is also in accordance with our *in silico* results described in previous sections (**Figure 2-2A** and **Figure 3-1A**). Next, we tested cell viability using the clinically relevant BRD4 inhibitors CPI203 and CN210, a novel, un-characterized pan-BETi (88, 89). Like other BETis, such as JQ1, these inhibitors bind directly to the BRD4 bromodomains and block BRD4's ability to interact with acetylated chromatin (**Figure 2-1B**) (35). Both 3-(4,5-dimethylthiazol-2-yl)-2,5-diphenyltetrazolium bromide (MTT) and colony formation assays using either compound showed a significant decrease in cell viability and growth, in association with treatment (**Figure 3-2C, D, E and F**). To determine that these effects were due to BRD4 inhibition, and not due to off-target effects of the compounds, we used siRNA to reduce BRD4 levels and then carried out MTT assays (**Figures 3-3A and B**). There was again a significant decrease in cell viability in MTT assays upon BRD4 knockdown (**Figure 3-3B**).

We next aimed to identify the biologic mechanisms underlying this decrease in cell viability. Ovarian cancer cells treated with either BRD4 inhibitor, compared with those treated with vehicle, demonstrated a significant decrease in 5-ethynyl-2′-deoxyuridine (EdU) incorporation in most of the cell lines tested, suggesting a decrease in proliferation (**Figure 3-4A and B**).
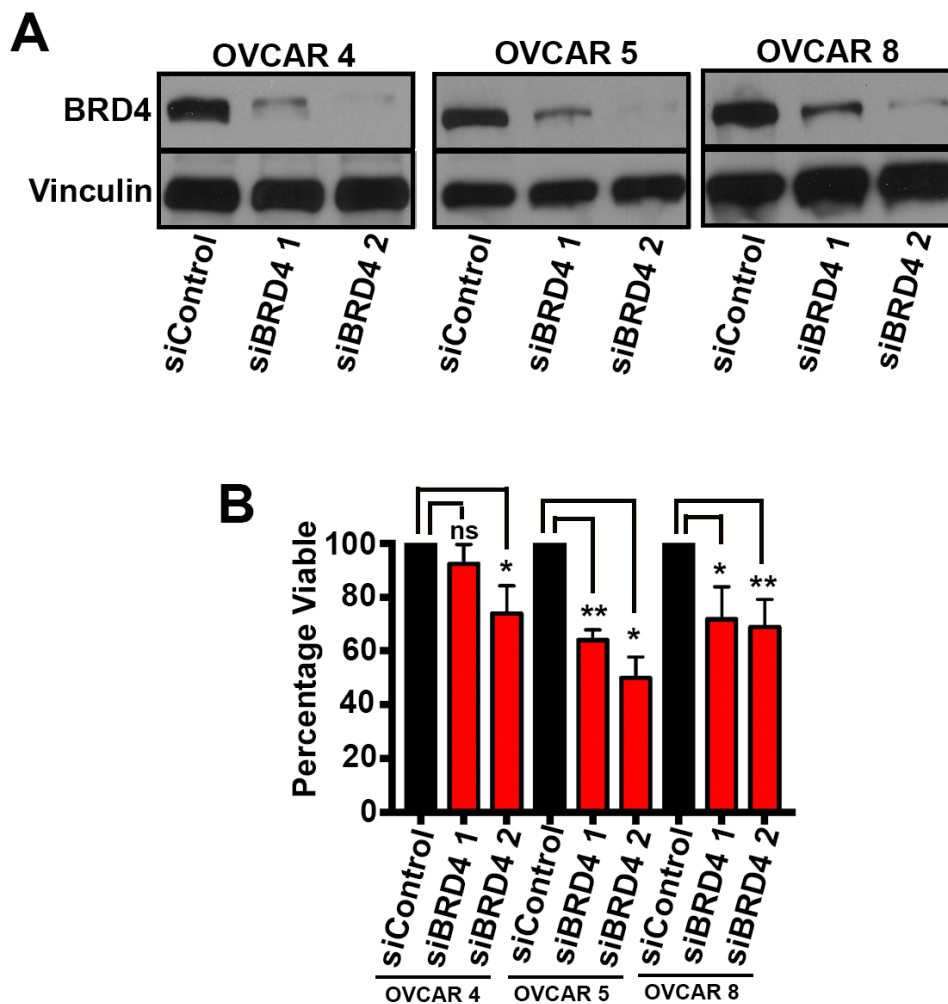
Figure 3-3. BRD4 knockdown reduces cell viability in ovarian cancer cell lines. (**A**) Confirmation of BRD4 protein knockdown in ovarian cancer cell lines 72 hours after siRNA transfection. Experiment conducted in 3 independent biological replicates (**B**) MTT viability assay of ovarian cancer cells transfected with BRD4 siRNA, 96 hours post transfections. Experiment conducted in 3 independent biological replicates.
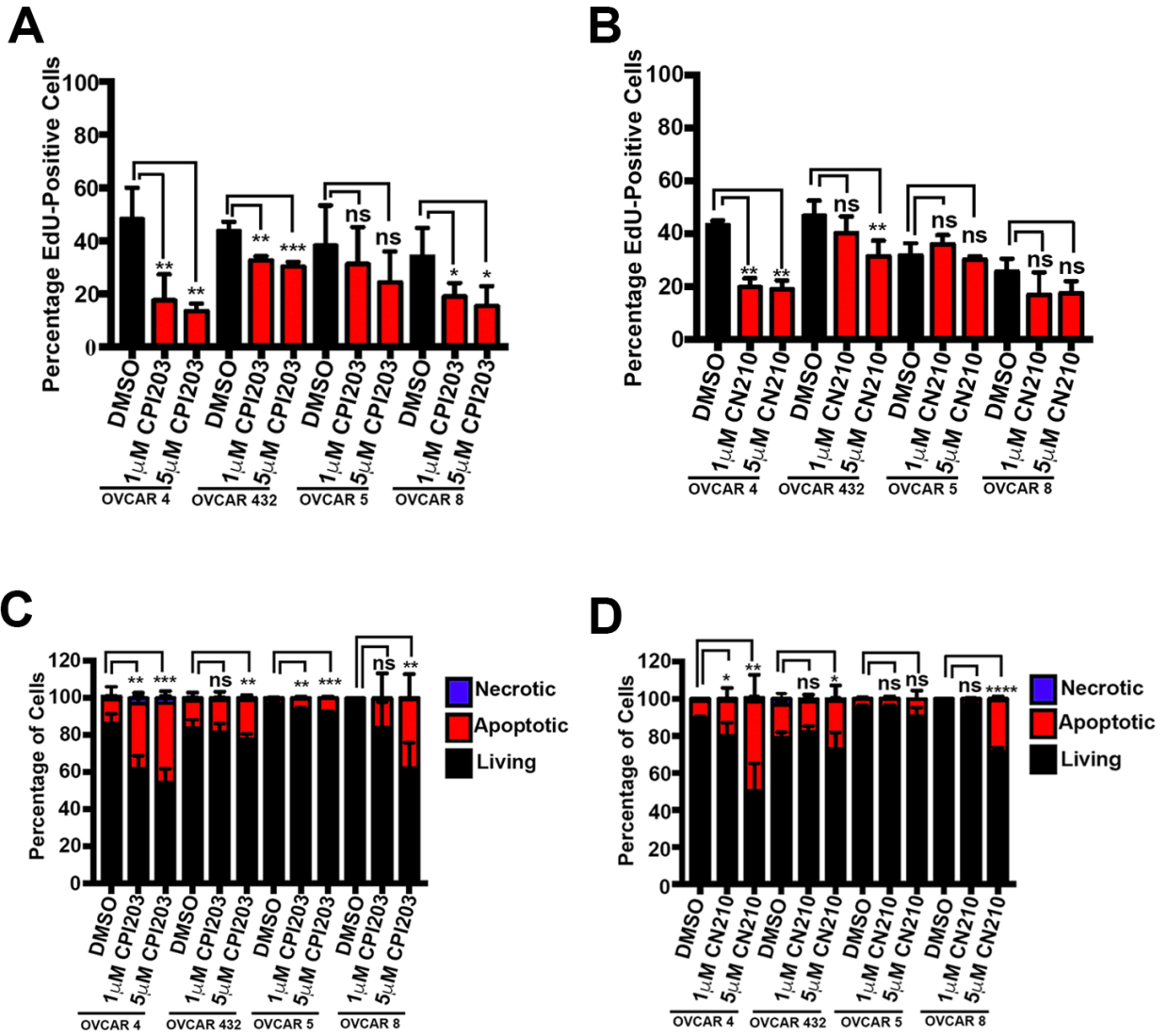
Figure 3-4. BETi treatment decreases cell proliferation and increases apoptosis in ovarian cancer cell lines. (**A** and **B**) EdU flow cytometry analysis of ovarian cancer cells treated with BETi CPI203 or CN210, respectively, for 72 hours. * $p < 0.05$, ** $p < 0.01$, *** $p < 0.001$, ns (non-significant). (**I** and **J**) Annexin V flow cytometry analysis of ovarian cancer cells treated with BETi CPI203 or CN210, respectively, for 72 hours. * $p < 0.05$, ** $p < 0.01$, *** $p < 0.001$, ns (non-significant). All experiment done in 3 independent biological duplicates. Statistical significance was determined by conducting unpaired Student t-test comparing vehicle control versus BETi treatments.
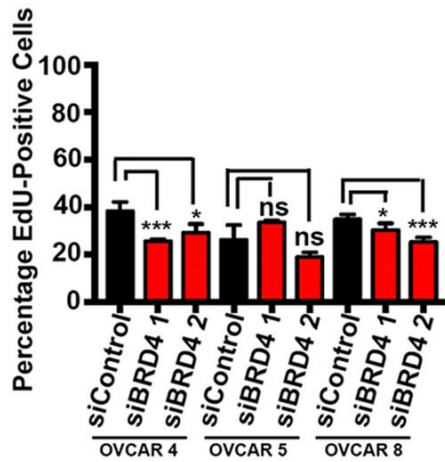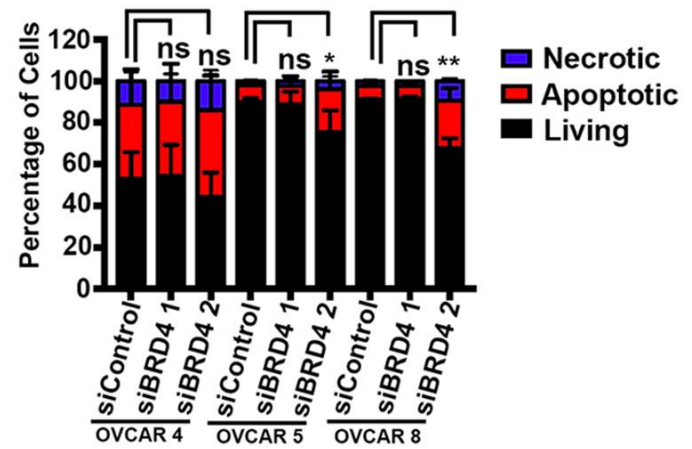
Figure 3-5. BRD4 knockdown decreases cell proliferation and increases apoptosis in ovarian cancer cell lines. (**A**) EdU incorporation 96 hours after BRD4 siRNA transfection, * p < 0.01. (**B**) Annexin V staining of ovarian cancer cells 96 hours after BRD4 siRNA transfection. * p < 0.05, ** p < 0.01. Statistical analysis was done by applying unpaired Student t-test for mean change in siControl group compared to either siBRD4 1 or siBRD4 2. All experiment conducted in 3 independent biological replicates.

Furthermore, we observed a significant increase in apoptosis upon treatment with either inhibitor (**Figure 3-4C and D**). We observed similar results upon siRNA knockdown of BRD4 (**Figure 3-5A and B**). These results show that BRD4 inhibition has a positive therapeutic effect in pre-clinical ovarian cancer models and provide a biologic basis for our TPT.

BRD4 inhibition decreases tumor growth and prolongs survival

On the basis of our *in vitro* results, we next aimed to investigate the anti-tumor and survival effects of BRD4 inhibition *in vivo.* We first asked whether targeting BRD4 using CPI203, which showed a more potent inhibitory effect than CN210 did *in vitro,* inhibits tumor growth in an OVCAR 5 orthotopic (intra-peritoneal) tumor model (90). Tumor-bearing mice were treated daily with 10 mg/kg CPI203 (injected intraperitoneally) for 21 days (**Figure 3-6A**). Compared with vehicle-treated mice, CPI203-treated mice had significantly decreased tumor weights ($p < 0.05$; **Figure 3-6B and 3C**) and non-significantly fewer tumor nodules ($p = 0.0596$; **Figure 3-7A**). To identify the biologic mechanism by which BRD4 inhibition decreased tumor growth in the OVCAR 5 tumor model, we performed immunohistochemical (IHC) staining on tumor sections with either the proliferative marker Ki67 or the apoptosis marker cleaved caspase-3. Tumors treated with CPI203 had a significant decrease in Ki67-positive cells compared with vehicle-treated controls (**Figure 3-6D and 3E**). No significant changes in cleaved Caspase-3 staining were observed between groups (**Figure 3-7B and C**).
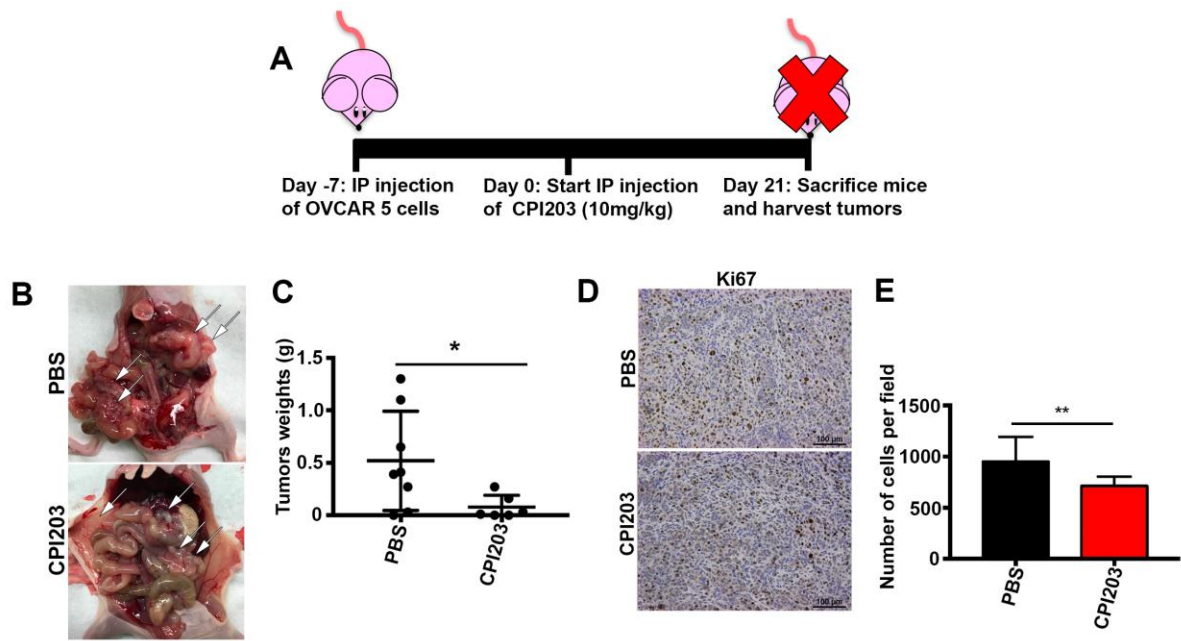
Figure 3-6. BETi CPI203 decelerates OVCAR 5 tumor growth by decreasing proliferation. (**A**) Schematic for CPI203 treatment in OVCAR 5 tumor-bearing mice. (**B**) Tumor nodules (white arrows) in CPI203- or PBS-treated mice. (**C**) Mean tumor weights in PBS (n = 8) and CPI203-treated mice (n = 6), * p < 0.05. Statistical significance was determined using Student t-test for mean difference in tumor weights. (**D**) IHC staining of OVCAR 5 tumors for Ki67. Scale bar, 100 μm. N = 4 per group. (**E**) Quantification of Ki67-positive cells from PBS- or CPI203-treated mice, n = 4 per group. Quantification was done using pictures of five random fields from OVCAR 5 tumors. Statistical significance was determined using Student t-test for mean difference in Ki67 positive cells.
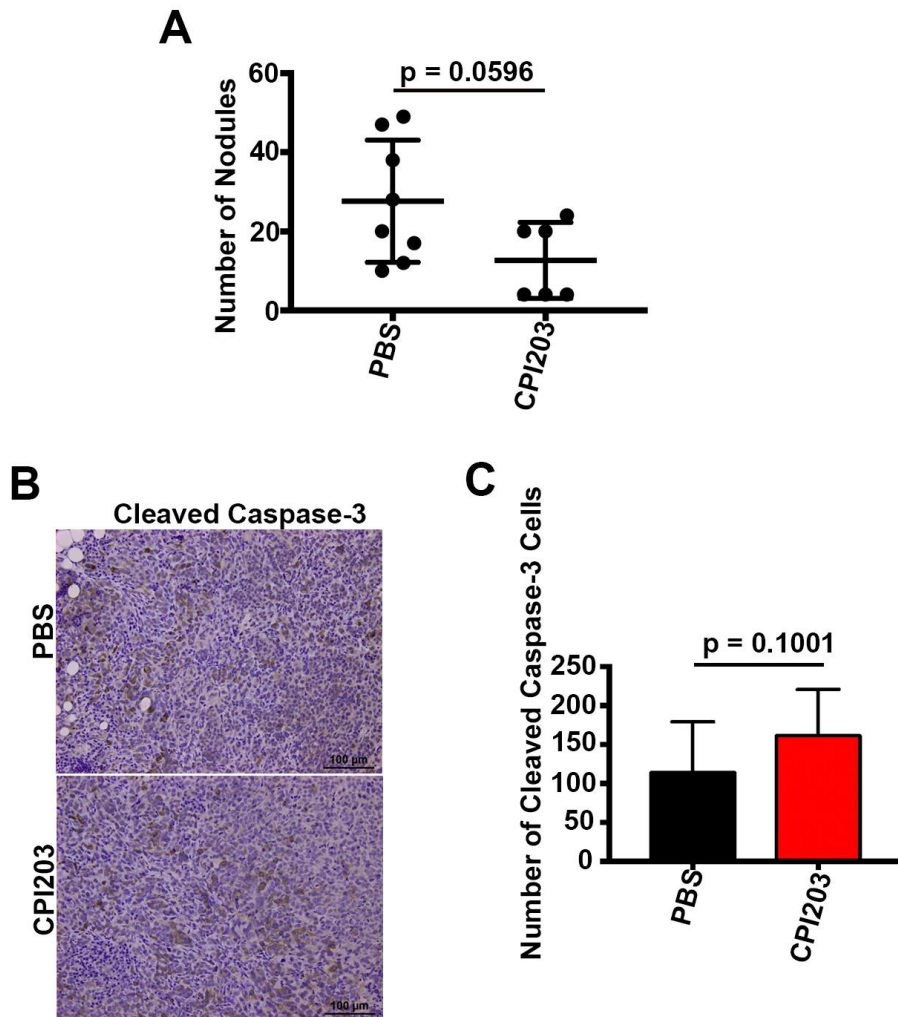
Figure 3-7. BETi treatment does not change number of tumor nodules or induce apoptosis in the OVCAR 5 tumor model. (**A**) Total nodule count of OVCAR 5 tumor-bearing mice treated with PBS vehicle control (n = 8) or CPI203 (n = 6). (**B**) IHC images of OVCAR 5 tumors harvested from mice and stained with cleaved caspase-3 (n = 5). Scale, 100 μm. (**C**) Quantification of cleaved caspase–positive cells from either PBS- or CPI203-treated mice (n = 5). Five random high-power fields from stained tumors were used for quantification. Statistical analysis was done by applying unpaired Student t-test for mean number of tumor nodules and mean number of positive cleaved Caspase 3 tumor cells.

To determine if these observations were unique to OVCAR 5 tumors, we conducted the same experiment using a newly generated second ovarian cancer tumor model, OVCAR 4ip1. Upon treatment with CPI203, we observed a significant decrease in both tumor weights (**Figure 3-8A and B**, $p < 0.05$) as well as the number of tumor nodules (**Figure 3-8C**, $p < 0.05$) in mice treated with CPI203 when compared to PBS treated controls. Furthermore, CPI203 treated mice demonstrated a significant increase in cleave Caspase-3 IHC staining (**Figure 3-9A and B**, $p < 0.001$) and a significant decrease in IHC Ki67 staining (**Figure 3-9C and D**, $p < 0.05$). These results indicate that decreased proliferation was the cause of decreased tumor growth in both OVCAR 5 and OVCAR4ip1 models as well as an increase in apoptosis in OVCAR 4ip1 model alone, which are also consistent with our *in vitro* findings described above.

Next, we examined whether long-term BRD4 downregulation resulted in increased survival, as predicted by the TPT. To do so, we generated a doxycycline-inducible shRNA system for luciferase-labeled OVCAR 5 cells, validated its function *in vitro,* and injected the cells into nude mice (**Figure 3-10A and B**). Upon tumor establishment, the mice were given a daily diet containing 200 mg/kg doxycycline to induce BRD4 shRNA expression in tumor cells and were killed when moribund (**Figure 3-11A**) (91). Luciferase (IVIS) imaging revealed that induction of shBRD4 decreased growth of tumors compared with induction of control shRNA, which is consistant with BETi treatment (**Figure 3-11B**). To confirm that BRD4 was indeed being downregulated in the OVCAR 5 tumors, we performed IHC. We observed that mice in which we induced BRD4 shRNA, had a significant decrease in BRD4 expression when compared to shBRD4 mice never exposed to doxycycline or mice expressing the non-targeting shRNA control sequence (**Figure 3-12A and B**).
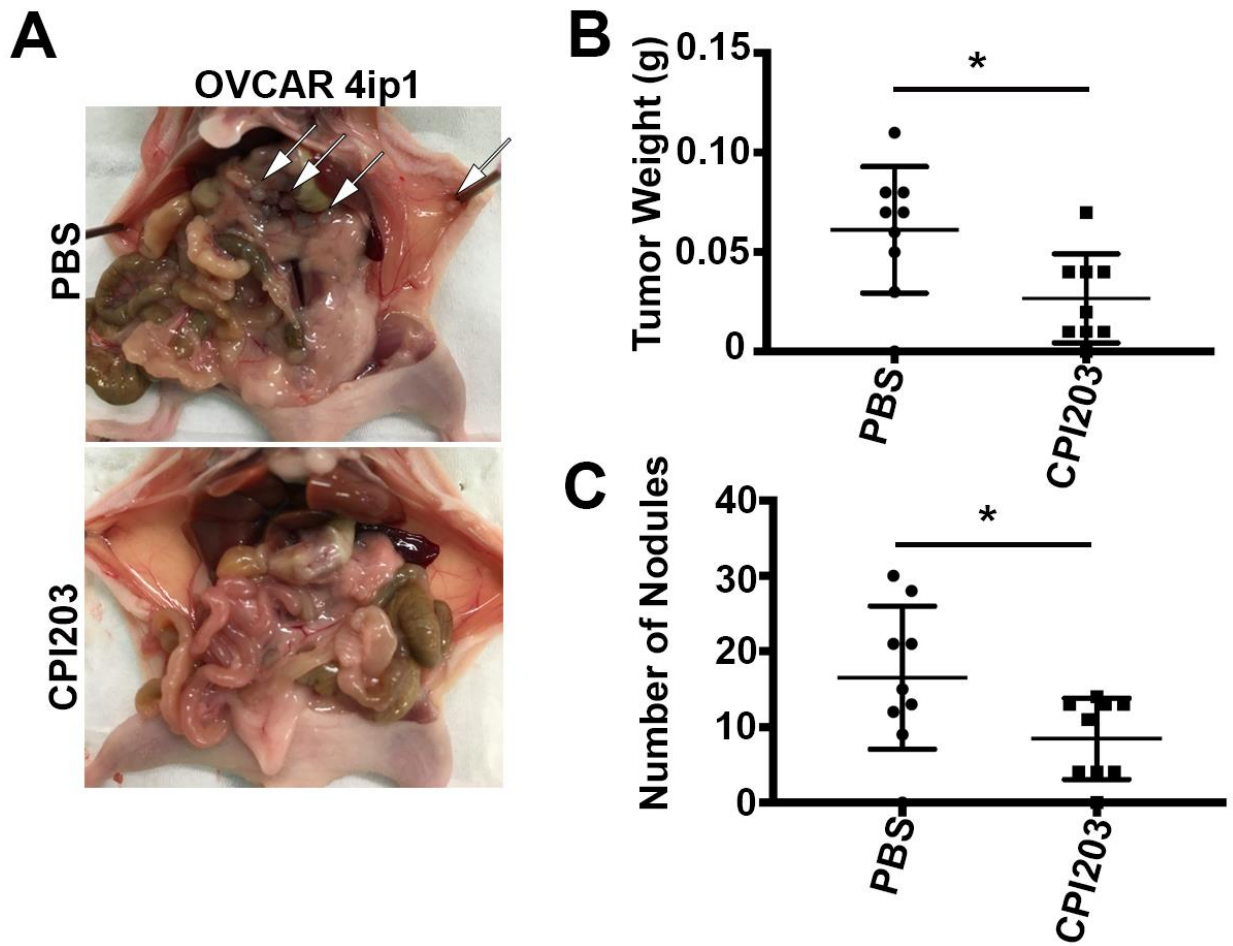
Figure 3-8. BETi treatment decreases tumor burden in OVCAR 4ip1 tumor-bearing mice. **(A)** Tumor nodules in PBS vehicle control–treated mice (white arrows) compared with CPI203-treated mice. (**B**) Quantification of total tumor weight per mouse in each group, n = 8 per group, * p = 0.0172. Statistical analysis was done by applying unpaired Student t-test comparing mean tumor weights between groups. (**C**) Quantification of total tumor nodule counts per dissected mouse. n = 8 per group, * p = 0.0400. Statistical analysis was done by applying unpaired Student t-test comparing mean tumor nodule counts between groups.
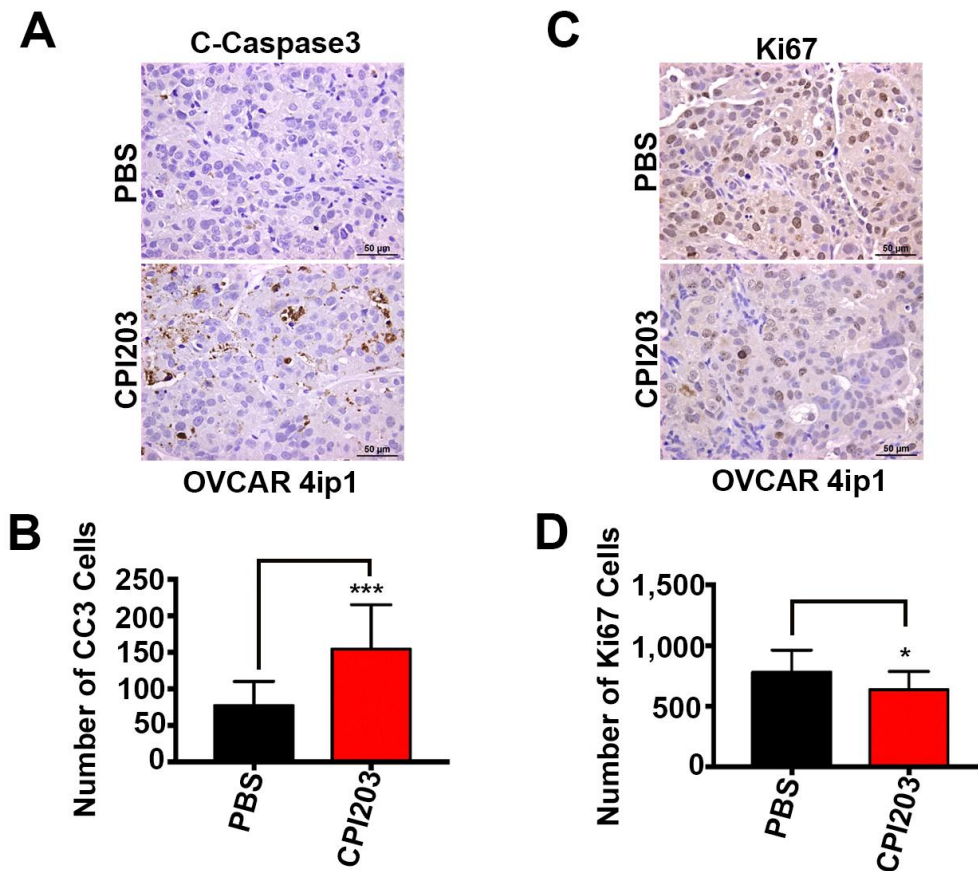
Figure 3-9. BETi treatment decreases proliferation and increases apoptosis in OVCAR 4ip1 tumor-bearing mice. (**A**) IHC staining of tumor nodules with cleaved Caspase-3 (CC3) antibody. Scale bar, 50μm (n = 5 per group). (**B**) Quantification of CC3 IHC images. Five random high-power fields from stained tumors were used for quantification. *** $p < 0.001$, statistical analysis was done by applying unpaired Student t-test comparing mean number of cleaved Caspase3 positive cells between groups (n =5 per group). (**C**) IHC staining of tumor nodules with Ki67 antibody. Scale bar, 50μm. (**D**) Quantification of Ki67 IHC images. Five random high-power fields from stained tumors were used for quantification (n = 5 per group). * $p < 0.05$. Statistical analysis was done by applying unpaired Student t-test comparing mean number of Ki67 positive cells per group.

Strikingly, mice with BRD4 knockdown had 50% increase in survival rate compared with controls (**Figure 3-12C**; p < 0.001). These results are consistent with our *in vitro* assays described above and provide further biologic support of the prediction given by our algorithm.

BRD4 inhibition decreases Notch3 expression in ovarian cancer

We next tested whether there is a functional relationship between BRD4 and Notch3 in ovarian cancer, as predicted by the TPT. Given not only the TPT prediction but also BRD4's known role as a transcriptional regulator, we hypothesized that BRD4 can directly regulate Notch3 expression in ovarian cancer (39, 40, 92). Treatment of various ovarian cancer cell lines with BETi CPI203 or BETi CN210 produced a decrease in Notch3 protein levels and mRNA levels (**Figure 3-13**). Notch3 protein and mRNA levels were also decreased upon BRD4 knockdown using two different siRNA sequences (**Figure 3-14**).

Next, we tested whether BRD4 knockdown downregulates Notch3 protein expression *in vivo* using our OVCAR 5 tumor model. Treating tumor-bearing mice with CN210 at 100 mg/kg resulted in decreased Notch3 staining on IHC analysis (**Figure 3-15**). To further validate these results, we used a previously described dioleoylphosphatidylcholine (DOPC) liposomal particle delivery system to deliver BRD4 siRNA in OVCAR 5 tumors (79, 93). Tumor-bearing mice were injected intraperitoneally with DOPC particles containing siBRD4 on days 1, 4 and 7 for a total of 3 treatments every 3 days
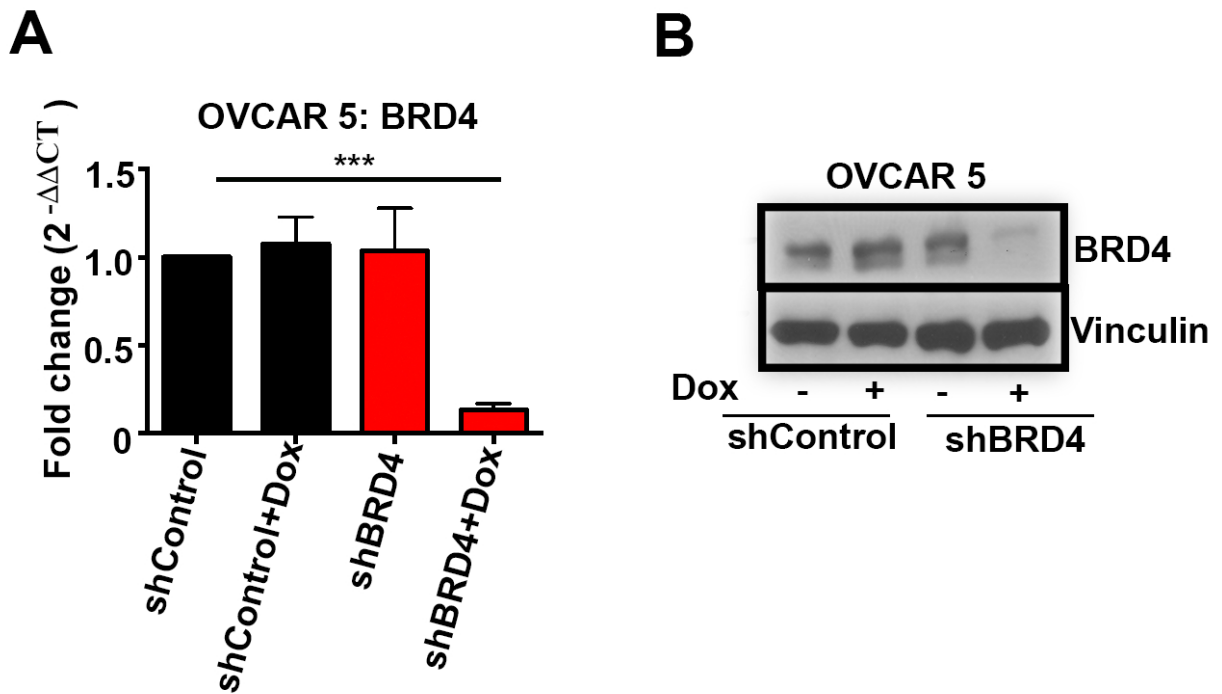
Figure 3-10. In vitro validation of doxycycline-inducible BRD4 shRNA system. (**A**) qPCR 48 hours after adding doxycycline to OVCAR 5 cells. Experiment conducted in 3 independent biological replicates. *** $p < 0.001$. Statistical analysis was done by applying one-way analysis of variance (ANOVA). (**B**) Verifying BRD4 expression 48 hours after exposure to doxycycline. Experiment done in 2 independent biological replicates.
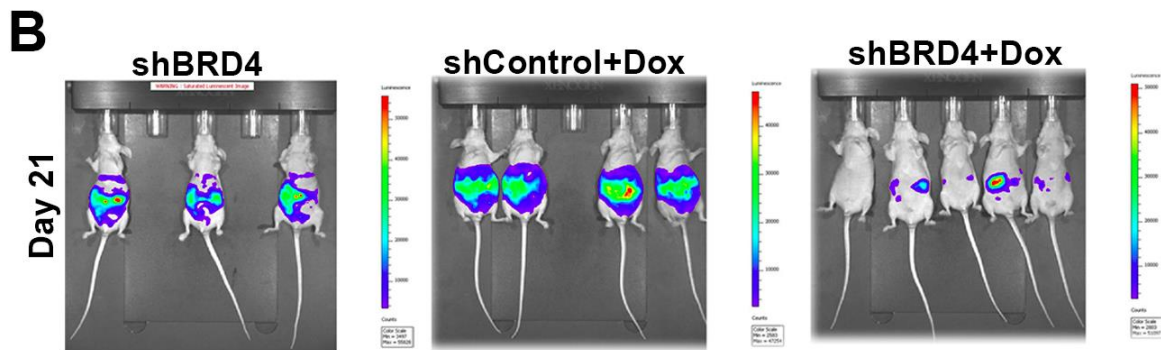
Figure 3-11. BRD4 knockdown reduces tumor growth in vivo. (**A**) Timeline for doxycycline-inducible shBRD4 survival experiment. (**B**) IVIS imaging of OVCAR 5 tumor-bearing mice 21 days after shRNA induction.
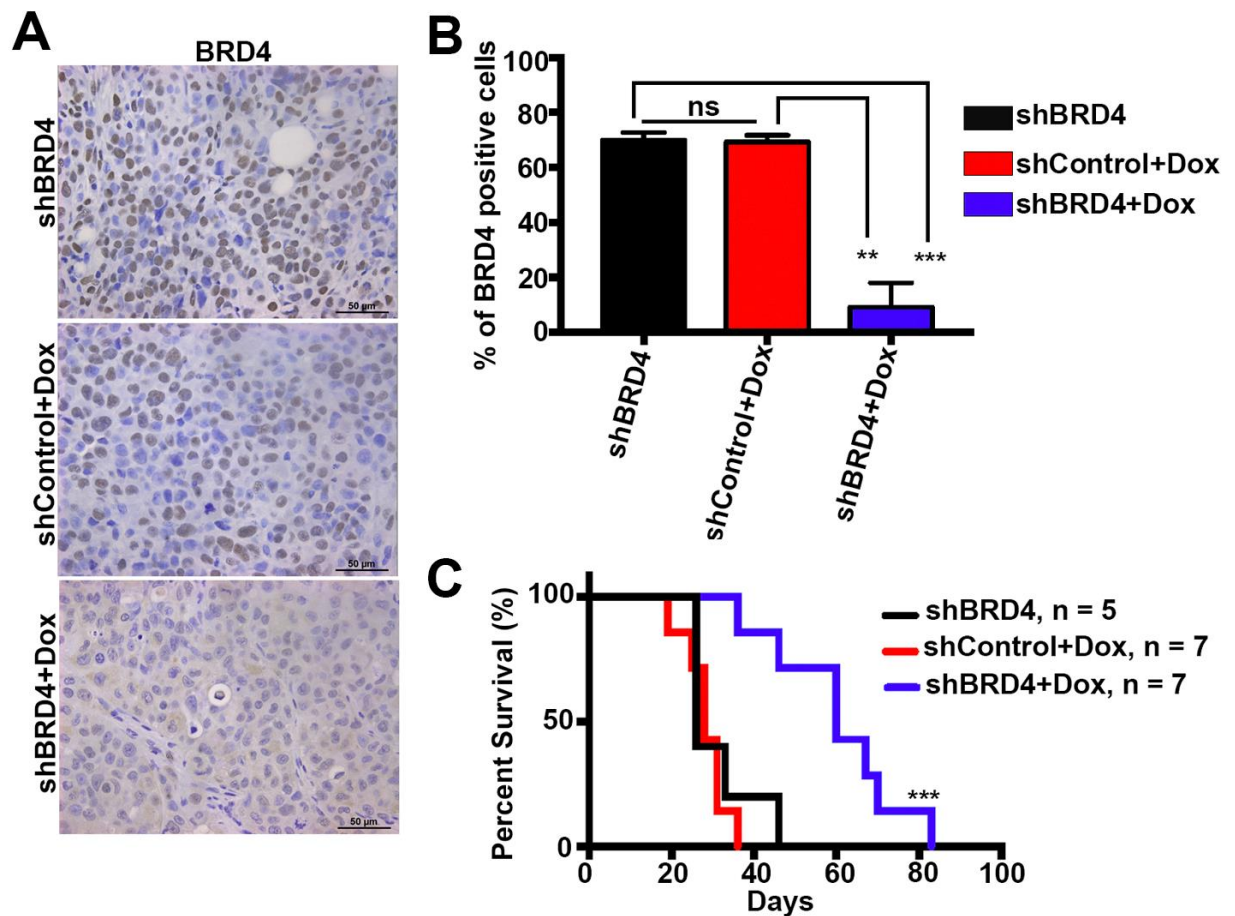
Figure 3-12. BRD4 knockdown prolongs survival in ovarian cancer. (**A**) IHC staining for BRD4 in OVCAR 5 tumor-bearing mice to confirm BRD4 knockdown in vivo. Scale bar, 50 μm. (**B**) Quantification of BRD4-positive cells from tumors in (**H**), ** p < 0.01, *** p < 0.001. Quantification was done using pictures of five random fields from OVCAR 5 tumors and statistical significance was determined using Student t-test for mean difference in BRD4 positive cells (n = 3 per indicated group). (**C**) Survival curve of each indicated group after shBRD4 induction, *** p < 0.001. Comparison was made to test for any significant difference between curves using Log-rank (Mantel-Cox) test.

On day 8 mice were euthanized and tumors were harvested for IHC. IHC analysis of harvested tumors showed that upon BRD4 knockdown, there was a marked decrease in Notch3 staining (**Figure 3-16**). These results are consistent with our *in vitro* findings and suggest that BRD4 has a direct role in Notch3 transcription and promotes Notch3 mRNA expression in ovarian cancer.

BRD4 directly regulates *NOTCH3* expression and impacts Notch3 downstream targets

Given our results so far, we wanted to test whether BRD4 directly promotes Notch3 transcription at the gene promoter level in ovarian cancer. Previous studies suggest that BRD4 regulates expression of genes, including *MYC,* by recruitment to the gene promoter (37, 44, 94). We performed chromatin immunoprecipitation (ChIP) of BRD4 and conducted PCR using previously described primers that flank the transcription start site of Notch3 (**Figure 3-17A**) (95). ChIP PCR demonstrated that BRD4 was enriched at the Notch3 promoter in both cell lines tested (**Figure 3-17B**). These results were quantified using qRT-PCR (Fig. 5C). BRD4 was also present at the *MYC* transcription start site, as described in other tumor models (**Figure 3-17C**) (44). Interestingly, BRD4 was not present at the *NOTCH2* promoter, suggesting that BRD4 directly and preferentially regulates *NOTCH3* gene expression in ovarian cancer (**Figure 3-17B**). These results indicate that BRD4 directly promotes Notch3 expression by enhancing its transcription at the gene promoter. Next, to understand the broader downstream effects of BRD4 inhibition, we conducted reverse phase protein array (RPPA) analysis in OVCAR 4 and OVCAR 5 cells that were treated with CPI203 for 48 hours.
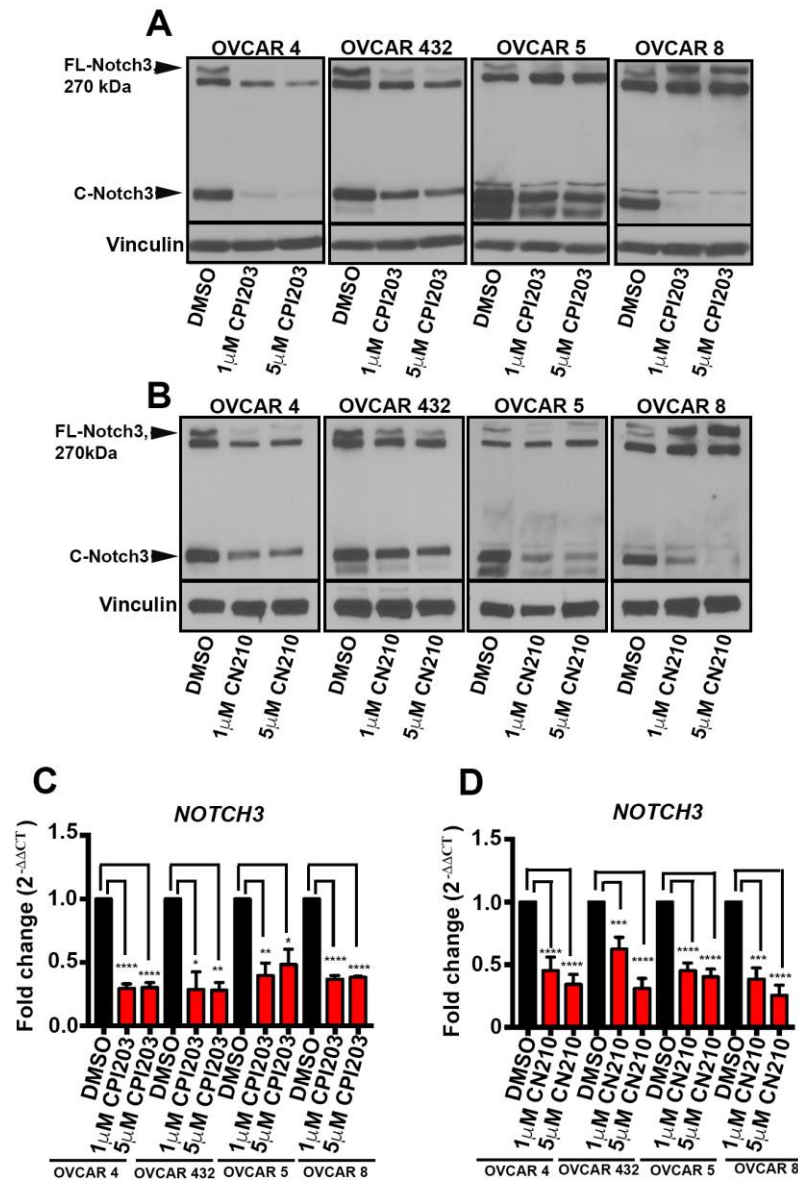
Figure 3-13. BETi treatment decreases Notch3 expression levels in ovarian cancer cells. (**A** and **B**) Protein expression analysis at 72 hours of full-length (FL) and cleaved (C) Notch3 after BRD4 inhibition using the BETi's indicated. (**C** and **D**) qRT-PCR analysis of NOTCH3 mRNA expression 48 hours after BRD4 inhibition using BETi. * $p < 0.05$, ** $p < 0.01$, *** $p < 0.001$, **** $p < 0.0001$). Statistical analysis was done by applying unpaired Student t-test of mean fold change for vehicle control cells compared to BETi treated cells. All experiments through have been repeated at least in 3 independent biological replicates.
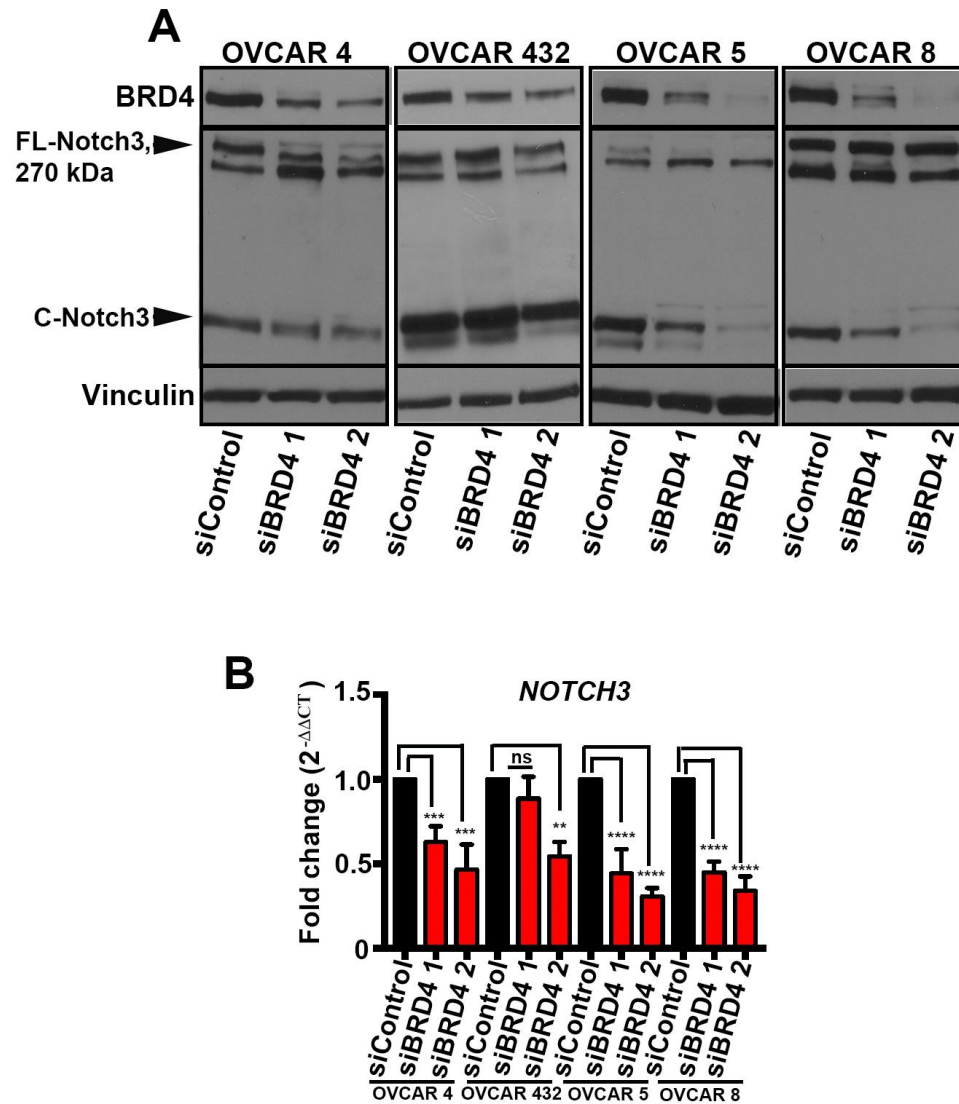
Figure 3-14. BRD4 knockdown decreases Notch3 expression levels in ovarian cancer cells. (**A**) Protein expression analysis at 72 hours of full-length (FL) and cleaved (C) Notch3 after BRD4 siRNA-mediated knockdown. (**B**) qRT-PCR analysis of NOTCH3 mRNA levels after BRD4 siRNA-mediated knockdown (**F**). * p < 0.05, ** p < 0.01, *** p < 0.001, **** p < 0.0001, ns (non-significant). Statistical analysis was done by applying unpaired Student t-test of mean fold change for vehicle control cells compared to BETi treated cells. All experiments have been repeated at least in 3 independent biological replicates.
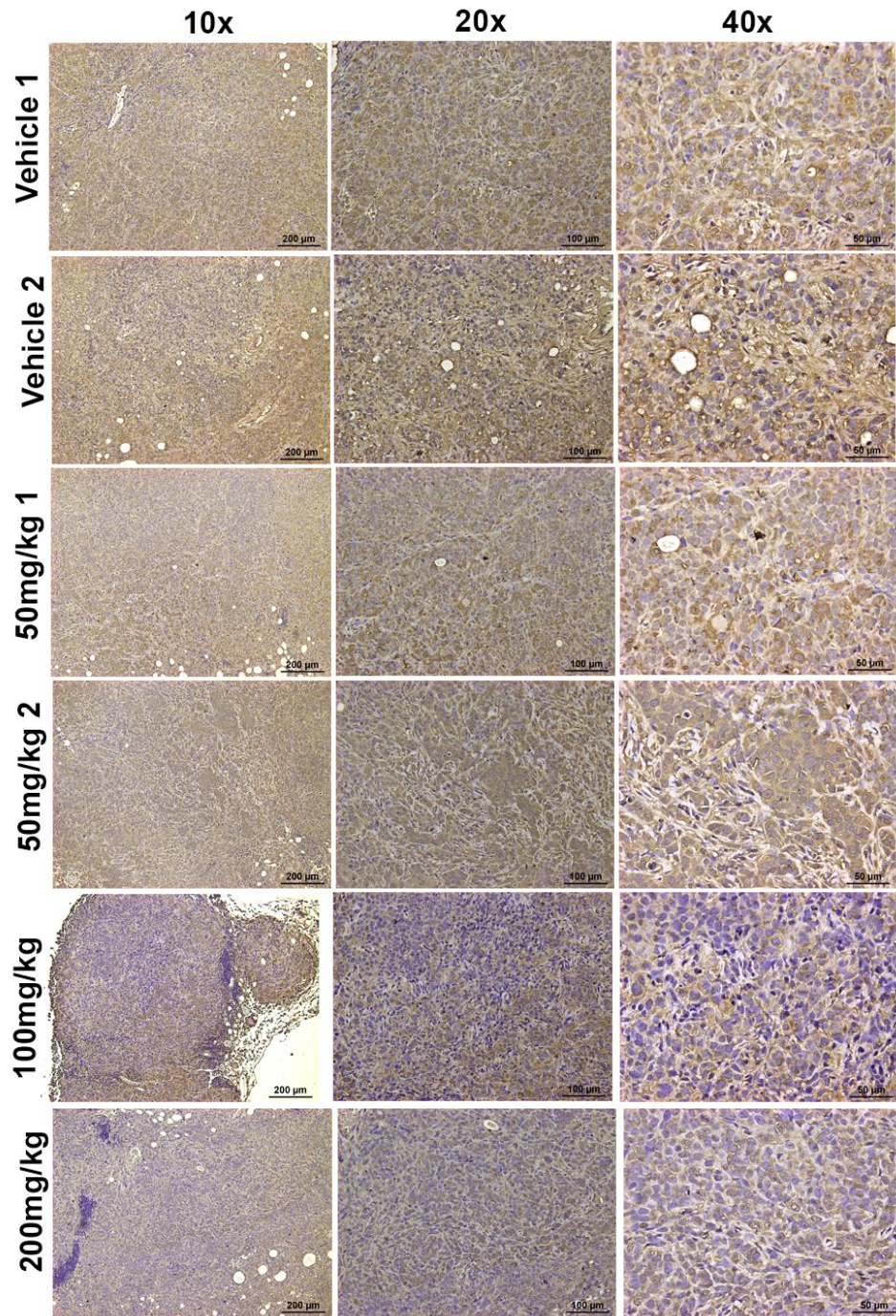
Figure 3-15. BETi decrease Notch3 protein expression in vivo. IHC images of OVCAR 5 tumors harvested from mice 24 hours after oral CN210 treatment at the indicated doses. N = 3 for each indicted treatment group. Scale bar for 10x images, 200 μm. Scale bar for 20x images, 100 μm. Scale bar for 40x images, 50 μm.
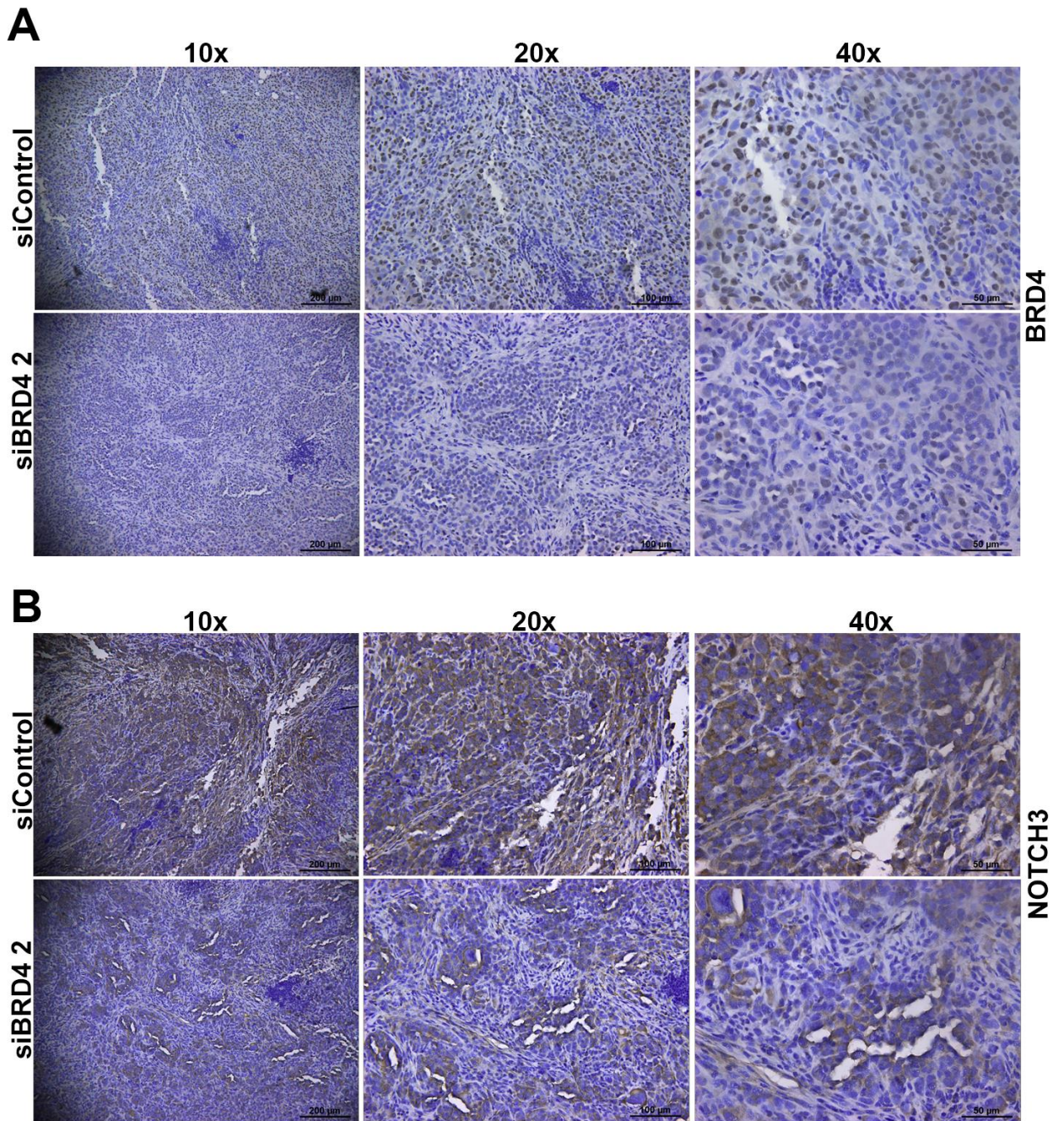
Figure 3-16. BRD4 knockdown decreases Notch3 protein expression levels in vivo. BRD4 (**A**) and Notch3 (**B**) IHC staining of OVCAR 5 tumors after Control (n = 5) or BRD4 (n = 5) siRNA delivery by DOPC nanoliposomes. Scale bar for 10x images, 200 μm. Scale bar for 20x images, 100 μm. Scale bar for 40x images, 50 μm.

RPPA allows for the rapid assessment of protein level changes in various cancer relevant signaling pathways, including Notch signaling. Based on our RPPA results, we generated a *NOTCH3* gene signature by combining previously identified Notch targets in ovarian cancer as well as the Broad Institute *NOTCH* gene signature to determine how protein levels of those targets would change in our RPPA data set after treatment with CPI203 compared with vehicle (57). The results showed that OVCAR 4 cells had an overall decrease in levels of Notch3 targets, including the previously described target Hes1 (**Figure 3-18**) (57). In OVCAR 5 cells, these changes were less prominent, but we also observed a downregulation of the Hes1 (**Figure 3-19**). We validated these results using both Western blot as well as qPCR analysis and observed that after BETi treatment, Hes1 protein (**Figure 3-20A** and **B**) and mRNA (**Figure 3-20C**) levels decrease in both OVCAR 4 and OVCAR 5 cells after BETi treatment. These results suggest that in ovarian cancer, BRD4 can directly regulate *NOTCH3* transcription and regulate *NOTCH3* downstream gene targets in ovarian cancer. We further validated the effect of BRD4 on *HES1* transcription using siRNA and observed that upon BRD4 knockdown, there was also a significant decrease in *HES1* transcription levels (**Figure 3-21**).
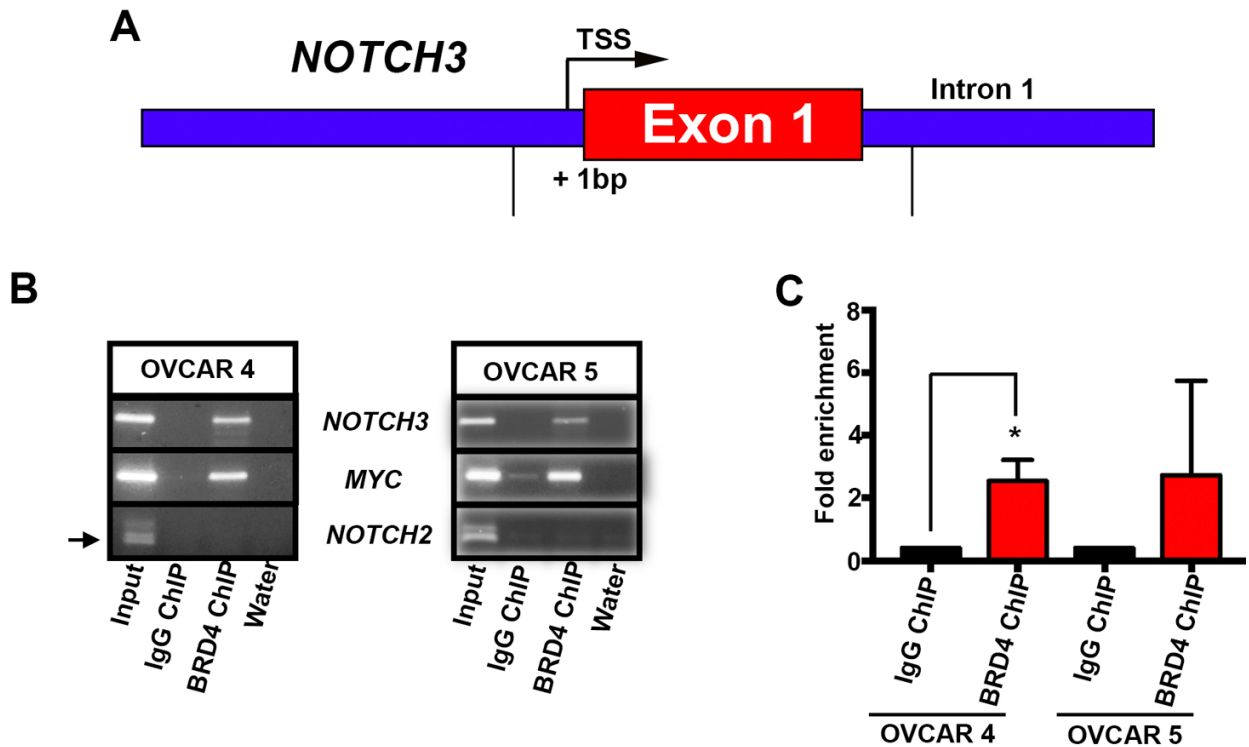
Figure 3-17. BRD4 is enriched at the NOTCH3 gene promoter. (A) Schematic of the
NOTCH3 promoter and transcription start site. (B) Chromatin immunoprecipitation
(ChIP) PCR reactions after BRD4 pulldown at the indicated gene promoter regions.
Experiments repeated in 3 independent biological duplicates. (C) ChIP qPCR of
NOTCH3 transcription start site after BRD4 pulldown, * p < 0.05. Experiments repeated
in 3 independent biological duplicates. Statistical analysis was done by applying
unpaired Student t-test for mean fold enrichment of BRD4 over IgG control.
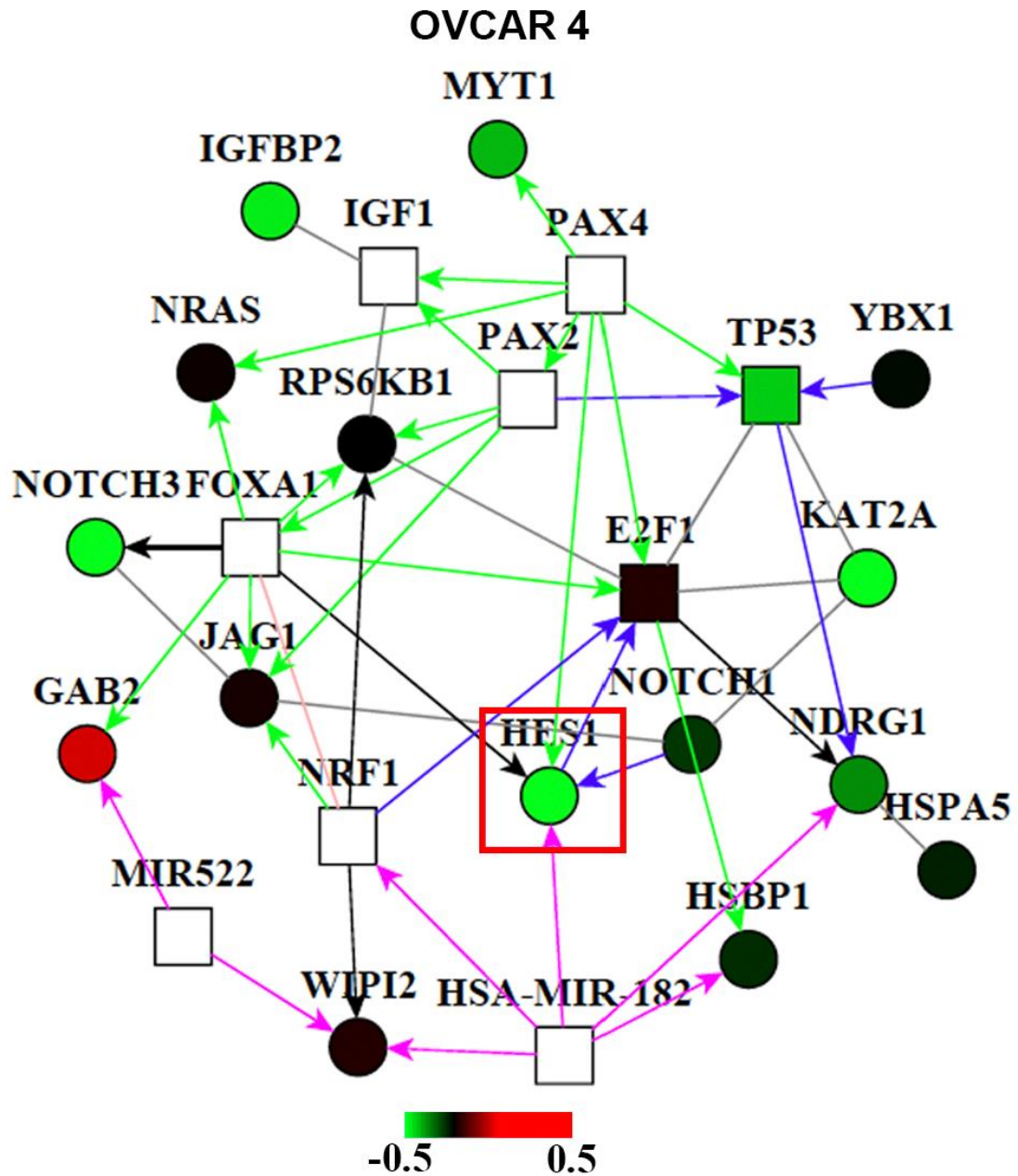
Figure 3-18. Defining Notch3 downstream targets impacted by BETi in OVCAR 4 cells. NOTCH3 gene signature generated from RPPA data using NetWalker software. Fold change calculated based on NormLog2 expression difference of DMSO treated cells versus CPI203 treated cells. Samples were submitted as 2 independent biological duplicates.
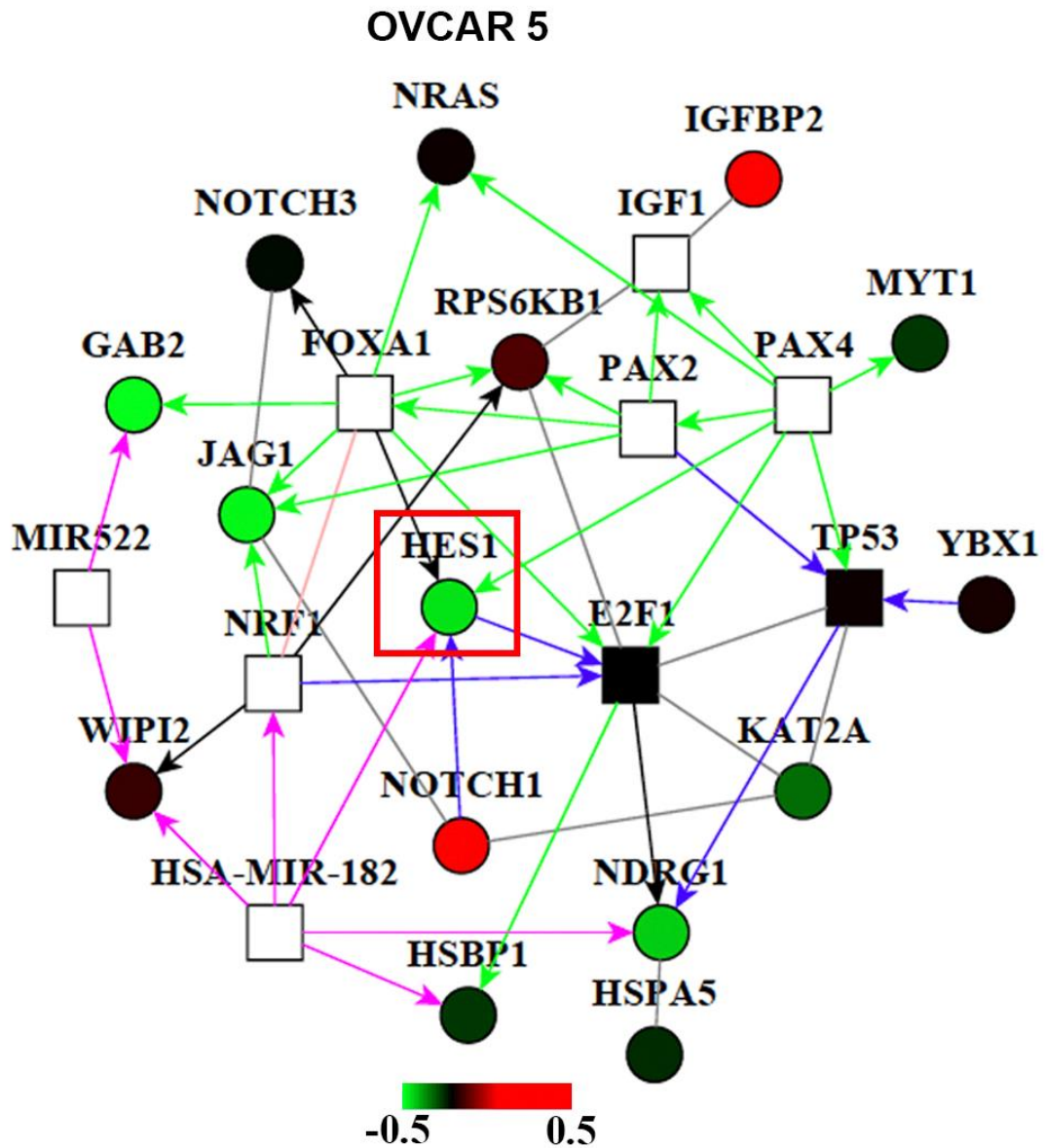
Figure 3-19. Defining Notch3 downstream targets impacted by BETi in OVCAR 5 cells. NOTCH3 gene signature generated from RPPA data using NetWalker software. Fold change calculated based on NormLog2 expression difference of DMSO treated cells versus CPI203 treated cells. Samples were submitted as 2 independent biological duplicates.
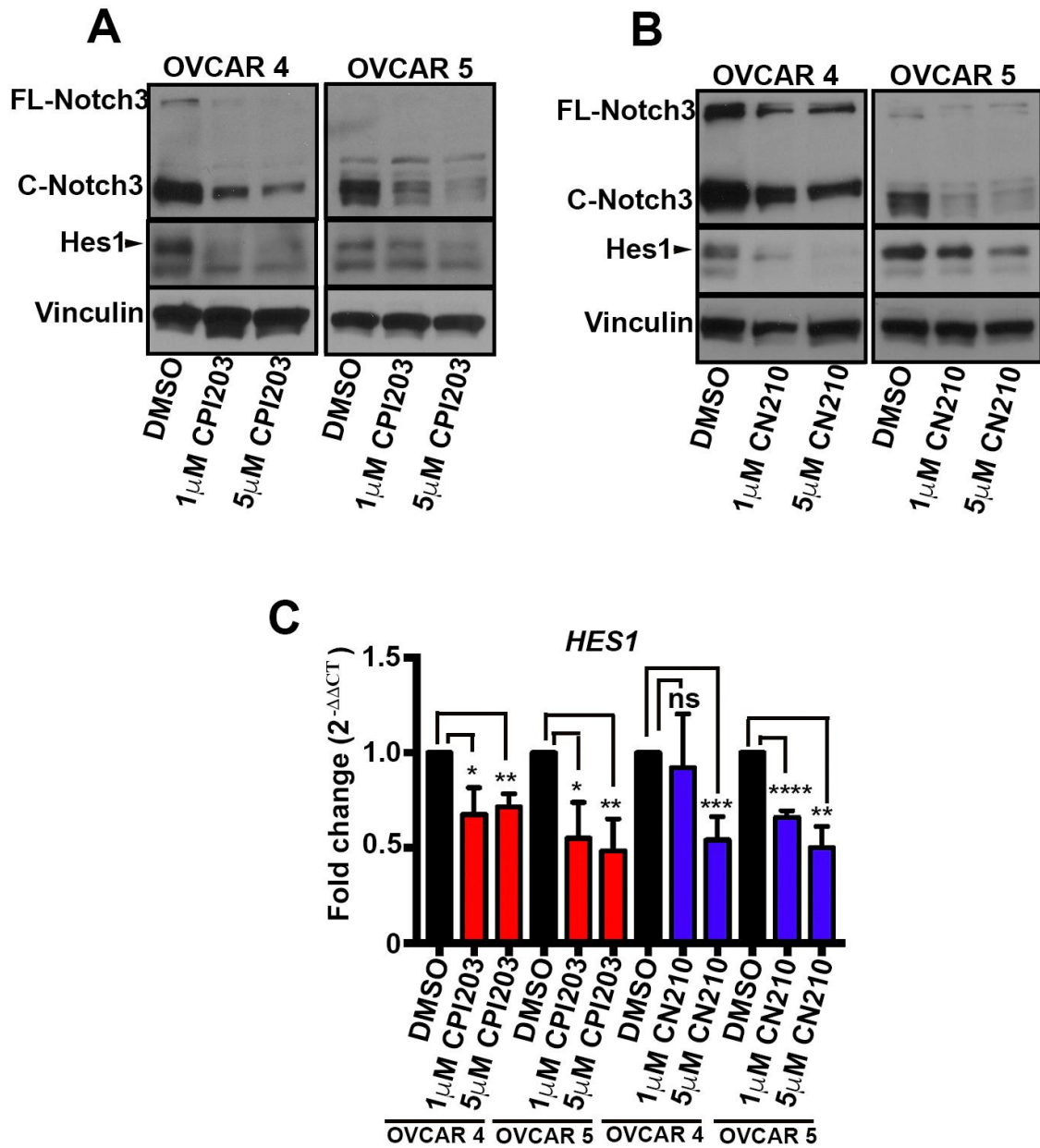
Figure 3-20. Downregulation of the Notch3 downstream target Hes1 after BETi treatment in ovarian cancer cells. (**A** and **B**) Hes1 Western blot of cells treated with BETi CPI203 (**A**) or CN210 (**B**). Experiments repeated in 2 independent biological duplicates (**C**) qRT-PCR analysis of HES1 after BETi treatment. * $p < 0.05$, ** $p < 0.01$, *** $p < 0.001$, **** $p < 0.0001$. Experiments repeated in 3 independent biological duplicates. Statistical analysis was done by applying unpaired Student t-test of mean fold change for vehicle control cells compared to BETi treated cells.
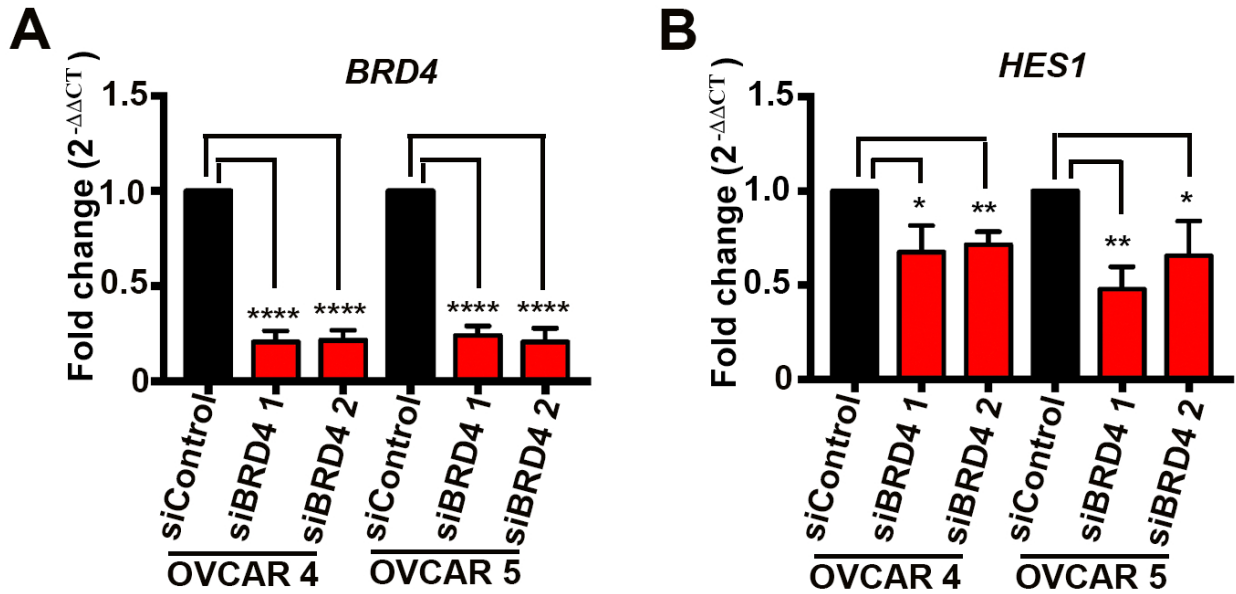
Figure 3-21. BRD4 knockdown decreases HES1 mRNA levels in ovarian cancer cell lines. qRT-PCR analysis after BRD4 siRNA mediated knockdown (**A**) of HES1 mRNA transcript levels (**B**). * $p < 0.05$, ** $p < 0.01$, **** $p < 0.0001$. Experiments repeated in 3 independent biological duplicates. Statistical analysis was done by applying unpaired Student t-test of mean fold change for siControl cells compared to siBRD4 knockdown treated cells.

SUMMARY

In this study, we took a multidisciplinary approach to identify and re-purpose clinically relevant targeted therapies. Our observations led us to characterize a novel molecular relationship between BRD4 and Notch3 in ovarian cancer. Using our TPT, we successfully predicted that early-stage BETis would provide significant therapeutic and survival benefits in pre-clinical ovarian cancer models. Furthermore, we uncovered BRD4's ability to regulate Notch3 expression both *in vitro* and *in vivo* in ovarian cancer models (**Figure 3-22**).
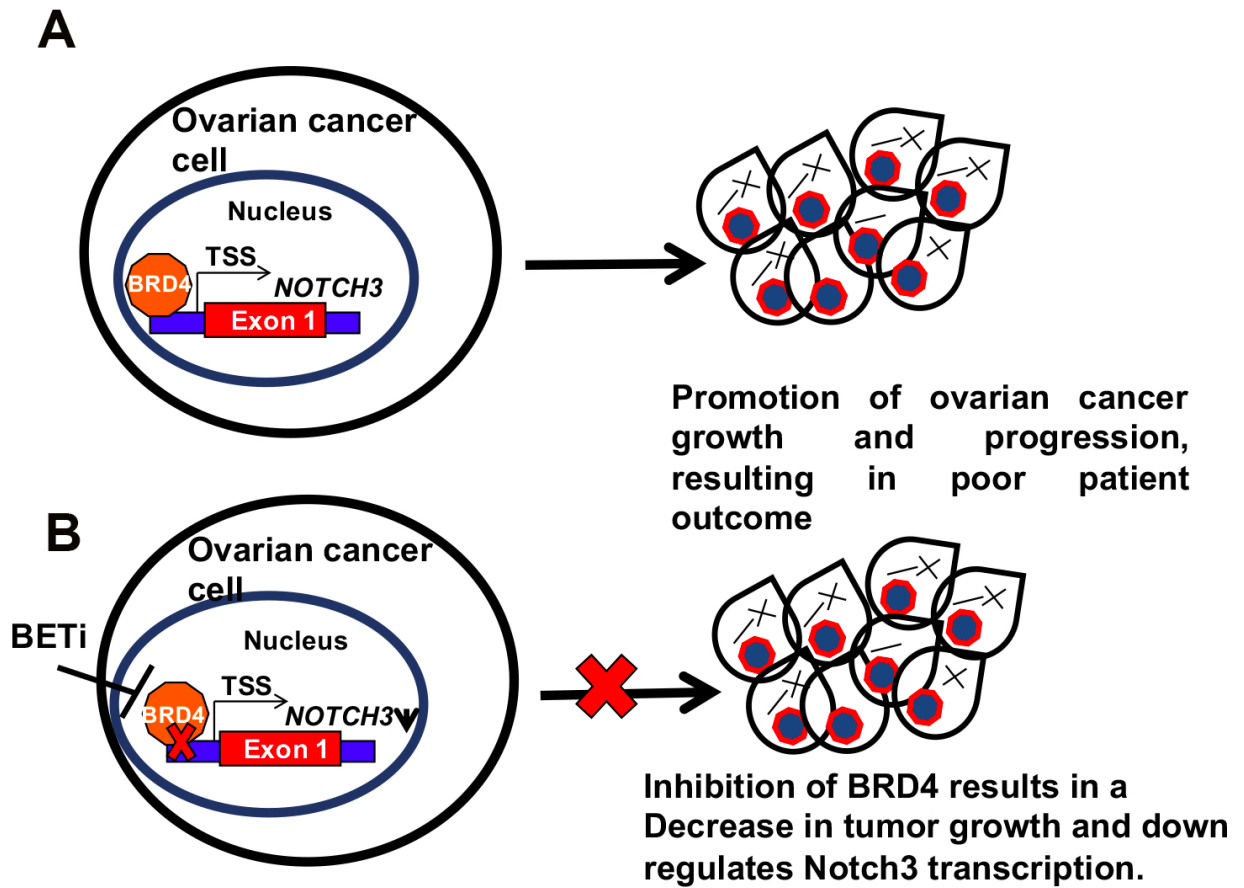
Figure 3-22. Working model. (**A**) BRD4 promotes NOTCH3 transcription and promotes ovarian cancer growth and progression. (**B**) BETi's inhibits ovarian cancer growth and decreases transcription of the BRD4 oncogenic target, NOTCH3.

CHAPTER IV

DISCUSSION AND FUTURE DIRECTIONS

DISCUSSION

Targeted cancer therapies and the TPT

The rise and development of targeted therapies has greatly impacted the perspective of basic and translational researchers, up to clinicians running multicenter clinical trials in how to approach cancer therapy (2). The ramifications of meticulous and rigorous pre-clinical studies that characterize the molecular mechanisms and genetic alterations which drive the growth and progression of specific cancer types can directly impact patient treatment options and outcomes. The fruits of these efforts have resulted in therapies that can range from small molecule inhibitors such as BETis and PARPi, to antibody therapies like bevacizumab, all of which target specific molecules (5, 12, 34). Furthermore, recent therapies are also designed to train the body's own immune system to attack tumor cells (96). With all these options, researchers and clinicians can put together an arsenal that targets both tumor cells themselves as well as their protective micro-environment. In spite of these advancements, due to the rapidly evolving nature of cancer cells, tumors can gain resistance to these promising therapeutics and fail to significantly improve patient outcomes for which they were designed for (3, 15, 16, 96).

Instead of discarding these therapies, researchers are turning to readily available and ever expanding bioinformatics databases (see **Chapter I**) to mine them in order to identify molecular and/or genetic signatures in specific cancer types which could be targeted by readily available targeted therapies (17). Even with these resources, determining an effective way to easily compile and centralize the breadth of information found in these databases to re-purpose targeted therapies remains

challenging (17). It is this need that propelled us to generate our Therapy Predicting Tool.

The design of the TPT is not the first of its kind. As described in Chapter I, other research groups have tried to compile the information various databases in order to generated predictive therapy response computational algorithms that have yielded promising results (17, 24-27, 97, 98). Our tool is different in critical ways. First, the TPT utilizes both TCGA and GTEx databases to generate its predictions for potential gene targets, which allows compared expression changes from patient tumor samples with normal tissue counterparts. This allows for more precise identification of targets that are potential drivers of tumor growth and less likely to be background noise inherent of large databases. Second, the TPT pairs the identified gene targets with phase I clinical trial targeted therapies. This aids in speeding up the use of these therapies in a clinical trial setting if pre-clinical studies demonstrate that the re-purposed therapy yields a therapeutic effect in the tumor of interest. Lastly, the TPT predicts potentially new downstream targets of the re-purposed targeted therapy in the tumor type of interest, providing further rational for using the re-purposed targeted therapy in the tumor of interest.

Based on the results presented in Chapter III, I was able to provide biological evidence which validates the accuracy of the TPT. Not only did BETis provide a beneficial therapeutic and survival effect, but it also uncovered a new molecular relationship between Notch3 and BRD4 in ovarian cancer. Although the results are highly encouraging, there also limitations to consider for the application of the TPT. Just like other computational algorithms before it, it is dependent on the accuracy of the original data sources such as TCGA and GTEx. This means that the accuracy of the TPT can be influenced by any error in the original data collection to

71

generate these databases and if the database is updated. Based on our biological results, the data set and correlations were robust enough to predict a significant anti-cancer effect of BETis in ovarian cancer. Furthermore, if any significant updates are made to the databases, we can simply incorporate those updated data sets in the TPT to ensure precision and accuracy of its predictions. Another consideration that applies to all computational approaches is that, regardless of what re-purposed therapy and target combination the TPT produces for the cancer of interest, the pre-clinical model systems may not respond as well as the TPT prediction (99, 100). Even within the standard ovarian cancer cell lines used, there was some variability in the response to the BETis used, both *in vitro* and *in vivo* (**Figures: 3-2, 3-4, 3-5, 3-6, 3-7, 3-8, 3-9**) (90). Thus, for future applications of the TPT, it is empirical that we test its effectiveness in different cancer types before moving forward with it in a clinical setting.

Implication of BETi usage in ovarian cancer

The study presented here highlights the potential of streamlining the process of rapidly identifying promising therapies, validating them and moving them to the clinical trial setting. From my work, I have determined that BETis are not only are a viable therapeutic avenue but can downregulate *NOTCH3* in ovarian cancer. Since their development, BETis have shown to be effective in a variety of cancers including: multiple myeloma, acute myelogenous leukemia, NUT midline carcinoma, pancreatic, breast and prostate (43, 44, 53, 54, 82, 83). This has lead the way to the set-up of a multitude of clinical trials (34).

Recently, multiple groups have independently explored the use of BETis in ovarian cancer (101-105). Consistent with these previous studies, BETis demonstrated beneficial anti-tumor effect in multiple ovarian cancer *in vitro* and *in vivo* pre-clinical models. Additionally, in my work I used a novel BETi, CN210, which is a prime candidate to be used in clinical trials. This is critical, given that there are currently no clinical trials designed for the BETi usage to specifically treat ovarian cancer. In most of the previous literature cited, the BETi predominantly used is JQ1, which is not suited for direct clinical use and can have some off-target effects (35). Furthermore, using the doxycycline inducible shRNA system, I was able to directly test the hypothesis that tumor intrinsic BRD4 downregulation not only slows down tumor growth but also significantly improves survival (**Figure 3-12**). This observation suggests that the anti-tumor effect of BETis is achieved by inhibiting BRD4 function within tumors.

BRD4 downstream targets in ovarian cancer

BRD4 is known to play an important part in regulating cell transcription (34, 39, 47). Depending on the biological context, such as disease or normal development, BRD4 may have a plethora of downstream transcriptional targets that can regulate specific cell functions (46, 47, 50, 106, 107). Previously published work through the use of BETis, have to identified novel BRD4 downstream transcriptional targets such as *FOXM1*, *MYCN* and *ALDH1A1* in ovarian cancer (101, 104, 105). Due to the initial prediction of the TPT in the study presented here, we can add *NOTCH3* to that list, which is known to play a role in ovarian cancer progression and is prognostic marker for worse survival outcomes (57, 108). However, due to BRD4's impact on multiple genes, its pro-tumorigenic effects are not exclusively due to promoting Notch3

expression. Regardless, similar to the *MYC* studies done in hematological malignancies, we can now consider in the future using BETis as means to target Notch3 signaling in ovarian cancer (42-44, 108). This is particularly exciting given the inherent difficulty of directly inhibiting Notch signaling in patients due to the high toxicity of γ-secretase inhibitors (76, 84). In comparison, BETis are better tolerated by patients in a clinical setting (34). In the work presented, we only focused on the effect of BETis in the perspective of BRD4 and Notch3, but generating specific gene networks and signatures encompassing all of these identified BRD4 downstream targets may hold promise in further personalizing the use of BETis in ovarian cancer.

Similar to BRD4, Notch signaling can have a broad effect in the transcriptional landscape of the cell and the physiological impact this can have is also biologically context dependent (**Figure 2-4**) (60, 65, 109). In the case of Notch3, its role in development is mostly attributed to the development of the mammalian arterial vascular system by promoting differentiation of arterial smooth muscle (66, 110). In the context of cancer, overexpression or constitutive activation of Notch3 signaling is shown to play a role in the progression of acute lymphoblastic leukemia as well as lung, breast, gallbladder and ovarian cancer (57, 62, 71-73, 111). One of the major challenges in understanding the role of Notch3 signaling in disease and development is identifying downstream targets. For ovarian cancer, this is of particular interest since identifying these downstream gene targets could present a novel avenue for developing targeted therapies (56, 57, 59). In the work presented here, by using RPPA and NetWalker analysis software, I was able to create a *NOTCH3* gene signature based on previously identified Notch targets in ovarian cancer as well as the Broad Institute *NOTCH* gene signature, that is impacted by the use of BETis (56, 57, 59). I biologically validated

these results by observing downregulation of Hes1 upon BETi treatment (**Figure 3-20**), but it remains to be determined what the overall impact of this network has in understanding the role of Notch3 signaling in ovarian cancer progression.

FUTURE DIRECTIONS

Further applications and biological validation of the TPT

Despite the extensive biological validation carried out in Chapter III, further biological testing has to be carried before the use of the TPT can be implemented in a clinical and patient setting. This implies not only further testing in ovarian cancer, but expanding the use of the TPT for other tumor types. To further evaluate the effect of chronic downregulation of BRD4 in ovarian, I am conducting a second survival using our doxycycline inducible system, described in Chapter III, using the OVCAR 4ip1 tumor model (**Figure 4-1**). Distinct to OVCAR 5, OVCAR 4 cells demonstrated more sensitivity to BETis both *in vitro* and *in vivo* (**Figures 3-4, 3-5, 3-6, 3-7, 3-8 and 3-9**)*.* This experiment is currently ongoing due to the much slower growth rate of OVCAR 4ip1 cells compared to OVCAR 5 cells *in vivo* (90)*.* Preliminary results demonstrate a decrease in tumor growth in mice with active expression of BRD4 shRNA when compared to mice expressing either shControl or shBRD4 mice never exposed to Dox-Chow (**Figure 4-1B**) (91). These results are consistent with the OVCAR 5 tumor model (**Figure 3-11**).
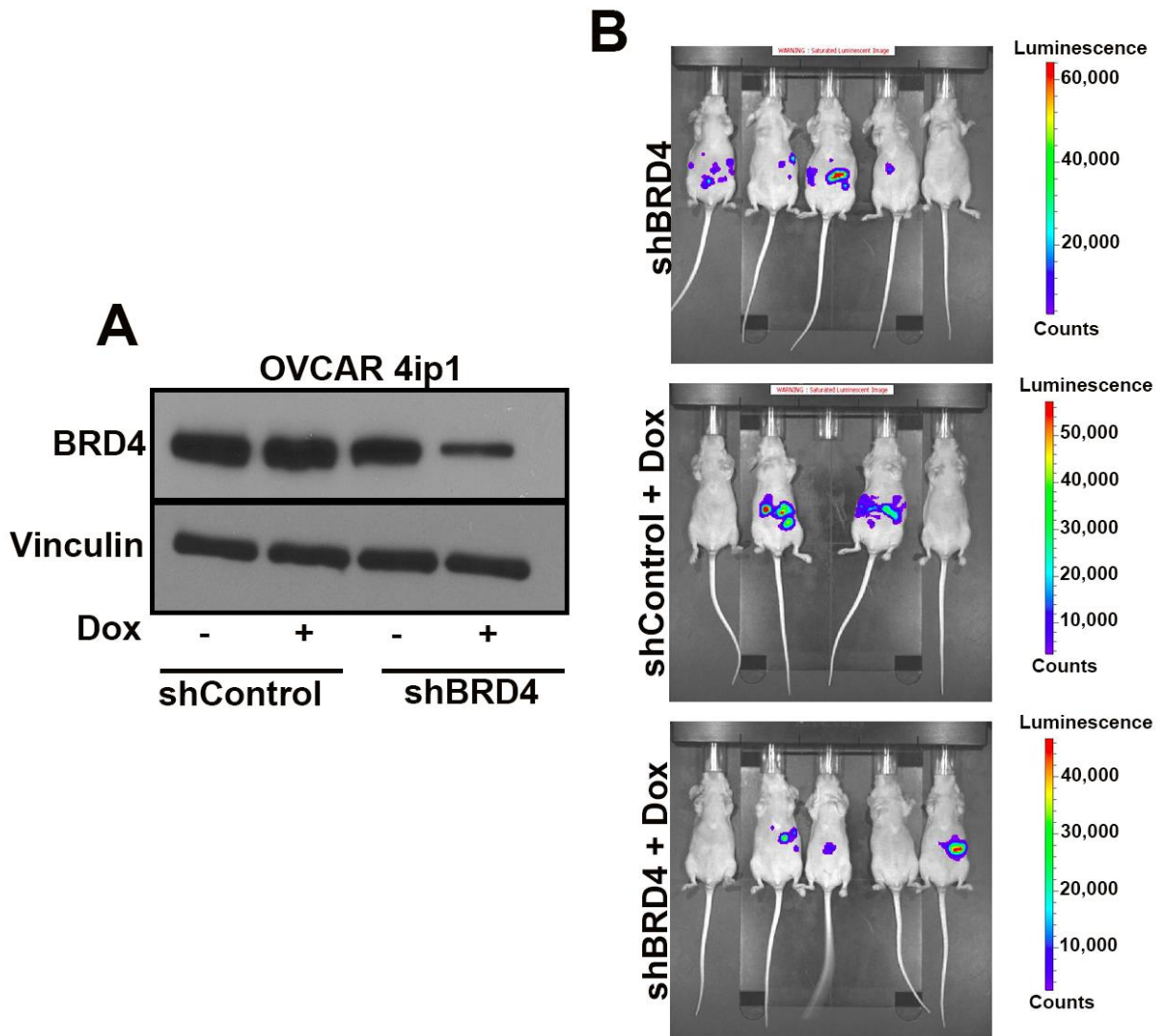
Figure 4-1. Testing the impact of survival of BRD4 knockdown in OVCAR4 ip1 tumor model. (**A**) In vitro validation of our doxycycline inducible shRNA system in OVCAR4 ip1 cells by Western blot. Cells were exposed to 100ng/mL of doxycycline and harvested to verify protein knockdown 48 hours later. (**B**) IVIS imaging of OVCAR 4ip1 tumor bearing mice, with indicated cell lines injected IP. IVIS imaging was conducted on day 59 after introduction of Dox-Chow and induction of shRNA constructs in tumor cells.

If we observed a similar increase in survival, as we did with OVCAR 5 (**Figure 3-12C**), after chronic tumor intrinsic BRD4 downregulation, this further strengthens the predictions of the TPT and prompt the use of BETis in ovarian cancer patients.

The goal of the TPT is to expand its use to a multitude of tumor types. To accomplish this, we need to ensure its biological accuracy in the tumor model of interest. To start addressing this, I chose another gynecological tumor model, endometrial cancer. Similar to ovarian cancer, patients that present with advance or recurrent disease do not respond as well to standard chemotherapies (112). The TPT predicted that BETis would provide a beneficial survival effect on endometrial cancer that trended towards significance ($p = 0.0618$, **Figure 4-2A**). One possible explanation for this result not being significant is because the TPT did not distinguish between the different subtypes of endometrial cancer, which have different clinical characteristics (112). We proceeded to test the effect of the BETi CPI203 and CN210 in two commonly used endometrial cancer cell lines: Hec1-b and Ishikawa (113). Results demonstrated that in both cell lines, BETis reduced cell viability by both colony formation and MTT assays (**Figure 4-2B-E**). These results are also consistent with recently published work using the BETi, JQ1 (48). I next used the TPT, to identify potentially novel downstream targets of BRD4 in endometrial cancer. The top prediction that emerged was Cyclin B1, which when upregulated is a marker for worse prognosis in endometrial cancer (114). Additionally, expression of Cyclin B1 increases during G2/M transition during the cell cycle, which is also a period where BRD4 is highly transcriptionally active (114-117). Treatment of endomentrial cancer cells with BETis, resulted in a decrease in Cyclin B1 mRNA expression in both cell lines tested (**Figure 4-3**). Taken together, the results in **Figures 4-2** and **4-3** suggests that the accuracy of the TPT can extend beyond ovarian cancer and merits future tests of drug/target combinations in other tumor types.
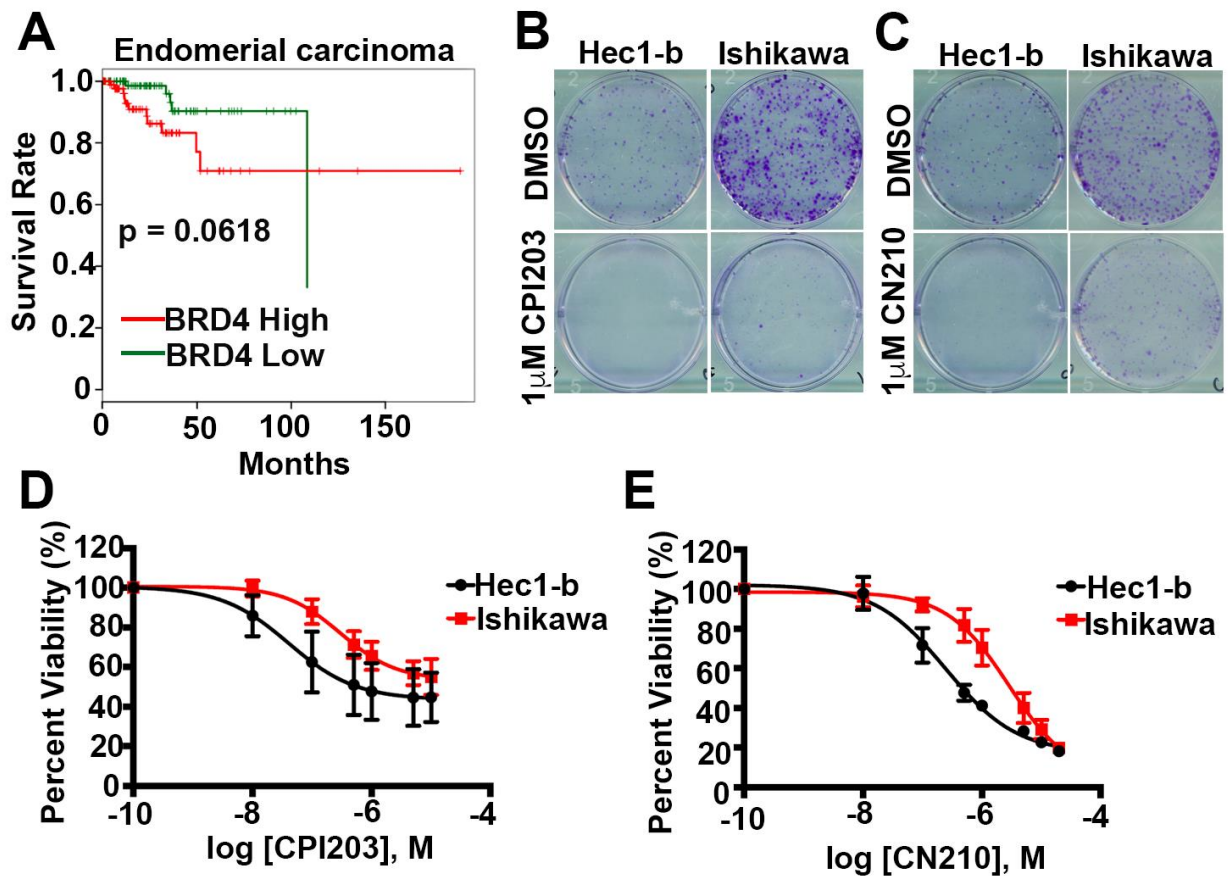
Figure 4-2. BETi inhibition produces beneficial therapeutic effect in endometrial cancer cell lines. (**A**) Survival curve based on TPT results showing a beneficial survival benefit of BETis in endometrial cancer, which trends to significance. (**B** and **C**) Colony formation assay of Hec1-b and Ishikawa cells treated with either CPI203 or CN210. (**D** and **E**) MTT viability assays for Hec1-b and Ishikawa cells after treatment with BETis CPI203 (**D**) or CN210 (**E**). All experiments from (**B**) to (**E**) have been done in 3 biological triplicates.
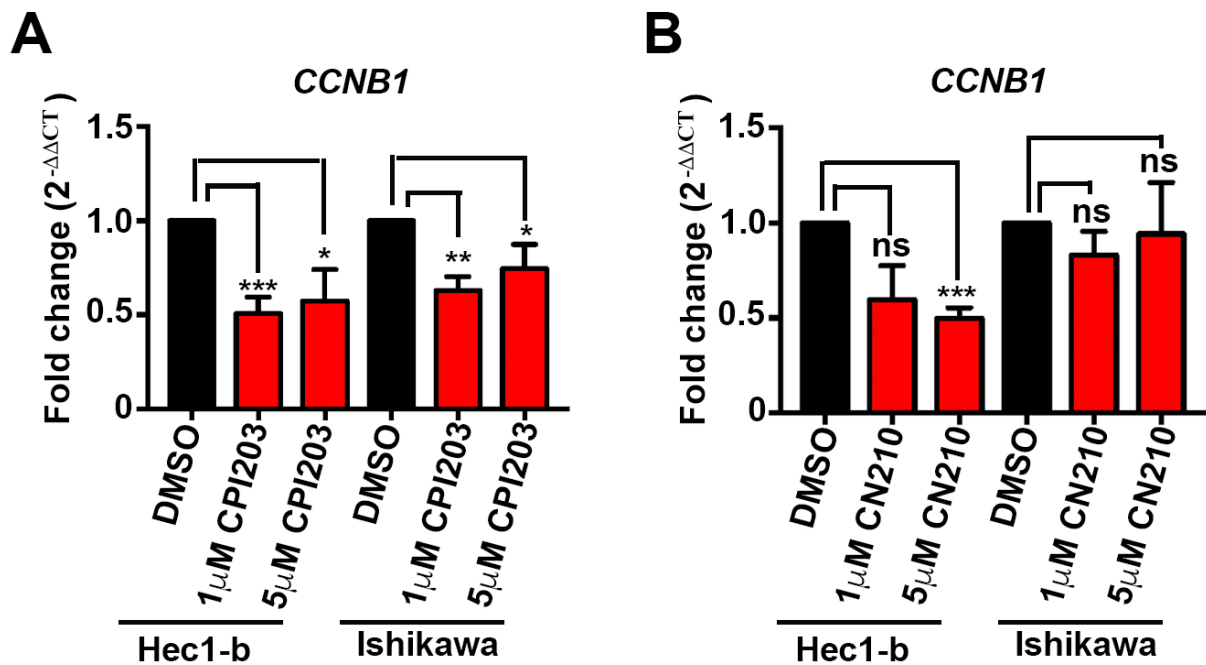
Figure 4-3. Targeting of BRD4 with BETis downregulates Cyclin B1 in endometrial cancer cell lines. (**A** and **B**) qRT-PCR analysis of CCB1 gene expression after treating with different concentrations of the BETis CPI203 (**A**) and CN210 (**B**) in Hec1-b and Ishikawa cells. Experiments were conducted in 3 independent biological replicates. * $p < 0.05$, ** $p < 0.01$, *** $p < 0.001$ and ns = not significant. Students t test was applied for determining statistical significance between fold change of BETi treated cells compared to DMSO vehicle controls.

Expanding the therapeutic potential of BETis in ovarian cancer

Ovarian cancer, particularly HGSC, is an extremely genetically complex disease (9). Due to this genomic instability, acquired drug resistance is quite common, even to promising targeted therapies (9, 15, 16). An alternative strategy to maximize the use of targeted therapies, is to incorporate them in combination with either conventional chemotherapies or with other targeted therapies (1, 3). The goal of this strategy is to identify combinations that produce synergistic effect and more effective killing of cancer cells.

In this study, we observed that as a monotherapy, BETi decreased tumor growth *in vivo*, but did not completely abolish tumor growth. In the setting of clinical trials for other tumor types, similar responses are observed in patients that are being treated with BETis as a monotherapy (34). Thus, understanding the adaptive changes that occur in a cell after BETi exposure may shed insight as to which patients will be the best responders to BETis and on what combination of therapies would be effective to shut down resistance inducing pathways. One modality that aids in identifying those adaptive changes is RPPA. We conducted RPPA analysis on cells treated with BETi to identify changes in downstream Notch3 proteins but the information provided by our RPPA data set can go further beyond than just the restriction of one cell signaling pathway (80). RPPA allows for the quantitative analysis of multiple proteins, as well as protein modifications such as phosphorylation and cleavage, that are central for a variety of major cancer related pathways (80). For the purpose of this study, RPPA provided in sight of major signaling pathways whose activity changed before and after BETi treatment. Using NetWalker network analysis software, I was able to determine which cellular processes were significantly changed after BRD4 inhibition (81). In

OVCAR 4 cells, which demonstrated higher sensitivity to BETis, BETi treatment decreased expression in proteins involved in cell cycle progression and transcriptional networks related to TP53, MYC and FOXM1 signaling, which has been previously described in other ovarian cancer cell lines (38, 101, 105) (**Table 4-1**). Conversely, there was an increase in proteins related to Insulin and mTOR signaling, which are related to metabolism, stress responses and associated with chemotherapy resistance in ovarian cancer (118) (**Table 4-1**). This suggests that in cells whereby BETi impacts proliferative capacity are more likely to respond better to BETis. Interestingly, for OVCAR 5, the more resistant cell line, there was an increase in proteins related to immune cell as well insulin signaling and a downregulation in proteins involved in overall tyrosine phosphorylation, leukocyte differentiation and cell adherens junctions (**Table 4-2**). A recent report suggests that in ovarian cancer, re-programing of the kinome may be responsible for acquired BETi resistance (103). One way to explore this hypothesis is to create ovarian cancer patient derived xenograph (PDX) models, treat them with BETis and run RPPA analysis on those tumors to observe if there are changes in mTOR signaling (119). This could be incorporated back to clinical care and decide if freshly resected tumors have high levels of BRD4 and Notch3, then adding mTOR pathway inhibitors would be highly beneficial as well.

Other groups have started to explore the idea of combination therapies in ovarian cancer that involve BETi (102, 120-122). Some of these reports have shown promising combination strategies with PARPi and BETis, due to the ability of BETis to stall the cell cycle (120, 121). It is yet to be determined whether these results are consistent using our novel and clinically ready BETi, CN210.

OVCAR 4 Upregulated Functional Pathways	Hypergeometric p Value
mTOR Signaling Pathway	2.51×10^{-10}
Insulin Receptor Signaling Pathway	4.84×10^{-9}
B Cell Receptor Signaling Pathway	1.06×10^{-9}
PI3K Cascade	1.38×10^{-9}
Cellular Response to Insulin Stimulus	2.74×10^{-9}
OVCAR 4 Downregulated Functional Pathways	**Hypergeometric p Value**
TP53 Network	9.29×10^{-13}
FOXM1 Transcription Factor Network	1.82×10^{-12}
Cyclin A/B1 Associated Events During G2/M Transition	2.10×10^{-12}
regulation of chromosome organization	1.33×10^{-10}
Validated Targets of C-MYC Transcriptional Activation	1.68×10^{-10}

Table 4-1. NetWalker analysis of functional pathways changes in OVCAR 4 cells after BETi treatment.

OVCAR 5 Upregulated Functional Pathways	Hypergeometric p Value
Acute Myeloid Leukemia	6.17×10^{-14}
Insulin Signaling Pathway	2.06×10^{-11}
G1 to S Cell Cycle Control	2.51×10^{-11}
B Cell Receptor Signaling Pathway	6.00×10^{-11}
Apoptosis	7.94×10^{-11}
OVCAR 5 Downregulated Functional Pathways	**Hypergeometric p Value**
Regulation of Peptidyl-Tyrosine Phosphorylation	1.47×10^{-11}
EGFR1 Signaling Pathway	2.15×10^{-10}
IL-3 Signaling Pathway	4.27×10^{-10}
Leukocyte Differentiation	1.80×10^{-8}
Adherens Junction	2.31×10^{-8}

Table 4-2. NetWalker analysis of functional pathways changes in OVCAR 5 cells after BETi treatment.

Furthermore, it would be beneficial to pursue combinations with mTOR pathway inhibitors or even drugs that can mitigate insulin signaling (123). Lastly, it would be beneficial to further characterize CN210 and whether this would create synergistic effect with immune checkpoint blockers, such as PDL-1, given the changes observed in immune related proteins in OVCAR 5 (122).

Further Exploring the Functional Relationship between BRD4 and Notch3 in Ovarian Cancer

In this study, I uncovered a novel functional relationship between BRD4 and Notch3 in ovarian cancer. Specifically, the ability of BRD4 to promote *NOTCH3* transcription by being enriched at the *NOTCH3* promoter (**Figure 3-22**). BRD4 is known to also regulate gene expression at enhancer sequences in association with the Mediator complex (**Figure 2-1**) (46, 83). A past report identified the presence of chromatin marks consistent with enhancer sequences within the *NOTCH3* gene body (110). To identify if BRD4 is present at these or other potential enhancer sequences for *NOTCH3*, I would conduct a ChIP sequencing assay. This would be give us more insight as to how BRD4 can directly regulate the expression of *NOTCH3,* as well as other gene targets, in ovarian cancer.

It still remains to be determined how much of BRD4's pro-tumorigenic effect in ovarian cancer is mediated by promoting Notch3 over-expression. To determine this, I attempted a rescue experiment where I stably over-expressed the cleaved, and transcriptionally active, Notch3 intracellular domain (NICD3) using a lentiviral vector. The rationale of this approach was that the expression of this active form of Notch3 does not depend on the presence or absence of BRD4 (**Figure 4-4A**). NICD3 over-

expression was able to increase mRNA expression of *HES1* (**Figure 4-4B**) but did not alter basal expression of BRD4 in the ovarian cancer cells tested (**Figure 4-4A**). Interestingly, when exposing these cells to the BETi CPI203, we observed that cells became more responsive to CPI203 when compared to their parental counter parts (**Figure 4-4C and D**). This effect may be in part due to off target effects produced by excessively high levels of NICD3. Additionally, it has been reported that over activation of Notch3 can also induce cell senescence (124). Several alternative approaches may be taken to rule out the potential toxic effect of constitutive NICD3. First, I could generate a doxycycline inducible NICD3 system to better control NICD3 expression levels during the rescue experiments. Another approach is to use a DNA construct with a much weaker promoter than pGK, such as the Ubiquitin C promoter to drive NICD3 expression and achieve more physiological expression levels (124). Lastly, another alternative to these rescue experiments, would be to express a Notch3 downstream gene target such as *HES1* and attempt the rescue experiments both *in vitro* and *in vivo.*

Another aspect to consider when trying to understand the regulation of Notch3 expression in ovarian cancer is the possibility that other entities, including micro RNAs (miR), may be independent of BRD4. A recent publication demonstrated that miR-150 can directly target Notch3 in ovarian cancer and increase sensitivity to paclitaxel (125). It would be of interesting to explore what occurs to levels of miR-150 after inhibition or knockdown of BRD4. Specifically, if miR-150 levels decrease after BETi treatment as a means of compensating for decrease of *NOTCH3* expression.

A second regulatory factor that may be impacting Notch3 expression in ovarian cancer is the protein CTCFL, which is a paralog of CCCTC-binding factor (CTCF) (95). In T-cell acute lymphoblastic leukemia, CTCFL was observed to occupy the *NOTCH3* promoter and promote its transcription (95).
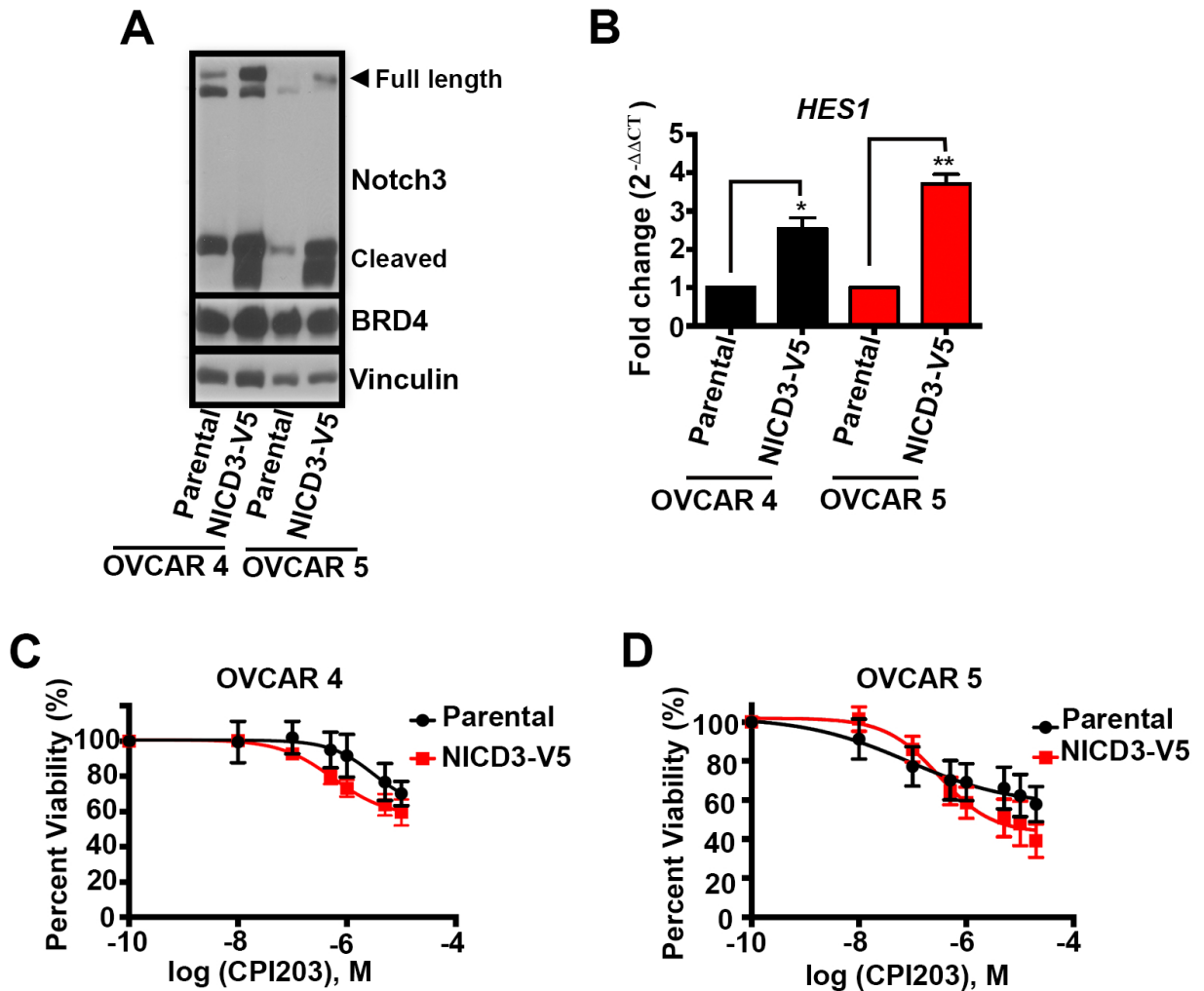
Figure 4-4. Over expression of Notch3 intracellular domain and response to BETi.
(**A**) Western blot confirmation of lentiviral over-expression of the Notch3 intra-cellular domain (NICD3) with a V5 protein tag. (**B**) qRT-PCR for HES1 expression after stable NICD3-V5 over-expression. * $p < 0.05$, ** $p < 0.01$. Experiment done in 3 biological replicates. Significance determined by Student t test. (**C** and **D**) MTT viability assay for OVCAR 4 and OVCAR 5 parental and NICD3-V5 over-expressing cells after treatment with CPI203.

Furthermore, analysis of the cBioportal TCGA data set for ovarian cancer demonstrates that *CTCFL* is amplified in a subset of ovarian cancer patients, alongside *BRD4* and *NOTCH3* (**Figure 4-5**) (19). Whether CTCFL regulates expression of Notch3 in ovarian and/or if BRD4 can recruit CTCFL to the *NOTCH3* promoter or vice versa, remains unknown. An initial experiment to start addressing this question would be to determine if gain or loss of CTCFL expression alter *NOTCH3* expression in ovarian cancer cells. Additionally, I would investigate if *CTCFL* expression levels change in response to BETi treatment. Lastly, I would determine whether CTCFL and BRD4 proteins interact with each other by conducting co-immunoprecipitation experiments.

The exact role of Notch3 and BRD4 regulation in ovarian cancer development is still not fully understood. BRD4 whole body knockout mice results in embryonic lethality (46, 66, 126). Notch3 mediates development of the vascular system and recent studies have shown the ability of BRD4 to induce expression of genes necessary for myogenesis, the development of muscle, and adipogenesis, the development of adipose tissue (46, 66). Little is known the role of these molecules in the development of the normal ovary. By understanding the gene networks that these molecules could regulate in development, this may shed more insight as to how those same gene networks play a role in ovarian cancer. A previous study has demonstrated that in the development of the mouse ovary, Notch3 mRNA is expressed in the granulosa cells (producers of sex hormones) of the ovarian follicle as well as the corpus luteum, but not in the oocyte itself (127). BRD4 on the other hand, has been reported to promote expression of the estrogen receptor in estrogen receptor positive cancers (128). This is particularly interesting because the use of oral contraceptives is regarded as a potential protective factor against ovarian cancer (9). The potential interplay between Notch3 and BRD4 in regulating hormone production and how this may impact both normal

BRD4   17%

Notch3 16%

CTCFL   11%

Genetic Alteration   ▪ Missense Mutation   ▐ No alteration

                           ▌ Deep Deletion   ▌ Amplification
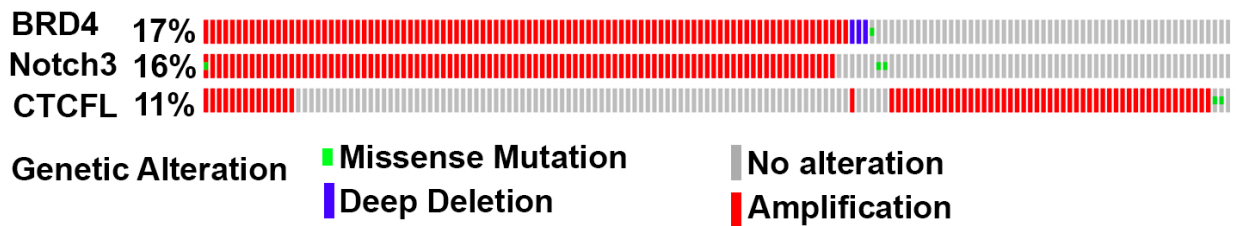
Figure 4-5. cBioportal oncoprint comparing expression of CTCFL and NOTCH3 in ovarian cancer. Oncoprint was generated and altered from the cBioportal tool (cbioportal.org) (19). To generate oncoprint, I first accessed the cbioportal home page and then I chose the TCGA data set available for ovarian cancer and input the genes BRD4, NOTCH3 and CTCFL in the gene entry box in order to compare genomic alterations found for these 3 genes in ovarian cancer. The oncoprint generate summarizes the results of the analysis, demonstrating what percent of patients in the dataset have alterations in each of the genes of interest.

development and ovarian cancer initiation and progression remains completely unknown. Despite this ambitious approach, exploring avenues to generate conditional knock out and knock in mouse ovary for BRD4 and Notch3 would start providing answers to these questions.

Clinical Relevance and Implications of the TPT

The use of the TPT opens a potential new door for clinicians. After further and extensive biological validation, the TPT could be easily applied in a clinical trial setting, particularly in the initial trial design. The TPT can systematically predict, biologically relevant targeted therapies which can be easily re-purposed and given in a novel combination with either standard chemotherapies or other FDA approved targeted therapies for the cancer of interest. By taking this approach, clinicians can help maximize the success of the trial and improve patient outcomes. This may be specifically relevant if the tool identifies a therapy that targets multiple downstream genes associated with poor survival in a specific tumor type. Another application for the TPT may be its use when having to take an adaptive clinical trial approach (129). In the unfortunate circumstance that a phase II or phase III clinical trial might not be producing the expected results, the TPT may aid in identifying new treatment arms to be added as an amendment to the trial instead of having to start all over again.

In the context of the results described in **Chapter III**, I demonstrated the anti-tumor effect provided by BETis in ovarian cancer pre-clinical models, based on the TPT's prediction. Based on this, we could incorporate the use of BETIs, such as CN210, and design a clinical trial to give in distinct combinations with platinum, taxol, PARPi or bevacizumab therapies (9). The use of BETis might be particularly useful in

the treatment of recurrent or advanced high grade serous ovarian cancer patients, as these cases not only have worse outcomes, but high a higher propensity for chemo-resistance (9). These applications demonstrate how the TPT and its ability to re-purpose targeted therapies may directly impact the future of cancer patient care.

BIBLIOGRAPHY

1.   Neal JW, Sledge GW. Decade in review-targeted therapy: successes, toxicities and challenges in solid tumours. Nat Rev Clin Oncol. 2014;11(11):627-8. doi: 10.1038/nrclinonc.2014.171. PubMed PMID: 25286974.

2.   Baudino TA. Targeted Cancer Therapy: The Next Generation of Cancer Treatment. Curr Drug Discov Technol. 2015;12(1):3-20. PubMed PMID: 26033233.

3.   Aggarwal S. Targeted cancer therapies. Nat Rev Drug Discov. 2010;9(6):427-8. doi: 10.1038/nrd3186. PubMed PMID: 20514063.

4.   Shih YC, Smieliauskas F, Geynisman DM, Kelly RJ, Smith TJ. Trends in the Cost and Use of Targeted Cancer Therapies for the Privately Insured Nonelderly: 2001 to 2011. J Clin Oncol. 2015;33(19):2190-6. doi: 10.1200/JCO.2014.58.2320. PubMed PMID: 25987701; PMCID: PMC4477789.

5.   Bitler BG, Watson ZL, Wheeler LJ, Behbakht K. PARP inhibitors: Clinical utility and possibilities of overcoming resistance. Gynecol Oncol. 2017;147(3):695-704. doi: 10.1016/j.ygyno.2017.10.003. PubMed PMID: 29037806; PMCID: PMC5698126.

6.   Morales J, Li L, Fattah FJ, Dong Y, Bey EA, Patel M, Gao J, Boothman DA. Review of poly (ADP-ribose) polymerase (PARP) mechanisms of action and rationale for targeting in cancer and other diseases. Crit Rev Eukaryot Gene Expr. 2014;24(1):15-28. PubMed PMID: 24579667; PMCID: PMC4806654.

7.   Farmer H, McCabe N, Lord CJ, Tutt AN, Johnson DA, Richardson TB, Santarosa M, Dillon KJ, Hickson I, Knights C, Martin NM, Jackson SP, Smith GC, Ashworth A. Targeting the DNA repair defect in BRCA mutant cells as a therapeutic strategy. Nature. 2005;434(7035):917-21. doi: 10.1038/nature03445. PubMed PMID: 15829967.

8.   Hanahan D, Weinberg RA. Hallmarks of cancer: the next generation. Cell. 2011;144(5):646-74. doi: 10.1016/j.cell.2011.02.013. PubMed PMID: 21376230.

9.   Matulonis UA, Sood AK, Fallowfield L, Howitt BE, Sehouli J, Karlan BY. Ovarian cancer. Nat Rev Dis Primers. 2016;2:16061. doi: 10.1038/nrdp.2016.61. PubMed PMID: 27558151.

10.   Kaufman B, Shapira-Frommer R, Schmutzler RK, Audeh MW, Friedlander M, Balmana J, Mitchell G, Fried G, Stemmer SM, Hubert A, Rosengarten O, Steiner M, Loman N, Bowen K, Fielding A, Domchek SM. Olaparib monotherapy in patients with advanced cancer and a germline BRCA1/2 mutation. J Clin Oncol. 2015;33(3):244-50. doi: 10.1200/JCO.2014.56.2728. PubMed PMID: 25366685.

11.   De Palma M, Biziato D, Petrova TV. Microenvironmental regulation of tumour angiogenesis. Nat Rev Cancer. 2017;17(8):457-74. doi: 10.1038/nrc.2017.51. PubMed PMID: 28706266.

12.   Keating GM. Bevacizumab: a review of its use in advanced cancer. Drugs. 2014;74(16):1891-925. doi: 10.1007/s40265-014-0302-9. PubMed PMID: 25315029.

13.   Norquist B, Wurz KA, Pennil CC, Garcia R, Gross J, Sakai W, Karlan BY, Taniguchi T, Swisher EM. Secondary somatic mutations restoring BRCA1/2 predict chemotherapy resistance in hereditary ovarian carcinomas. J Clin Oncol. 2011;29(22):3008-15. doi: 10.1200/JCO.2010.34.2980. PubMed PMID: 21709188; PMCID: PMC3157963.

14.   Barber LJ, Sandhu S, Chen L, Campbell J, Kozarewa I, Fenwick K, Assiotis I, Rodrigues DN, Reis Filho JS, Moreno V, Mateo J, Molife LR, De Bono J, Kaye S, Lord CJ, Ashworth A. Secondary mutations in BRCA2 associated with clinical resistance to a PARP inhibitor. J Pathol. 2013;229(3):422-9. doi: 10.1002/path.4140. PubMed PMID: 23165508.

15.   Lyons YA, Pradeep S, Wu SY, Haemmerle M, Hansen JM, Wagner MJ, Villar-Prados A, Nagaraja AS, Dood RL, Previs RA, Hu W, Zhao Y, Mak DH, Xiao Z, Melendez BD, Lizee GA, Mercado-Uribe I, Baggerly KA, Hwu P, Liu J, Overwijk WW, Coleman RL, Sood AK. Macrophage depletion through colony stimulating factor 1 receptor pathway blockade overcomes adaptive resistance to anti-VEGF therapy. Oncotarget. 2017;8(57):96496-505. doi: 10.18632/oncotarget.20410. PubMed PMID: 29228548; PMCID: PMC5722500.

16.   Mitamura T, Pradeep S, McGuire M, Wu SY, Ma S, Hatakeyama H, Lyons YA, Hisamatsu T, Noh K, Villar-Prados A, Chen X, Ivan C, Rodriguez-Aguayo C, Hu W, Lopez-Berestein G, Coleman RL, Sood AK. Induction of anti-VEGF therapy resistance by upregulated expression of microseminoprotein (MSMP). Oncogene. 2018;37(6):722-31. doi: 10.1038/onc.2017.348. PubMed PMID: 29059175.

17.   Azuaje F. Computational models for predicting drug responses in cancer research. Brief Bioinform. 2017;18(5):820-9. doi: 10.1093/bib/bbw065. PubMed PMID: 27444372.

18.   Gao J, Aksoy BA, Dogrusoz U, Dresdner G, Gross B, Sumer SO, Sun Y, Jacobsen A, Sinha R, Larsson E, Cerami E, Sander C, Schultz N. Integrative analysis of complex cancer genomics and clinical profiles using the cBioPortal. Sci Signal. 2013;6(269):pl1. doi: 10.1126/scisignal.2004088. PubMed PMID: 23550210; PMCID: PMC4160307.

19.   Cerami E, Gao J, Dogrusoz U, Gross BE, Sumer SO, Aksoy BA, Jacobsen A, Byrne CJ, Heuer ML, Larsson E, Antipin Y, Reva B, Goldberg AP, Sander C, Schultz N. The cBio cancer genomics portal: an open platform for exploring multidimensional cancer genomics data. Cancer Discov. 2012;2(5):401-4. doi: 10.1158/2159-8290.CD-12-0095. PubMed PMID: 22588877; PMCID: PMC3956037.

20.   Edgar R, Domrachev M, Lash AE. Gene Expression Omnibus: NCBI gene expression and hybridization array data repository. Nucleic Acids Res. 2002;30(1):207-10. PubMed PMID: 11752295; PMCID: PMC99122.

21.   Barretina J, Caponigro G, Stransky N, Venkatesan K, Margolin AA, Kim S, Wilson CJ, Lehar J, Kryukov GV, Sonkin D, Reddy A, Liu M, Murray L, Berger MF, Monahan JE, Morais P, Meltzer J, Korejwa A, Jane-Valbuena J, Mapa FA, Thibault J, Bric-Furlong E, Raman P, Shipway A, Engels IH, Cheng J, Yu GK, Yu J, Aspesi P, Jr., de Silva M, Jagtap K, Jones MD, Wang L, Hatton C, Palescandolo E, Gupta S, Mahan S, Sougnez C, Onofrio RC, Liefeld T, MacConaill L, Winckler W, Reich M, Li N, Mesirov JP, Gabriel SB, Getz G, Ardlie K, Chan V, Myer VE, Weber BL, Porter J, Warmuth M, Finan P, Harris JL, Meyerson M, Golub TR, Morrissey MP, Sellers WR, Schlegel R, Garraway LA. The Cancer Cell Line Encyclopedia

enables predictive modelling of anticancer drug sensitivity. Nature. 2012;483(7391):603-7. doi: 10.1038/nature11003. PubMed PMID: 22460905; PMCID: PMC3320027.

22.   Garnett MJ, Edelman EJ, Heidorn SJ, Greenman CD, Dastur A, Lau KW, Greninger P, Thompson IR, Luo X, Soares J, Liu Q, Iorio F, Surdez D, Chen L, Milano RJ, Bignell GR, Tam AT, Davies H, Stevenson JA, Barthorpe S, Lutz SR, Kogera F, Lawrence K, McLaren-Douglas A, Mitropoulos X, Mironenko T, Thi H, Richardson L, Zhou W, Jewitt F, Zhang T, O'Brien P, Boisvert JL, Price S, Hur W, Yang W, Deng X, Butler A, Choi HG, Chang JW, Baselga J, Stamenkovic I, Engelman JA, Sharma SV, Delattre O, Saez-Rodriguez J, Gray NS, Settleman J, Futreal PA, Haber DA, Stratton MR, Ramaswamy S, McDermott U, Benes CH. Systematic identification of genomic markers of drug sensitivity in cancer cells. Nature. 2012;483(7391):570-5. doi: 10.1038/nature11005. PubMed PMID: 22460902; PMCID: PMC3349233.

23.   Lamb J, Crawford ED, Peck D, Modell JW, Blat IC, Wrobel MJ, Lerner J, Brunet JP, Subramanian A, Ross KN, Reich M, Hieronymus H, Wei G, Armstrong SA, Haggarty SJ, Clemons PA, Wei R, Carr SA, Lander ES, Golub TR. The Connectivity Map: using gene-expression signatures to connect small molecules, genes, and disease. Science. 2006;313(5795):1929-35. doi: 10.1126/science.1132939. PubMed PMID: 17008526.

24.   Louhimo R, Laakso M, Belitskin D, Klefstrom J, Lehtonen R, Hautaniemi S. Data integration to prioritize drugs using genomics and curated data. BioData Min. 2016;9:21. doi: 10.1186/s13040-016-0097-1. PubMed PMID: 27231484; PMCID: PMC4881054.

25.   San Lucas FA, Fowler J, Chang K, Kopetz S, Vilar E, Scheet P. Cancer in silico drug discovery: a systems biology tool for identifying candidate drugs to target specific molecular tumor subtypes. Mol Cancer Ther. 2014;13(12):3230-40. doi: 10.1158/1535-7163.MCT-14-0260. PubMed PMID: 25349306; PMCID: PMC4341901.

26.   Sheng J, Li F, Wong ST. Optimal drug prediction from personal genomics profiles. IEEE J Biomed Health Inform. 2015;19(4):1264-70. doi: 10.1109/JBHI.2015.2412522. PubMed PMID: 25781964; PMCID: PMC4532321.

27. Huang C, Mezencev R, McDonald JF, Vannberg F. Open source machine-learning algorithms for the prediction of optimal cancer drug therapies. PLoS One. 2017;12(10):e0186906. doi: 10.1371/journal.pone.0186906. PubMed PMID: 29073279; PMCID: PMC5658085.

28. Siegel RL, Miller KD, Jemal A. Cancer statistics, 2016. CA Cancer J Clin. 2016;66(1):7-30. doi: 10.3322/caac.21332. PubMed PMID: 26742998.

29. Romero I, Bast RC, Jr. Minireview: human ovarian cancer: biology, current management, and paths to personalizing therapy. Endocrinology. 2012;153(4):1593-602. doi: 10.1210/en.2011-2123. PubMed PMID: 22416079; PMCID: PMC3320264.

30. Kindelberger DW, Lee Y, Miron A, Hirsch MS, Feltmate C, Medeiros F, Callahan MJ, Garner EO, Gordon RW, Birch C, Berkowitz RS, Muto MG, Crum CP. Intraepithelial carcinoma of the fimbria and pelvic serous carcinoma: Evidence for a causal relationship. Am J Surg Pathol. 2007;31(2):161-9. doi: 10.1097/01.pas.0000213335.40358.47. PubMed PMID: 17255760.

31. George SH, Garcia R, Slomovitz BM. Ovarian Cancer: The Fallopian Tube as the Site of Origin and Opportunities for Prevention. Front Oncol. 2016;6:108. doi: 10.3389/fonc.2016.00108. PubMed PMID: 27200296; PMCID: PMC4852190.

32. Chang SJ, Hodeib M, Chang J, Bristow RE. Survival impact of complete cytoreduction to no gross residual disease for advanced-stage ovarian cancer: a meta-analysis. Gynecol Oncol. 2013;130(3):493-8. doi: 10.1016/j.ygyno.2013.05.040. PubMed PMID: 23747291.

33. Choi YE, Meghani K, Brault ME, Leclerc L, He YJ, Day TA, Elias KM, Drapkin R, Weinstock DM, Dao F, Shih KK, Matulonis U, Levine DA, Konstantinopoulos PA, Chowdhury D. Platinum and PARP Inhibitor Resistance Due to Overexpression of MicroRNA-622 in BRCA1-Mutant Ovarian Cancer. Cell Rep. 2016;14(3):429-39. doi: 10.1016/j.celrep.2015.12.046. PubMed PMID: 26774475; PMCID: PMC4731274.

34. Stathis A, Bertoni F. BET Proteins as Targets for Anticancer Treatment. Cancer Discov. 2018;8(1):24-36. doi: 10.1158/2159-8290.CD-17-0605. PubMed PMID: 29263030.

35.   Filippakopoulos P, Knapp S. Targeting bromodomains: epigenetic readers of lysine acetylation. Nat Rev Drug Discov. 2014;13(5):337-56. doi: 10.1038/nrd4286. PubMed PMID: 24751816.

36.   Taniguchi Y. The Bromodomain and Extra-Terminal Domain (BET) Family: Functional Anatomy of BET Paralogous Proteins. Int J Mol Sci. 2016;17(11). doi: 10.3390/ijms17111849. PubMed PMID: 27827996; PMCID: PMC5133849.

37.   Kanno T, Kanno Y, LeRoy G, Campos E, Sun HW, Brooks SR, Vahedi G, Heightman TD, Garcia BA, Reinberg D, Siebenlist U, O'Shea JJ, Ozato K. BRD4 assists elongation of both coding and enhancer RNAs by interacting with acetylated histones. Nat Struct Mol Biol. 2014;21(12):1047-57. doi: 10.1038/nsmb.2912. PubMed PMID: 25383670; PMCID: PMC4720983.

38.   Wu SY, Lee AY, Lai HT, Zhang H, Chiang CM. Phospho switch triggers Brd4 chromatin binding and activator recruitment for gene-specific targeting. Mol Cell. 2013;49(5):843-57. doi: 10.1016/j.molcel.2012.12.006. PubMed PMID: 23317504; PMCID: PMC3595396.

39.   Yang Z, He N, Zhou Q. Brd4 recruits P-TEFb to chromosomes at late mitosis to promote G1 gene expression and cell cycle progression. Mol Cell Biol. 2008;28(3):967-76. doi: 10.1128/MCB.01020-07. PubMed PMID: 18039861; PMCID: PMC2223388.

40.   Wang R, Li Q, Helfer CM, Jiao J, You J. Bromodomain protein Brd4 associated with acetylated chromatin is important for maintenance of higher-order chromatin structure. J Biol Chem. 2012;287(14):10738-52. doi: 10.1074/jbc.M111.323493. PubMed PMID: 22334664; PMCID: PMC3322821.

41.   Wu SY, Chiang CM. The double bromodomain-containing chromatin adaptor Brd4 and transcriptional regulation. J Biol Chem. 2007;282(18):13141-5. doi: 10.1074/jbc.R700001200. PubMed PMID: 17329240.

42.   Zuber J, Shi J, Wang E, Rappaport AR, Herrmann H, Sison EA, Magoon D, Qi J, Blatt K, Wunderlich M, Taylor MJ, Johns C, Chicas A, Mulloy JC, Kogan SC, Brown P, Valent P, Bradner JE, Lowe SW, Vakoc CR. RNAi screen identifies Brd4 as a therapeutic target in acute

myeloid leukaemia. Nature. 2011;478(7370):524-8. doi: 10.1038/nature10334. PubMed PMID: 21814200; PMCID: PMC3328300.

43.   Delmore JE, Issa GC, Lemieux ME, Rahl PB, Shi J, Jacobs HM, Kastritis E, Gilpatrick T, Paranal RM, Qi J, Chesi M, Schinzel AC, McKeown MR, Heffernan TP, Vakoc CR, Bergsagel PL, Ghobrial IM, Richardson PG, Young RA, Hahn WC, Anderson KC, Kung AL, Bradner JE, Mitsiades CS. BET bromodomain inhibition as a therapeutic strategy to target c-Myc. Cell. 2011;146(6):904-17. doi: 10.1016/j.cell.2011.08.017. PubMed PMID: 21889194; PMCID: PMC3187920.

44.   Mertz JA, Conery AR, Bryant BM, Sandy P, Balasubramanian S, Mele DA, Bergeron L, Sims RJ, 3rd. Targeting MYC dependence in cancer by inhibiting BET bromodomains. Proc Natl Acad Sci U S A. 2011;108(40):16669-74. doi: 10.1073/pnas.1108190108. PubMed PMID: 21949397; PMCID: PMC3189078.

45.   Filippakopoulos P, Qi J, Picaud S, Shen Y, Smith WB, Fedorov O, Morse EM, Keates T, Hickman TT, Felletar I, Philpott M, Munro S, McKeown MR, Wang Y, Christie AL, West N, Cameron MJ, Schwartz B, Heightman TD, La Thangue N, French CA, Wiest O, Kung AL, Knapp S, Bradner JE. Selective inhibition of BET bromodomains. Nature. 2010;468(7327):1067-73. doi: 10.1038/nature09504. PubMed PMID: 20871596; PMCID: PMC3010259.

46.   Lee JE, Park YK, Park S, Jang Y, Waring N, Dey A, Ozato K, Lai B, Peng W, Ge K. Brd4 binds to active enhancers to control cell identity gene induction in adipogenesis and myogenesis. Nat Commun. 2017;8(1):2217. doi: 10.1038/s41467-017-02403-5. PubMed PMID: 29263365; PMCID: PMC5738375.

47.   Wadhwa E, Nicolaides T. Bromodomain Inhibitor Review: Bromodomain and Extra-terminal Family Protein Inhibitors as a Potential New Therapy in Central Nervous System Tumors. Cureus. 2016;8(5):e620. doi: 10.7759/cureus.620. PubMed PMID: 27382528; PMCID: PMC4917374.

48.	Qiu H, Li J, Clark LH, Jackson AL, Zhang L, Guo H, Kilgore JE, Gehrig PA, Zhou C, Bae-Jump VL. JQ1 suppresses tumor growth via PTEN/PI3K/AKT pathway in endometrial cancer. Oncotarget. 2016;7(41):66809-21. doi: 10.18632/oncotarget.11631. PubMed PMID: 27572308; PMCID: PMC5341839.

49.	Wu T, Donohoe ME. The converging roles of BRD4 and gene transcription in pluripotency and oncogenesis. RNA Dis. 2015;2(3). PubMed PMID: 26405693; PMCID: PMC4578175.

50.	Bryant JM, Donahue G, Wang X, Meyer-Ficca M, Luense LJ, Weller AH, Bartolomei MS, Blobel GA, Meyer RG, Garcia BA, Berger SL. Characterization of BRD4 during mammalian postmeiotic sperm development. Mol Cell Biol. 2015;35(8):1433-48. doi: 10.1128/MCB.01328-14. PubMed PMID: 25691659; PMCID: PMC4372693.

51.	Liu W, Stein P, Cheng X, Yang W, Shao NY, Morrisey EE, Schultz RM, You J. BRD4 regulates Nanog expression in mouse embryonic stem cells and preimplantation embryos. Cell Death Differ. 2014;21(12):1950-60. doi: 10.1038/cdd.2014.124. PubMed PMID: 25146928; PMCID: PMC4227152.

52.	Asangani IA, Dommeti VL, Wang X, Malik R, Cieslik M, Yang R, Escara-Wilke J, Wilder-Romans K, Dhanireddy S, Engelke C, Iyer MK, Jing X, Wu YM, Cao X, Qin ZS, Wang S, Feng FY, Chinnaiyan AM. Therapeutic targeting of BET bromodomain proteins in castration-resistant prostate cancer. Nature. 2014;510(7504):278-82. doi: 10.1038/nature13229. PubMed PMID: 24759320; PMCID: PMC4075966.

53.	Sahai V, Kumar K, Knab LM, Chow CR, Raza SS, Bentrem DJ, Ebine K, Munshi HG. BET bromodomain inhibitors block growth of pancreatic cancer cells in three-dimensional collagen. Mol Cancer Ther. 2014;13(7):1907-17. doi: 10.1158/1535-7163.MCT-13-0925. PubMed PMID: 24807963; PMCID: PMC4090266.

54.	French CA, Rahman S, Walsh EM, Kuhnle S, Grayson AR, Lemieux ME, Grunfeld N, Rubin BP, Antonescu CR, Zhang S, Venkatramani R, Dal Cin P, Howley PM. NSD3-NUT fusion oncoprotein in NUT midline carcinoma: implications for a novel oncogenic mechanism.

Cancer Discov. 2014;4(8):928-41. doi: 10.1158/2159-8290.CD-14-0014. PubMed PMID: 24875858; PMCID: PMC4125436.

55.   French CA, Ramirez CL, Kolmakova J, Hickman TT, Cameron MJ, Thyne ME, Kutok JL, Toretsky JA, Tadavarthy AK, Kees UR, Fletcher JA, Aster JC. BRD-NUT oncoproteins: a family of closely related nuclear proteins that block epithelial differentiation and maintain the growth of carcinoma cells. Oncogene. 2008;27(15):2237-42. doi: 10.1038/sj.onc.1210852. PubMed PMID: 17934517.

56.   Jung JG, Stoeck A, Guan B, Wu RC, Zhu H, Blackshaw S, Shih Ie M, Wang TL. Notch3 interactome analysis identified WWP2 as a negative regulator of Notch3 signaling in ovarian cancer. PLoS Genet. 2014;10(10):e1004751. doi: 10.1371/journal.pgen.1004751. PubMed PMID: 25356737; PMCID: PMC4214668.

57.   Hu W, Liu T, Ivan C, Sun Y, Huang J, Mangala LS, Miyake T, Dalton HJ, Pradeep S, Rupaimoole R, Previs RA, Han HD, Bottsford-Miller J, Zand B, Kang Y, Pecot CV, Nick AM, Wu SY, Lee JS, Sehgal V, Ram P, Liu J, Tucker SL, Lopez-Berestein G, Baggerly KA, Coleman RL, Sood AK. Notch3 pathway alterations in ovarian cancer. Cancer Res. 2014;74(12):3282-93. doi: 10.1158/0008-5472.CAN-13-2066. PubMed PMID: 24743243; PMCID: PMC4058356.

58.   Rahman MT, Nakayama K, Rahman M, Katagiri H, Katagiri A, Ishibashi T, Ishikawa M, Iida K, Nakayama S, Otsuki Y, Miyazaki K. Notch3 overexpression as potential therapeutic target in advanced stage chemoresistant ovarian cancer. Am J Clin Pathol. 2012;138(4):535-44. doi: 10.1309/AJCPKDLRQ8F3EWNS. PubMed PMID: 23010708.

59.   Chen X, Thiaville MM, Chen L, Stoeck A, Xuan J, Gao M, Shih Ie M, Wang TL. Defining NOTCH3 target genes in ovarian cancer. Cancer Res. 2012;72(9):2294-303. doi: 10.1158/0008-5472.CAN-11-2181. PubMed PMID: 22396495; PMCID: PMC3342447.

60.   Andersson ER, Sandberg R, Lendahl U. Notch signaling: simplicity in design, versatility in function. Development. 2011;138(17):3593-612. doi: 10.1242/dev.063610. PubMed PMID: 21828089.

61.   Kopan R, Ilagan MX. The canonical Notch signaling pathway: unfolding the activation mechanism. Cell. 2009;137(2):216-33. doi: 10.1016/j.cell.2009.03.045. PubMed PMID: 19379690; PMCID: PMC2827930.

62.   Osanyingbemi-Obidi J, Dobromilskaya I, Illei PB, Hann CL, Rudin CM. Notch signaling contributes to lung cancer clonogenic capacity in vitro but may be circumvented in tumorigenesis in vivo. Mol Cancer Res. 2011;9(12):1746-54. doi: 10.1158/1541-7786.MCR-11-0286. PubMed PMID: 21994468; PMCID: PMC3243765.

63.   Vermezovic J, Adamowicz M, Santarpia L, Rustighi A, Forcato M, Lucano C, Massimiliano L, Costanzo V, Bicciato S, Del Sal G, d'Adda di Fagagna F. Notch is a direct negative regulator of the DNA-damage response. Nat Struct Mol Biol. 2015;22(5):417-24. doi: 10.1038/nsmb.3013. PubMed PMID: 25895060.

64.   Tanigaki K, Nogaki F, Takahashi J, Tashiro K, Kurooka H, Honjo T. Notch1 and Notch3 instructively restrict bFGF-responsive multipotent neural progenitor cells to an astroglial fate. Neuron. 2001;29(1):45-55. PubMed PMID: 11182080.

65.   Bellavia D, Checquolo S, Campese AF, Felli MP, Gulino A, Screpanti I. Notch3: from subtle structural differences to functional diversity. Oncogene. 2008;27(38):5092-8. doi: 10.1038/onc.2008.230. PubMed PMID: 18758477.

66.   Domenga V, Fardoux P, Lacombe P, Monet M, Maciazek J, Krebs LT, Klonjkowski B, Berrou E, Mericskay M, Li Z, Tournier-Lasserve E, Gridley T, Joutel A. Notch3 is required for arterial identity and maturation of vascular smooth muscle cells. Genes Dev. 2004;18(22):2730-5. doi: 10.1101/gad.308904. PubMed PMID: 15545631; PMCID: PMC528893.

67.   Joutel A, Monet M, Domenga V, Riant F, Tournier-Lasserve E. Pathogenic mutations associated with cerebral autosomal dominant arteriopathy with subcortical infarcts and leukoencephalopathy differently affect Jagged1 binding and Notch3 activity via the RBP/JK signaling Pathway. Am J Hum Genet. 2004;74(2):338-47. doi: 10.1086/381506. PubMed PMID: 14714274; PMCID: PMC1181931.

68.   Li X, Zhang X, Leathers R, Makino A, Huang C, Parsa P, Macias J, Yuan JX, Jamieson SW, Thistlethwaite PA. Notch3 signaling promotes the development of pulmonary arterial hypertension. Nat Med. 2009;15(11):1289-97. doi: 10.1038/nm.2021. PubMed PMID: 19855400; PMCID: PMC2780347.

69.   Dang TP, Gazdar AF, Virmani AK, Sepetavec T, Hande KR, Minna JD, Roberts JR, Carbone DP. Chromosome 19 translocation, overexpression of Notch3, and human lung cancer. J Natl Cancer Inst. 2000;92(16):1355-7. PubMed PMID: 10944559.

70.   Dang TP, Eichenberger S, Gonzalez A, Olson S, Carbone DP. Constitutive activation of Notch3 inhibits terminal epithelial differentiation in lungs of transgenic mice. Oncogene. 2003;22(13):1988-97. doi: 10.1038/sj.onc.1206230. PubMed PMID: 12673204.

71.   Bernasconi-Elias P, Hu T, Jenkins D, Firestone B, Gans S, Kurth E, Capodieci P, Deplazes-Lauber J, Petropoulos K, Thiel P, Ponsel D, Hee Choi S, LeMotte P, London A, Goetcshkes M, Nolin E, Jones MD, Slocum K, Kluk MJ, Weinstock DM, Christodoulou A, Weinberg O, Jaehrling J, Ettenberg SA, Buckler A, Blacklow SC, Aster JC, Fryer CJ. Characterization of activating mutations of NOTCH3 in T-cell acute lymphoblastic leukemia and anti-leukemic activity of NOTCH3 inhibitory antibodies. Oncogene. 2016;35(47):6077-86. doi: 10.1038/onc.2016.133. PubMed PMID: 27157619; PMCID: PMC5102827.

72.   Yamaguchi N, Oyama T, Ito E, Satoh H, Azuma S, Hayashi M, Shimizu K, Honma R, Yanagisawa Y, Nishikawa A, Kawamura M, Imai J, Ohwada S, Tatsuta K, Inoue J, Semba K, Watanabe S. NOTCH3 signaling pathway plays crucial roles in the proliferation of ErbB2-negative human breast cancer cells. Cancer Res. 2008;68(6):1881-8. doi: 10.1158/0008-5472.CAN-07-1597. PubMed PMID: 18339869.

73.   Guest RV, Boulter L, Dwyer BJ, Kendall TJ, Man TY, Minnis-Lyons SE, Lu WY, Robson AJ, Gonzalez SF, Raven A, Wojtacha D, Morton JP, Komuta M, Roskams T, Wigmore SJ, Sansom OJ, Forbes SJ. Notch3 drives development and progression of cholangiocarcinoma. Proc Natl Acad Sci U S A. 2016;113(43):12250-5. doi: 10.1073/pnas.1600067113. PubMed PMID: 27791012; PMCID: PMC5086988.

74.   Park JT, Chen X, Trope CG, Davidson B, Shih Ie M, Wang TL. Notch3 overexpression is related to the recurrence of ovarian cancer and confers resistance to carboplatin. Am J Pathol. 2010;177(3):1087-94. doi: 10.2353/ajpath.2010.100316. PubMed PMID: 20671266; PMCID: PMC2928943.

75.   Jung SG, Kwon YD, Song JA, Back MJ, Lee SY, Lee C, Hwang YY, An HJ. Prognostic significance of Notch 3 gene expression in ovarian serous carcinoma. Cancer Sci. 2010;101(9):1977-83. doi: 10.1111/j.1349-7006.2010.01641.x. PubMed PMID: 20624166.

76.   Takebe N, Nguyen D, Yang SX. Targeting notch signaling pathway in cancer: clinical development advances and challenges. Pharmacol Ther. 2014;141(2):140-9. doi: 10.1016/j.pharmthera.2013.09.005. PubMed PMID: 24076266; PMCID: PMC3982918.

77.   McAuliffe SM, Morgan SL, Wyant GA, Tran LT, Muto KW, Chen YS, Chin KT, Partridge JC, Poole BB, Cheng KH, Daggett J, Jr., Cullen K, Kantoff E, Hasselbatt K, Berkowitz J, Muto MG, Berkowitz RS, Aster JC, Matulonis UA, Dinulescu DM. Targeting Notch, a key pathway for ovarian cancer stem cells, sensitizes tumors to platinum therapy. Proc Natl Acad Sci U S A. 2012;109(43):E2939-48. doi: 10.1073/pnas.1206400109. PubMed PMID: 23019585; PMCID: PMC3491453.

78.   Ucar D, Lin DI. Amplification of the bromodomain-containing protein 4 gene in ovarian high-grade serous carcinoma is associated with worse prognosis and survival. Mol Clin Oncol. 2015;3(6):1291-4. doi: 10.3892/mco.2015.622. PubMed PMID: 26807235; PMCID: PMC4667564.

79.   Landen CN, Jr., Chavez-Reyes A, Bucana C, Schmandt R, Deavers MT, Lopez-Berestein G, Sood AK. Therapeutic EphA2 gene targeting in vivo using neutral liposomal small interfering RNA delivery. Cancer Res. 2005;65(15):6910-8. doi: 10.1158/0008-5472.CAN-05-0530. PubMed PMID: 16061675.

80.   Tibes R, Qiu Y, Lu Y, Hennessy B, Andreeff M, Mills GB, Kornblau SM. Reverse phase protein array: validation of a novel proteomic technology and utility for analysis of primary

leukemia specimens and hematopoietic stem cells. Mol Cancer Ther. 2006;5(10):2512-21. doi: 10.1158/1535-7163.MCT-06-0334. PubMed PMID: 17041095.

81.   Komurov K, Dursun S, Erdin S, Ram PT. NetWalker: a contextual network analysis tool for functional genomics. BMC Genomics. 2012;13:282. doi: 10.1186/1471-2164-13-282. PubMed PMID: 22732065; PMCID: PMC3439272.

82.   Asangani IA, Wilder-Romans K, Dommeti VL, Krishnamurthy PM, Apel IJ, Escara-Wilke J, Plymate SR, Navone NM, Wang S, Feng FY, Chinnaiyan AM. BET Bromodomain Inhibitors Enhance Efficacy and Disrupt Resistance to AR Antagonists in the Treatment of Prostate Cancer. Mol Cancer Res. 2016;14(4):324-31. doi: 10.1158/1541-7786.MCR-15-0472. PubMed PMID: 26792867; PMCID: PMC4834259.

83.   Shu S, Lin CY, He HH, Witwicki RM, Tabassum DP, Roberts JM, Janiszewska M, Huh SJ, Liang Y, Ryan J, Doherty E, Mohammed H, Guo H, Stover DG, Ekram MB, Brown J, D'Santos C, Krop IE, Dillon D, McKeown M, Ott C, Qi J, Ni M, Rao PK, Duarte M, Wu SY, Chiang CM, Anders L, Young RA, Winer E, Letai A, Barry WT, Carroll JS, Long H, Brown M, Liu XS, Meyer CA, Bradner JE, Polyak K. Response and resistance to BET bromodomain inhibitors in triple-negative breast cancer. Nature. 2016;529(7586):413-7. doi: 10.1038/nature16508. PubMed PMID: 26735014; PMCID: PMC4854653.

84.   Shah MM, Zerlin M, Li BY, Herzog TJ, Kitajewski JK, Wright JD. The role of Notch and gamma-secretase inhibition in an ovarian cancer model. Anticancer Res. 2013;33(3):801-8. PubMed PMID: 23482747; PMCID: PMC3893696.

85.   Campos MP, Konecny GE. The target invites a foe: antibody-drug conjugates in gynecologic oncology. Curr Opin Obstet Gynecol. 2017. doi: 10.1097/GCO.0000000000000432. PubMed PMID: 29227302.

86.   Chaidos A, Caputo V, Karadimitris A. Inhibition of bromodomain and extra-terminal proteins (BET) as a potential therapeutic approach in haematological malignancies: emerging preclinical and clinical evidence. Ther Adv Hematol. 2015;6(3):128-41. doi: 10.1177/2040620715576662. PubMed PMID: 26137204; PMCID: PMC4480520.

87.   Corzo C, Iniesta MD, Patrono MG, Lu KH, Ramirez PT. Role of Fallopian Tubes in the Development of Ovarian Cancer. J Minim Invasive Gynecol. 2017;24(2):230-4. doi: 10.1016/j.jmig.2016.12.007. PubMed PMID: 28007588.

88.   Wong C, Laddha SV, Tang L, Vosburgh E, Levine AJ, Normant E, Sandy P, Harris CR, Chan CS, Xu EY. The bromodomain and extra-terminal inhibitor CPI203 enhances the antiproliferative effects of rapamycin on human neuroendocrine tumors. Cell Death Dis. 2014;5:e1450. doi: 10.1038/cddis.2014.396. PubMed PMID: 25299775; PMCID: PMC4237236.

89.   Moros A, Rodriguez V, Saborit-Villarroya I, Montraveta A, Balsas P, Sandy P, Martinez A, Wiestner A, Normant E, Campo E, Perez-Galan P, Colomer D, Roue G. Synergistic antitumor activity of lenalidomide with the BET bromodomain inhibitor CPI203 in bortezomib-resistant mantle cell lymphoma. Leukemia. 2014;28(10):2049-59. doi: 10.1038/leu.2014.106. PubMed PMID: 24721791.

90.   Mitra AK, Davis DA, Tomar S, Roy L, Gurler H, Xie J, Lantvit DD, Cardenas H, Fang F, Liu Y, Loughran E, Yang J, Sharon Stack M, Emerson RE, Cowden Dahl KD, M VB, Nephew KP, Matei D, Burdette JE. In vivo tumor growth of high-grade serous ovarian cancer cell lines. Gynecol Oncol. 2015;138(2):372-7. doi: 10.1016/j.ygyno.2015.05.040. PubMed PMID: 26050922; PMCID: PMC4528621.

91.   Cawthorne C, Swindell R, Stratford IJ, Dive C, Welman A. Comparison of doxycycline delivery methods for Tet-inducible gene expression in a subcutaneous xenograft model. J Biomol Tech. 2007;18(2):120-3. PubMed PMID: 17496224; PMCID: PMC2062538.

92.   Devaiah BN, Lewis BA, Cherman N, Hewitt MC, Albrecht BK, Robey PG, Ozato K, Sims RJ, 3rd, Singer DS. BRD4 is an atypical kinase that phosphorylates serine2 of the RNA polymerase II carboxy-terminal domain. Proc Natl Acad Sci U S A. 2012;109(18):6927-32. doi: 10.1073/pnas.1120422109. PubMed PMID: 22509028; PMCID: PMC3345009.

93.   Wagner MJ, Mitra R, McArthur MJ, Baze W, Barnhart K, Wu SY, Rodriguez-Aguayo C, Zhang X, Coleman RL, Lopez-Berestein G, Sood AK. Preclinical Mammalian Safety Studies of EPHARNA   (DOPC   Nanoliposomal   EphA2-Targeted   siRNA).   Mol   Cancer   Ther.

2017;16(6):1114-23. doi: 10.1158/1535-7163.MCT-16-0541. PubMed PMID: 28265009; PMCID: PMC5457703.

94.   Wu X, Liu D, Tao D, Xiang W, Xiao X, Wang M, Wang L, Luo G, Li Y, Zeng F, Jiang G. BRD4 Regulates EZH2 Transcription through Upregulation of C-MYC and Represents a Novel Therapeutic Target in Bladder Cancer. Mol Cancer Ther. 2016;15(5):1029-42. doi: 10.1158/1535-7163.MCT-15-0750. PubMed PMID: 26939702.

95.   Zampieri M, Ciccarone F, Palermo R, Cialfi S, Passananti C, Chiaretti S, Nocchia D, Talora C, Screpanti I, Caiafa P. The epigenetic factor BORIS/CTCFL regulates the NOTCH3 gene expression in cancer cells. Biochim Biophys Acta. 2014;1839(9):813-25. doi: 10.1016/j.bbagrm.2014.06.017. PubMed PMID: 24984200.

96.   Peters S, Kerr KM, Stahel R. PD-1 blockade in advanced NSCLC: A focus on pembrolizumab. Cancer Treat Rev. 2018;62:39-49. doi: 10.1016/j.ctrv.2017.10.002. PubMed PMID: 29156447.

97.   Martz CA, Ottina KA, Singleton KR, Jasper JS, Wardell SE, Peraza-Penton A, Anderson GR, Winter PS, Wang T, Alley HM, Kwong LN, Cooper ZA, Tetzlaff M, Chen PL, Rathmell JC, Flaherty KT, Wargo JA, McDonnell DP, Sabatini DM, Wood KC. Systematic identification of signaling pathways with potential to confer anticancer drug resistance. Sci Signal. 2014;7(357):ra121. doi: 10.1126/scisignal.aaa1877. PubMed PMID: 25538079; PMCID: PMC4353587.

98.   Qin Y, Conley AP, Grimm EA, Roszik J. A tool for discovering drug sensitivity and gene expression associations in cancer cells. PLoS One. 2017;12(4):e0176763. doi: 10.1371/journal.pone.0176763. PubMed PMID: 28453553; PMCID: PMC5409143.

99.   Plenge RM, Scolnick EM, Altshuler D. Validating therapeutic targets through human genetics. Nat Rev Drug Discov. 2013;12(8):581-94. doi: 10.1038/nrd4051. PubMed PMID: 23868113.

100.   Horvath P, Aulner N, Bickle M, Davies AM, Nery ED, Ebner D, Montoya MC, Ostling P, Pietiainen V, Price LS, Shorte SL, Turcatti G, von Schantz C, Carragher NO. Screening out

irrelevant cell-based models of disease. Nat Rev Drug Discov. 2016;15(11):751-69. doi: 10.1038/nrd.2016.175. PubMed PMID: 27616293.

101.   Baratta MG, Schinzel AC, Zwang Y, Bandopadhayay P, Bowman-Colin C, Kutt J, Curtis J, Piao H, Wong LC, Kung AL, Beroukhim R, Bradner JE, Drapkin R, Hahn WC, Liu JF, Livingston DM. An in-tumor genetic screen reveals that the BET bromodomain protein, BRD4, is a potential therapeutic target in ovarian carcinoma. Proc Natl Acad Sci U S A. 2015;112(1):232-7. doi: 10.1073/pnas.1422165112. PubMed PMID: 25535366; PMCID: PMC4291641.

102.   Jing Y, Zhang Z, Ma P, An S, Shen Y, Zhu L, Zhuang G. Concomitant BET and MAPK blockade for effective treatment of ovarian cancer. Oncotarget. 2016;7(3):2545-54. doi: 10.18632/oncotarget.6309. PubMed PMID: 26575423; PMCID: PMC4823054.

103.   Kurimchak AM, Shelton C, Duncan KE, Johnson KJ, Brown J, O'Brien S, Gabbasov R, Fink LS, Li Y, Lounsbury N, Abou-Gharbia M, Childers WE, Connolly DC, Chernoff J, Peterson JR, Duncan JS. Resistance to BET Bromodomain Inhibitors Is Mediated by Kinome Reprogramming in Ovarian Cancer. Cell Rep. 2016;16(5):1273-86. doi: 10.1016/j.celrep.2016.06.091. PubMed PMID: 27452461; PMCID: PMC4972668.

104.   Yokoyama Y, Zhu H, Lee JH, Kossenkov AV, Wu SY, Wickramasinghe JM, Yin X, Palozola KC, Gardini A, Showe LC, Zaret KS, Liu Q, Speicher D, Conejo-Garcia JR, Bradner JE, Zhang Z, Sood AK, Ordog T, Bitler BG, Zhang R. BET Inhibitors Suppress ALDH Activity by Targeting ALDH1A1 Super-Enhancer in Ovarian Cancer. Cancer Res. 2016;76(21):6320-30. doi: 10.1158/0008-5472.CAN-16-0854. PubMed PMID: 27803105; PMCID: PMC5117661.

105.   Zhang Z, Ma P, Jing Y, Yan Y, Cai MC, Zhang M, Zhang S, Peng H, Ji ZL, Di W, Gu Z, Gao WQ, Zhuang G. BET Bromodomain Inhibition as a Therapeutic Strategy in Ovarian Cancer by Downregulating FoxM1. Theranostics. 2016;6(2):219-30. doi: 10.7150/thno.13178. PubMed PMID: 26877780; PMCID: PMC4729770.

106.   You J, Li Q, Wu C, Kim J, Ottinger M, Howley PM. Regulation of aurora B expression by the bromodomain protein Brd4. Mol Cell Biol. 2009;29(18):5094-103. doi: 10.1128/MCB.00299-09. PubMed PMID: 19596781; PMCID: PMC2738288.

107.   Rodriguez RM, Suarez-Alvarez B, Salvanes R, Huidobro C, Torano EG, Garcia-Perez JL, Lopez-Larrea C, Fernandez AF, Bueno C, Menendez P, Fraga MF. Role of BRD4 in hematopoietic differentiation of embryonic stem cells. Epigenetics. 2014;9(4):566-78. doi: 10.4161/epi.27711. PubMed PMID: 24445267; PMCID: PMC4121367.

108.   Chen C, Wang X, Huang S, Wang L, Han L, Yu S. Prognostic roles of Notch receptor mRNA expression in human ovarian cancer. Oncotarget. 2017;8(20):32731-40. doi: 10.18632/oncotarget.16387. PubMed PMID: 28415574; PMCID: PMC5464823.

109.   Wang H, Zang C, Liu XS, Aster JC. The role of Notch receptors in transcriptional regulation. J Cell Physiol. 2015;230(5):982-8. doi: 10.1002/jcp.24872. PubMed PMID: 25418913; PMCID: PMC4442318.

110.   Gagan J, Dey BK, Layer R, Yan Z, Dutta A. Notch3 and Mef2c proteins are mutually antagonistic via Mkp1 protein and miR-1/206 microRNAs in differentiating myoblasts. J Biol Chem. 2012;287(48):40360-70. doi: 10.1074/jbc.M112.378414. PubMed PMID: 23055528; PMCID: PMC3504751.

111.   Choi SH, Severson E, Pear WS, Liu XS, Aster JC, Blacklow SC. The common oncogenomic program of NOTCH1 and NOTCH3 signaling in T-cell acute lymphoblastic leukemia. PLoS One. 2017;12(10):e0185762. doi: 10.1371/journal.pone.0185762. PubMed PMID: 29023469; PMCID: PMC5638296.

112.   Buhtoiarova TN, Brenner CA, Singh M. Endometrial Carcinoma: Role of Current and Emerging Biomarkers in Resolving Persistent Clinical Dilemmas. Am J Clin Pathol. 2016;145(1):8-21. doi: 10.1093/ajcp/aqv014. PubMed PMID: 26712866.

113.   Wang Y, Yang D, Cogdell D, Hu L, Xue F, Broaddus R, Zhang W. Genomic characterization of gene copy-number aberrations in endometrial carcinoma cell lines derived from endometrioid-type endometrial adenocarcinoma. Technol Cancer Res Treat.

2010;9(2):179-89. doi: 10.1177/153303461000900207. PubMed PMID: 20218740; PMCID: PMC5120669.

114.   Santala S, Talvensaari-Mattila A, Soini Y, Santala M. Prognostic value of cyclin B in endometrial endometrioid adenocarcinoma. Tumour Biol. 2015;36(2):953-7. doi: 10.1007/s13277-014-2676-4. PubMed PMID: 25315186.

115.   Jackman M, Lindon C, Nigg EA, Pines J. Active cyclin B1-Cdk1 first appears on centrosomes in prophase. Nat Cell Biol. 2003;5(2):143-8. doi: 10.1038/ncb918. PubMed PMID: 12524548.

116.   Kramer A, Mailand N, Lukas C, Syljuasen RG, Wilkinson CJ, Nigg EA, Bartek J, Lukas J. Centrosome-associated Chk1 prevents premature activation of cyclin-B-Cdk1 kinase. Nat Cell Biol. 2004;6(9):884-91. doi: 10.1038/ncb1165. PubMed PMID: 15311285.

117.   Dey A, Nishiyama A, Karpova T, McNally J, Ozato K. Brd4 marks select genes on mitotic chromatin and directs postmitotic transcription. Mol Biol Cell. 2009;20(23):4899-909. doi: 10.1091/mbc.E09-05-0380. PubMed PMID: 19812244; PMCID: PMC2785733.

118.   Foster H, Coley HM, Goumenou A, Pados G, Harvey A, Karteris E. Differential expression of mTOR signalling components in drug resistance in ovarian cancer. Anticancer Res. 2010;30(9):3529-34. PubMed PMID: 20944133.

119.   Jung J, Seol HS, Chang S. The Generation and Application of Patient-Derived Xenograft Model for Cancer Research. Cancer Res Treat. 2018;50(1):1-10. doi: 10.4143/crt.2017.307. PubMed PMID: 28903551; PMCID: PMC5784646.

120.   Yang L, Zhang Y, Shan W, Hu Z, Yuan J, Pi J, Wang Y, Fan L, Tang Z, Li C, Hu X, Tanyi JL, Fan Y, Huang Q, Montone K, Dang CV, Zhang L. Repression of BET activity sensitizes homologous recombination-proficient cancers to PARP inhibition. Sci Transl Med. 2017;9(400). doi: 10.1126/scitranslmed.aal1645. PubMed PMID: 28747513; PMCID: PMC5705017.

121.   Karakashev S, Zhu H, Yokoyama Y, Zhao B, Fatkhutdinov N, Kossenkov AV, Wilson AJ, Simpkins F, Speicher D, Khabele D, Bitler BG, Zhang R. BET Bromodomain Inhibition

Synergizes with PARP Inhibitor in Epithelial Ovarian Cancer. Cell Rep. 2017;21(12):3398-405. doi: 10.1016/j.celrep.2017.11.095. PubMed PMID: 29262321; PMCID: PMC5745042.

122.   Zhu H, Bengsch F, Svoronos N, Rutkowski MR, Bitler BG, Allegrezza MJ, Yokoyama Y, Kossenkov AV, Bradner JE, Conejo-Garcia JR, Zhang R. BET Bromodomain Inhibition Promotes Anti-tumor Immunity by Suppressing PD-L1 Expression. Cell Rep. 2016;16(11):2829-37. doi: 10.1016/j.celrep.2016.08.032. PubMed PMID: 27626654; PMCID: PMC5177024.

123.   Mabuchi S, Hisamatsu T, Kimura T. Targeting mTOR signaling pathway in ovarian cancer. Curr Med Chem. 2011;18(19):2960-8. PubMed PMID: 21651485.

124.   Cui H, Kong Y, Xu M, Zhang H. Notch3 functions as a tumor suppressor by controlling cellular senescence. Cancer Res. 2013;73(11):3451-9. doi: 10.1158/0008-5472.CAN-12-3902. PubMed PMID: 23610446; PMCID: PMC3674178.

125.   Kim TH, Jeong JY, Park JY, Kim SW, Heo JH, Kang H, Kim G, An HJ. miR-150 enhances apoptotic and anti-tumor effects of paclitaxel in paclitaxel-resistant ovarian cancer cells by targeting Notch3. Oncotarget. 2017;8(42):72788-800. doi: 10.18632/oncotarget.20348. PubMed PMID: 29069826; PMCID: PMC5641169.

126.   Houzelstein D, Bullock SL, Lynch DE, Grigorieva EF, Wilson VA, Beddington RS. Growth and early postimplantation defects in mice deficient for the bromodomain-containing protein Brd4. Mol Cell Biol. 2002;22(11):3794-802. PubMed PMID: 11997514; PMCID: PMC133820.

127.   Johnson J, Espinoza T, McGaughey RW, Rawls A, Wilson-Rawls J. Notch pathway genes are expressed in mammalian ovarian follicles. Mech Dev. 2001;109(2):355-61. PubMed PMID: 11731249.

128.   Nagarajan S, Hossan T, Alawi M, Najafova Z, Indenbirken D, Bedi U, Taipaleenmaki H, Ben-Batalla I, Scheller M, Loges S, Knapp S, Hesse E, Chiang CM, Grundhoff A, Johnsen SA. Bromodomain protein BRD4 is required for estrogen receptor-dependent enhancer activation and gene transcription. Cell Rep. 2014;8(2):460-9. doi: 10.1016/j.celrep.2014.06.016. PubMed PMID: 25017071; PMCID: PMC4747248.

129.   Chow SC. Adaptive clinical trial design. Annu Rev Med. 2014;65:405-15. doi: 10.1146/annurev-med-092012-112310. PubMed PMID: 24422576.

VITA

Alejandro O. Villar-Prados was born in San Juan, Puerto Rico, the son of Carmen Belen-Prados and Alejandro Villar-Rabell. After completing his work at Cupeyville Highschool, San Juan, Puerto Rico in 2005, he entered The University of Puerto Rico, Rio Piedras Campus in San Juan, Puerto Rico. He received the degree of Bachelor of Sciences with a major in General Biology in May, 2009. In August 2009, he entered The University of Puerto Rico Medical School to pursue his medical degree and shortly after entered the joint combined M.D./Ph.D. program between The University of Puerto Rico Medical School and The University of Texas MD Anderson Cancer Center UTHealth Graduate School of Biomedical Sciences. In August 2012, he began the Ph.D. portion of the program at The University of Texas MD Anderson Cancer Center UTHealth Graduate School of Biomedical Sciences.

Permanent address:

Urb. Paseo Mayor, Street 5, House B-1
San Juan, Puerto Rico, 00926